ΕΘΝΙΚΟ & ΚΑΠΟΔΙΣΤΡΙΑΚΟ
ΠΑΝΕΠΙΣΤΗΜΙΟ ΑΘΗΝΩΝ
Τμήμα Φυσικής,
Τομέας Αστροφυσικής, Αστρονομίας
και Μηχανικής

Διπλωματικη Εργασια

Απομονωμένοι Αστέρες Νετρονίων ως Πηγές Βαρυτικών Κυμάτων

Πάτσαρη Ευθυμία
Α.Μ. 201739

Επιβλέπων:
Αν. Καθηγητής, Θεοχάρης Αποστολάτος

Τριμελής εξεταστική επιτροπή:
Θ. Αποστολάτος, Αν. Καθηγητής
Ν. Βλαχάκης, Αν. Καθηγητής
Δ. Χατζηδημητρίου, Αν. Καθηγήτρια

Αθήνα 2019

Ευχαριστίες

Από τη θέση αυτή θα ήθελα να ευχαριστήσω θερμά τον Καθηγητή μου κ. Αποστολάτο Θεοχάρη για τις πολύτιμες συμβουλές του και την καθοδήγησή του σε κάθε στάδιο της διπλωματικής αυτής εργασίας, αφού με τη συνεχή και συστηματική του βοήθεια καθώς και με τις συζητήσεις μας επί του θέματος και τις στοχευμένες παρατηρήσεις του, συνέβαλε ουσιαστικά στην πραγματοποίηση αυτής της εργασίας.

Περίληψη

Σκοπός αυτής της εργασίας είναι να κατανοήσουμε τους βασικούς μηχανισμούς παραγωγής βαρυτικών κυμάτων από απομονωμένους αστέρες νετρονίων. Αρχικά, παρουσιάζουμε συνοπτικά κάποιους από τους επικρατέστερους μηχανισμούς για την παραγωγή βαρυτικών κυμάτων από μεμονωμένους αστέρες νετρονίων για να σταθούμε και να μελετήσουμε εκτενέστερα στη συνέχεια τον CFS μηχανισμό παραγωγής ασταθειών. Έπειτα, μελετάμε τις εξισώσεις του Einstein στο πλαίσιο της γραμμικοποιημένης Θεωρίας της Σχετικότητας, με σκοπό να εξάγουμε τα χαρακτηριστικά των βαρυτικών κυμάτων, συναρτήσει της τετραπολικής ροπής της μάζας που είναι υπεύθυνη για την παραγωγή τους. Τέλος, επειδή ο μηχανισμός CFS οδηγεί σε δυναμικές μεταβολές που συνδέονται με παραμορφώσεις του σχήματος του αστέρα, στο τελευταίο μέρος αυτής της εργασίας μελετάμε τα σχήματα των περιστρεφόμενων σωμάτων που υπόκεινται στην ιδιοβαρύτητά τους και βρίσκονται σε υδροστατική ισορροπία.

Abstract

The aim of this thesis is to understand the fundamental mechanisms that are responsible for gravitational wave emission from isolated neutron stars. We start by briefly presenting some of the dominant mechanisms that produce gravitational waves from single neutron stars, in order to, delve later into the CFS instability mechanism. Following, we study the Einstein's equations in the linearized approximation of General Theory of Relativity, with the aim of extracting the characteristic features of the gravitational waves as a function of the quadrupole moment tensor, which is responsible for their excitation. Finally, due to the fact that the CFS mechanism can lead to dynamical changes linked to deformations of the shape of the star, we dedicate the last part of this thesis, to study the figures of equilibrium of self-gravitating, rotating masses.

Contents

Chapter 1

Neutron stars

1.1 From the theoretical conception to the detection of neutron stars

A few years after Chadwick's discovery of the neutron in 1932, Baade and Zwicky [1] proposed the existence of a neutron star. While they were studying the origin of supernovae, they proposed that a supernova explosion could be linked to the transition of an ordinary star to a neutron star, an extremely dense star with a small radius, that consists almost entirely of neutron matter.

If one assumes this mechanism to study the birth of a neutron star, the surface temperature is expected to be around $10^6 K$ for the first few hundred years. The electromagnetic emission at this temperature, corresponds to a black body whose spectrum peaks in the X-ray region. Using the technology of that time, observations at the X-ray band were not possible. Furthermore, neutron star's radiation in the optical band of the spectrum would be too faint to be observed with optical telescopes. As a result, most of the community did not further pursue the discovery of these objects for the next years.

Zwicky, however, was intrigued by these objects and kept on studying neutron stars theoretically. In 1938, he calculated the binding energy of a neutron star with mass M at approximately $0.4Mc^2$ and the next year, the gravitational redshift of the surface photons, due to the star's strong gravitational field. Apart from Zwicky, Tolman, Oppenheimer and Volkkoff also contributed to the theoretical study of neutron star's. Working independently, Tolman [2] and Oppenheimer & Volkoff [3] published their work on the hydrostatic equilibrium of a self- gravitating spherical mass in the context of Einstein's theory of General Relativity, in 1939 at the same volume of Physical Review. For their calculations, they used the equation of state of non-interacting pure neutron matter. Although this equation of state is not realistic, it provides some qualitative results, such as the existence of a maximum mass limit for the neutron stars, similar to Chandrasekhar's maximum mass limit for the white dwarfs. Using the equation of state for non-interacting pure neutron matter, this maximum mass limit was calculated to be $0.7M_\odot$. Since this number is significantly smaller than $1.4M_\odot$, which is the maximum mass for white dwarfs, Tolman, Oppenheimer&Volkoff (we will use the abbreviation TOV for further references) concluded that neutron stars could not

exist, at least, having the aforementioned properties. As a result, they started questioning their assumptions, but without any significant remarks.

The discussion on the equation of state of the neutron star continued for the following decades. In 1959, Cameron [4] proved that nucleon-nucleon interactions have a significant impact on neutron star structure. Accounting for the nuclear interactions, Cameron estimated that the maximum mass of neutron stars would be significantly higher than the TOV limit, at $2M_{\odot}$. This finding once again brought under consideration the scenario that neutron stars can form during supernovae and as a result the interest of the community turned to these objects.

Another significant contribution to neutron star structure, is attributed to Migdal [5]. While he was studying the physics of superfluidity and superconductivity, he proposed that the neutron star interior provides the necessary conditions so that a superfluid and a superconducting component can occur. The existence of such components has been proven to significantly affect neutron star's cooling, which is happening due to neutrino emission produced via Urca process [1]. The neutrino emission from cooling neutron stars, inspired the community to study the possible cooling mechanisms in depth, as the potential detection of these neutrinos would provide evidence on the existence of neutron stars, and furthermore, they would reveal information concerning the equation of state that governs the neutron stars.

In the early 1960s, the X-ray astronomy was developing so the direct detection of a neutron star was anticipated. From 1962 to 1964 several X-ray cosmic sources were detected, but none of them would fit to the neutron star theoretical profile. One of these sources, was the Crab nebula, which as we know today, is home of a neutron star, the Crab pulsar. However, at the time, Bowyer [6] estimated that the source of the X-ray emission in the Crab nebula should have dimensions about 10^{13}km, which is extremely large to be associated to the dimensions of a neutron star. At the same time, Kardashev [7] considered the case of a collapsing, magnetized rotating star, forming a compact object. He noticed that the spin of the collapsing star could be faster during the first stages, at the birth of the star, slowing down as the magnetic field decayed, thus explaining the dimensions of X-ray source in the Crab nebula.

In 1965 at Cambridge England, started the construction of a new radio - telescope, sensitive at 3.7 m wavelength with very high resolution, in order to study the changes in radio photons as they pass through non-uniform regions of the interstellar and interplanetary medium. By July 1967 the telescope was fully operational, and in August of the same year, Jocelyn Bell, while a PhD student under the supervision of A. Hewish, discovered faint pulses from a radio-source. This signal could not be attributed to any known radio source. In the next few months, while they kept studying that source, they discovered that the pulses

[1] An Urca process is a reaction between a baryon and a lepton, which results to a neutrino emission. The direct Urca process in general form is described by the reaction

$$b_1 \to b_2 + \ell + \bar{\nu},$$

where b_1, b_2 are the baryons, ℓ is the lepton, and $\bar{\nu}$ is the antineutrino that take part in the reaction. The Urca process that takes place in neutron stars is the inverse beta reaction, which happens as the electrons acquire enough energy to enter inside the nucleus of the atoms and react with the protons, producing neutrons - hence the name of the neutron star- and neutrinos.

Figure 1.1: A composite image of the Crab Nebula showing the X-ray (blue), and optical (red) images superimposed. The size of the X-ray image is smaller because the higher energy X-ray emitting electrons radiate away their energy more quickly than the lower energy optically emitting electrons as they move. Source: http://hubblesite.org/image/1248/news_release/2002-24.

were periodical, and in fact extremely accurate with a period of 1.333012 s. The source was located beyond our solar system and the group that was studying it, named it pulsar, an abbreviation for pulsating radio star [8]. In the next months, the team discovered three more signals, similar to the first one and soon came up a few attempts to explain these pulses mentioning pulsating white dwarfs and neutron stars as the sources of the signals, but these theories were soon abandoned.

In 1967, Pacini published a paper in Nature [9] in which he showed that a rapidly rotating neutron star, with a strong dipole magnetic field, can turn its rotational kinetic energy to electromagnetic radiation. The electromagnetic radiation that is produced by this mechanism, will in turn accelerate particles to very high energies. In addition to Pacini's work. in 1968, Gold [10] suggested that pulsars are in fact magnetized, rotating neutron stars, supporting his argument by the discovery of the Crab pulsar, at the same year. When the Crab pulsar was detected, its period was measured to be 33 ms, which implies that the central compact object could not be a white dwarf since it would be torn apart by the centrifugal forces due to the rapid rotation. This observation established that pulsars are actually neutron stars.

The radio wave pulses that we observe are thought to originate from the neutron star magnetosphere. The pulses are explained if one assumes that the radio waves are emitted

along the axis of the magnetic field and that the dipole magnetic moment of the neutron star is not aligned with the axis of rotation. As the star is spinning, we perceive pulses as the magnetic dipole moment vector passes by the Earth, similar to the lighthouse beam. Another significant finding, is that the period of the pulsar is growing larger with the time, meaning that neutron stars are spinning down. The fact that one can measure the pulsar spin down rate comes from the precise measurement of the neutron star period itself.

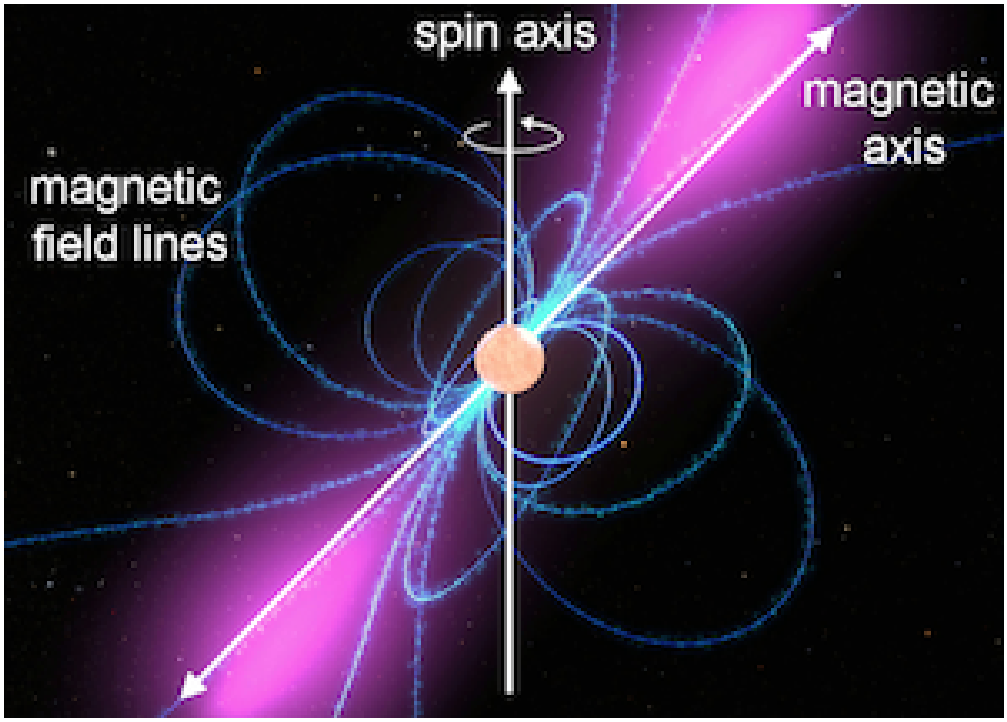

Figure 1.2: Artistic presentation of a pulsar. In the general case, where the spin axis is not aligned with the magnetic axis, radiation emitted along the magnetic axis appears as pulses to a distant observer whenever the magnetic axis passes by the observer's line of sight. Source: https://imagine.gsfc.nasa.gov/science/objects/neutron_stars1.html

1.2 The structure of a neutron star

In this section, we will briefly present an overview of the current theoretical understanding of the neutron star structure. With a mass, around $1 - 1.5 M_{\odot}$, packed in a radius of approximately 10 km, they are among the densest objects in the Universe. As a result, the conditions that dominate their interior lead to some of the most extreme states of matter. Apart from a thin atmosphere, which has a few centimeters height from the neutron star surface, the neutron star interior can be subdivided into four main regions:

- the outer crust,
- the inner crust,

- the outer core and
- the inner core,

as shown in figure 1.3. Each region is characterized by different composition, and is described by a different equation of state. We will briefly describe the key characteristics of each region.

Outer crust

The outer crust, extends from the neutron star surface to a few hundred meters, where the density reaches the neutron drip point $\rho_{ND} \approx 10^{11}$ g/cm^3. This region consists mainly of ions and electrons. At density $\rho \approx 10^6$g/cm^3 the pressure is provided by strongly degenerate, almost ideal gas of electrons. When the electrons become relativistic, they enter the nucleus and react with the protons via inverse beta-decay,

$$p + e \rightarrow n + \nu, \tag{1.1}$$

forming neutron-rich nuclei. Neutrons, are fermions, thus there is a critical density, which signifies that they can no longer occupy the nuclear energy states, thus they leave the nuclei and form a gas of free neutrons. The point where the density reaches this critical value is called neutron drip point and is approximately $\rho_{ND} \approx 4 \times 10^{11}$ g/cm^3.

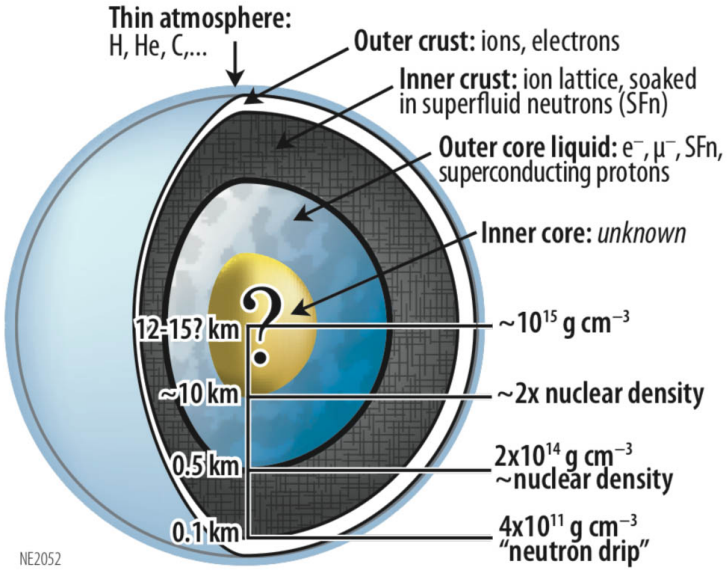

Figure 1.3: Schematic structure of a neutron star.

Inner crust

The inner crust may extend to about one kilometer. It occupies the region where the pressure extends between the neutron drip point and approximately $0.5\rho_0$ at the base, where $\rho_0 = 2.8 \times 10^{14}$ g/cm^3 is the saturation nuclear matter density. The inner crust consists mainly of free neutrons neutron rich nuclei and electrons. The fraction of free neutrons increases with the density and in the bottom layers of the crust, the nuclei disappear. The free neutrons in the inner crust and the atomic nuclei can be in superfluid state.

Outer core

The density in the outer core ranges between $\rho \approx 0.5\rho_0$ to $\rho \approx 2\rho_0$ and is several kilometers thick. The composition of the outer core is mainly neutrons, with an admixture of protons, electrons and possibly muons ($npe\mu$ composistion). Electrons and muons form almost ideal Fermi gases, while the protons and neutrons form a Fermi liquid which can be in superfluid state. The outer core is thought to extend to the very center of low-mass neutron stars.

Inner core

The inner core occupies the central region of the more massive neutron stars. The density in this region ranges from $2\rho_0$ to as much as $10 - 15\rho_0$, in the most extreme theories that have been proposed. Since there are several ambiguities concerning the nucleon-nucleon interaction and many-body interactions, the equation of state of nuclear matter at supra-nuclear densities is an open question, so there have been proposed many different theories concerning the composition of the core. Some of the hypotheses proposed for the composition of the inner core, include hyperon matter, pion or kaon condensation and quark matter, composed of deconfined light u and d quarks and strange s quarks, and possibly a small admixture of electrons.

1.3 Observational physical quantities of neutron stars

Depending on their surrounding environment, neutron stars can be detected in all the electromagnetic spectrum, from radio waves to the very high frequency gamma-rays. Although the mechanism that produces the radio emission in the pulsar's magnetosphere is not entirely determined, the emission is associated with the spin of the neutron star. Based on this we are able to infer the pulsar's spin period, and in some cases pulsar's period is more accurate than atomic clocks.

Since pulsars are the most accurate clocks, one can not only measure the spin period, but also the rate of change of that period, i.e. the first - order time derivative of the period. In the case of isolated neutron stars, it is found that the pulsar rotation decelerates with time. This is attributed to the conversion of a portion of rotational kinetic energy to rotating magnetic dipole emission, and another portion to accelerate relativistic particles. As a result, the pulsar period is growing with time.

As we stated above, the values of the pulsar period, P and the time derivative of the period, $\dot{P}$ inferred from the observational data, are widely used to estimate the magnetic field strength and the pulsar characteristic age. Let us assume that the magnetic field is given by the dipole approximation

$$\vec{m} = \frac{1}{2} B_{\rm surf} R^3 (\sin\theta \cos(\Omega t)\hat{i} + \sin\theta \sin(\Omega t)\hat{j} + \cos\theta \hat{k}) \tag{1.2}$$

where $B_{\rm surf}$, is the surface magnetic field strength, R the radius of the neutron star, θ the angle between the rotation axis and the magnetic field vector and Ω the angular velocity of

the neutron star $\Omega = 2\pi/P$. Furthermore, the magnetic dipole energy loss rate is given by equation

$$\dot{E} = -\frac{2}{3c^3}\|\vec{\ddot{m}}\|^2, \tag{1.3}$$

and the pulsar change in rotational energy,

$$E_{\rm rot} = \frac{1}{2}I\Omega^2 \rightarrow \dot{E}_{\rm rot} = I\Omega\dot{\Omega}, \tag{1.4}$$

where I is the moment of inertia. If we assume that the energy changes according to equation (1.3), then one can estimate the magnetic field using the relation

$$\dot{\Omega} = -\frac{B_{surf}^2 R^6 \sin^2\theta}{6Ic^3}\Omega^3. \tag{1.5}$$

The significance of this relation comes from the fact that it links the observational parameters $\omega, \dot{\omega}$ and $\dot{E}$ to the surface magnetic field and the radius of the pulsar.

The basic equation for estimating the pulsar age also comes from equation (1.5). We express the spin-down rate as

$$\dot{\Omega} = -k\Omega^n \tag{1.6}$$

where n is the braking index, and for the case of magnetic dipole, $n = 3$. Using equation (1.6) and assuming that the braking index remains constant, we can integrate from the pulsar birth $t = 0$ to a current age t

$$\int_{\Omega_0}^{\Omega}\frac{d\Omega'}{\Omega'^n} = -\int_0^T kdt \Rightarrow -kT = \frac{\Omega^{1-n} - \Omega_0^{1-n}}{1-n} \rightarrow T = \frac{\Omega}{(n-1)\dot{\Omega}} \rightarrow$$

$$T = \frac{\Omega}{(n-1)\dot{\Omega}} = \frac{P}{(n-1)\dot{P}}\ , \tag{1.7}$$

where we assumed that a newly born neutron star rotates much faster than now. If one assumes a dipole magnetic field for the pulsar, i.e. the $n = 3$ case, then the formula for the pulsar characteristic age yields

$$T = \frac{P}{2\dot{P}}\ . \tag{1.8}$$

For some pulsars, we can measure not only their spin-down rate $\dot{P}$, but also $\ddot{P}$. Taking the time derivative of (1.6) and substituting to equation (1.7) we can measure the braking index, which is linked to the magnetic field configuration, as a function of observable parameters,

$$n = \frac{\Omega\ddot{\Omega}}{\dot{\Omega}^2}. \tag{1.9}$$

This last relation is important to check the assumptions regarding the magnetic field of a particular neutron star that one has to make and furthermore, when combined, equations (1.7), (1.8) and (1.9) provide information about the true pulsar age and the initial pulsar spin period.

A very useful plot, that is often used when one studies the evolution of pulsars, is the $P - \dot{P}$ diagram. In this plot, one can distinguish three dominant regions. The central region,

where most of the pulsar population lies, is composed mainly by what we call "normal" pulsars.

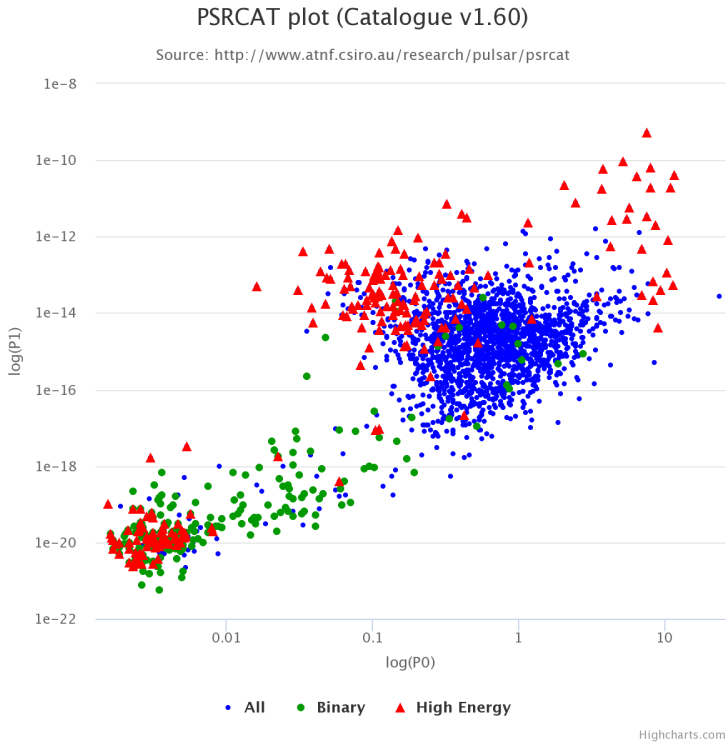

Figure 1.4: Pulsar distribution in the logarithmic $P - \dot{P}$ plane. Most of the pulsar population is located in the central region, and we will refer to them as normal pulsars. In the bottom left corner of the diagram, lie the MSPs, having very slow spin-down rates and weak magnetic fields compared to the normal pulsars. On the other hand, in the top right corner lie the magnetars, with longer period, faster spin-down rates than normal pulsars and very strong magnetic fields, up to 10^{15} G. Source:http://www.atnf.csiro.au/people/pulsar/psrcat/

The bottom left region of the diagram is occupied by millisecond pulsars (MSPs). These are old pulsars, members of the Low-mass X-ray binary systems (LMXRB), that have been presumably recycled due to accretion from a companion star, hence their rapid spin. MSPs have very slow spin-down rates and weak magnetic fields - compared to normal pulsars - around 10^8 G. Lying between the MSPs and the region of the normal pulsar distribution, there is a group of binary pulsars. These systems, are characterized by relatively massive companions in High-mass X-ray binary systems (HMXRB), and include all of the known double neutron star systems. Since more massive stars evolve faster, the pulsar's recycling phase did not last as long as the corresponding phase in a LMXRB system, so these pulsars end up with intermediate periods, in the range of 10 - 100 ms. Last but not least, in the top right corner of the $P - \dot{P}$ diagram, lie the magnetars. These neutron stars have very strong magnetic fields, up to 10^{15} G and their high-energy emission is thought to be coming from the decay of their magnetic field.

Another observational quantity that is of great interest is the neutron star mass. Figuring out the mass of an isolated neutron star is a very difficult task, since it depends highly on

the equation of state of its interior, which still remains an open question.

The simplest way to measure the neutron star mass, is when it is a part of a binary system, using Kepler's laws of motion. However, neutron star mass measurements determined in this way, have huge error bars, as depicted in figure 1.5.

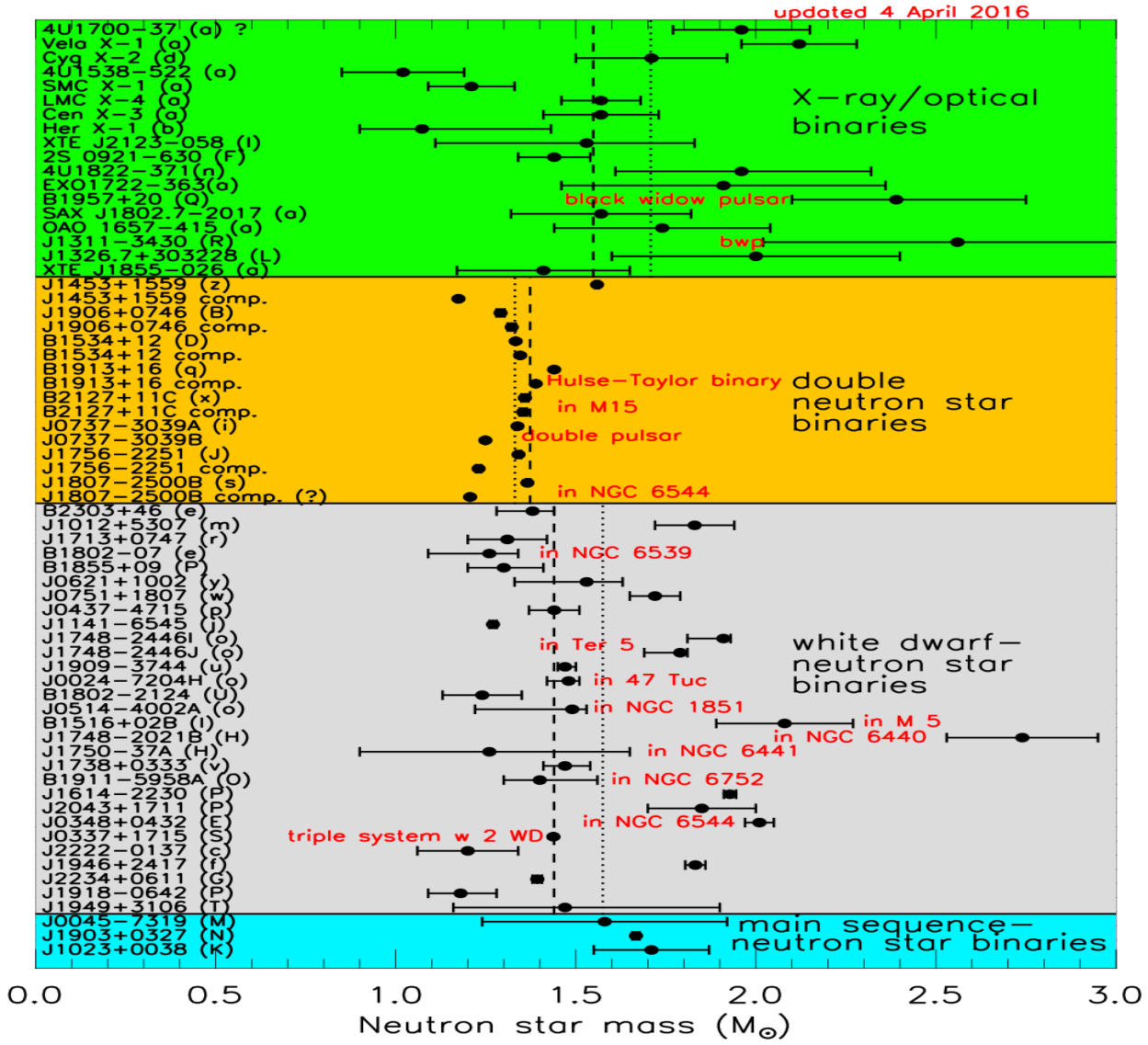

Figure 1.5: Neutron star masses. This list was last updated in April 4, 2016. Source: https://stellarcollapse.org/nsmasses

In the few cases where we have a double neutron star system, those error bars are significantly smaller. When a binary neutron star system is in close orbit, Kepler's laws are not sufficient to describe the motions of the system, so we need to correct our equations using General theory of Relativity. If we apply General Relativity to the problem, the relativistic corrections to the problem, are parametrized in terms of post-Keplerian parameters. These are similar to the advance of the periastron of the orbit, the combined effect of gravitational redshift and Doppler shift, around the elliptical orbit, the orbital change due to emission

of quadrupole gravitational radiation and the range and shape of the Shapiro time delay of the pulsar signal, as it propagates through the gravitational field of its companion. If one can measure any two of the post-Keplerian parameters that we mentioned, then one can uniquely determine the masses of the neutron stars involved. For more details on neutron star mass measurements, we refer the interested reader to Thorsett & Chakrabarty [11].

1.4 Gravitational waves from single neutron stars

In the previous section, we discussed some of the key physical quantities of a neutron star, that can be inferred from electromagnetic observations. In this section, we will briefly mention some of the possible theoretical mechanisms that could trigger neutron stars so as to produce gravitational waves. It should be made clear, that by the term "single" neutron star, we imply that we will focus on either isolated neutron stars, or neutron stars that are members of a LMXRB system.

Neutron star Asteroseismology

Much like the main-sequence stars that oscillate, neutron stars can be pulsating and produce gravitational waves. These gravitational waves, if detected, can be used as probes to the neutron star interior, using techniques of asteroseismology. The key idea in neutron star asteroseismology is to parametrize an oscillation mode's frequency f and gravitational wave damping timescale τ_{GW} in terms of fundamental neutron star parameters, i.e. the mass M, radius R and angular velocity Ω. If one manages to combine these parameters, then it would lead to a relation between them that is independent of the equation of state, which is still unknown. Moreover, if the neutron star mass is known, then a measurement of its oscillation modes would provide extra information that could be used to determine the neutron star equation of state.

Unstable oscillation modes in rotating stars - CFS instabilities

The theory of instabilities of rotating self-gravitating fluid systems dates back to 1970s, when Chandrasekhar, Friedman and Schutz developed a mechanism that describes them, today known as CFS theory, or CFS instability mechanism. We have a separate section entirely dedicated to the CFS theory, where we present in a greater detail the instability mechanism, but we will briefly present some key points here for the sake of completeness.

The CFS theory includes two types of instabilities, the secular and the dynamical instability. Both are based on the notion that the canonical energy of the perturbation, if conserved, can become either zero, which leads to the dynamical instabilities, or negative, in the case of secular instabilities, above a certain rotational frequency threshold. The two types of instabilities are fundamentally different; the secular instability requires the fluid to be coupled to some dissipative mechanism, such as the gravitational wave emission or viscosity[2] while the dynamical instability can take place in completely dissipationless systems.

[2]The CFS instability is not strictly a gravitational-wave driven instability. Electromagnetic radiation or normal shear viscosity can also lead to unstable oscillation modes, but it turns out that gravitational radiation is almost always the dominant mechanism.

The names "secular" and "dynamical" given to the two types of instabilities have been used to describe the time on which the instabilities manifest. The dynamical instabilities can take place for very brief periods of time and are linked to shape deformations of the star. For instance, a dynamical CFS instability could manifest during the merging process of two neutron stars. On the other hand, secular instabilities manifest in much longer periods of time.

Among the various neutron star oscillation modes, the most promising ones to turn the neutron stars into a potential source of gravitational waves and play an important role in the dynamics of a neutron stars via the CFS mechanism are the fundamental f-mode and the inertial r-mode.

The f-mode is associated with the dynamical CFS instability with the dominant multipole being the $l = 2$, leading to the so-called bar-mode instability. The dynamical f-mode instability is likely to appear in fast, differentially rotating systems, such as the immediate neutron star outcome of a binary neutron star merger.

Neutron star mountains

A spherically symmetric rotating neutron star with respect to the axis of rotation, cannot emit gravitational radiation. However, there are cases where non-axisymmetric distortions, called "mountains", can occur on the neutron star surface, which lead to deviation from the spherical symmetry of the star, thus producing gravitational waves. This deviation from axisymmetry is described by the quadrupole ellipticity

$$\epsilon = \frac{Q}{I}, \tag{1.10}$$

where Q is the mass quadrupole moment associated to the distortion, and I is the moment of inertia of the rotation axis.

These mountains can be frozen into the crust or core of the neutron star after it was born in a supernova, or it can form later in the crust and be supported by the star's magnetic field (magnetic mountains) or can be caused by temperature gradients in the crust (thermal mountains) [3]. For a neutron star crust made up of ordinary matter, these mountains can be as high as 10 cm[4].

Although LIGO and VIRGO interferometers are thought to be sensitive to the expected gravitational wave emission from neutron star mountains, there have been no signs of such detection up to now. This negative result, however, places an upper limit on the maximum value of the quadrupole ellipticity on neutron stars.

[3]Thermal mountains, require that the neutron star is in an accreting LMXRB system, because the temperature gradients are created by asymmetries in the accreting matter from the companion star. Magnetic mountains can occur to both isolated neutron stars or members of a LMXRB system

[4]A source, where these estimates can be found, is https://www.ligo.org/science/Publication-S6VSR24KnownPulsar/

Chapter 2

CFS Instability

In this chapter, we will delve into the calculations of the CFS instability mechanism, following the original works of Friedman and Schutz [12], [13]. We will consider the case of a self gravitating, perfect fluid to study its perturbations, in the Cowling approximation[1]. The problem will be studied in terms of the Lagrangian displacement vector. First we will derive the equation of motion that characterize our perturbations and then we will focus on the conserved quantities of our configuration, i.e. the canonical energy and angular momentum. At the end of this chapter, we will apply the results to study the case of secular instability in stars.

2.1 Lagrangian perturbation theory

We will consider the perturbations of a stationary perfect fluid with density ρ, pressure p, entropy per baryon s and fluid velocity u^i. The present study will be purely Newtonian. The parameters (ρ, p, s, u^i) are solutions to the equations:

$$p = p(\rho, s) \tag{2.1}$$

$$\nabla_i(\rho u^i) = 0 \tag{2.2}$$

$$u^i \nabla_i s = 0 \tag{2.3}$$

$$u^j \nabla_j u_i + \frac{1}{\rho}\nabla_i p + \nabla_i \Phi = 0 \tag{2.4}$$

where Φ is the gravitational potential, defined by the equation:

$$\nabla^2 \Phi = 4\pi G\rho. \tag{2.5}$$

There are two ways, in which one can study small perturbations of a fluid. One way is by using the Eulerian approach, where one considers the change in a fluid variable Q,

[1] In the Cowling approximation, we only consider perturbations of the fluid, while the spacetime metric is assumed to be described as a fixed background.

namely δQ, at a particular point in space. Through this approach, we end up having the quantities $\delta\rho, \delta p, \delta s$ and δu^i as the perturbations of our fluid. The other way is by defining a Lagrangian displacement vector field ξ^i which connects fluid elements in the equilibrium with corresponding ones in the perturbed configuration. If we represent the Lagrangian change of a quantity Q, as ΔQ, then we can relate it to the Eulerian change δQ through the equation:

$$\Delta Q = \delta Q + \pounds_\xi Q, \tag{2.6}$$

where the Lie derivative $\pounds_\xi$ is defined as:

$$\pounds_\xi f = \xi^i \nabla_i f \qquad \text{for scalars } f, \tag{2.7}$$

$$\pounds_\xi u^i = \xi^j \nabla_j u^i - u^j \nabla_j \xi^i \qquad \text{for contravariant vectors,} \tag{2.8}$$

$$\pounds_\xi u_i = \xi^j \nabla_j u_i + u_j \nabla_i \xi^j \quad \text{for covariant vectors.} \tag{2.9}$$

We will begin our analysis, by extracting the equation of motion for the perturbed fluid configuration. To do that, we will consider that a fluid element follows a perturbed trajectory $c^i(t) + \xi^i[c(t), t]$, where $c^i(t)$ is the trajectory of the fluid element in the equilibrium configuration. In that context, the Lagrangian change in the fluid velocity Δu^i, is:

$$\Delta u^i = \partial_t \xi^i. \tag{2.10}$$

Given this, and:

$$\pounds_\xi g_{ij} = \nabla_i \xi_j + \nabla_j \xi_i,$$

we compute that:

$$\Delta u_i = \Delta(g_{ij} u^j) = u^j \Delta g_{ij} + g_{ij} \Delta u^j = u^j \nabla_i \xi_j + u^j \nabla_j \xi_i + g_{ij} \partial_t \xi^j \rightarrow$$

$$\Delta u_i = \partial_t \xi_i + u^j \nabla_i \xi_j + u^j \nabla_j \xi_i. \tag{2.11}$$

Furthermore, using relation (2.6), it can be easily shown that:

$$\delta u_i = \partial_t \xi_i + u^j \nabla_j \xi_i - \xi^j \nabla_j u_i. \tag{2.12}$$

The conservation of mass is expressed by:

$$\Delta \rho = -\rho \nabla_i \xi^i. \tag{2.13}$$

Assuming adiabatic perturbations, which implies

$$\Delta s = 0, \tag{2.14}$$

we could assume that the equation of state (2.1) is described by the general polytropic form:

$$p = k\rho^\gamma \tag{2.15}$$

where γ is the adiabatic index. It then follows that:

$$\Delta p = \Delta(k\rho^\gamma) \rightarrow \Delta p = k\Delta(\rho^\gamma) \rightarrow \Delta p = \frac{p}{\rho^\gamma}\left[\delta(\rho^\gamma) + \pounds_\xi(\rho^\gamma)\right] \rightarrow$$
$$\frac{\Delta p}{p} = \frac{1}{\rho^\gamma}\left[\gamma\rho^{\gamma-1}\delta\rho + \xi^i\nabla_i(\rho^\gamma)\right] \rightarrow \frac{\Delta p}{p} = \frac{1}{\rho^\gamma}\left[\gamma\rho^{\gamma-1}\delta\rho + \gamma\rho^{\gamma-1}\xi^i\nabla_i\rho\right] \rightarrow$$
$$\frac{\Delta p}{p} = \gamma\frac{1}{\rho}\left(\delta\rho + \xi^i\nabla_i\rho\right) \rightarrow$$
$$\frac{\Delta p}{p} = \gamma\frac{\Delta\rho}{\rho}. \tag{2.16}$$

In terms of Eulerian perturbations, equations (2.10), (2.13), (2.14) and (2.16) can be written as follows.

For the density, we have:

$$\Delta\rho = \delta\rho + \pounds_\xi\rho \rightarrow \delta\rho = -\rho\nabla_i\xi^i - \xi^i\nabla_i\rho \rightarrow$$
$$\delta\rho = -\nabla_i(\rho\xi^i). \tag{2.17}$$

From adiabatic perturbations, we have:

$$\Delta s = 0 \rightarrow \delta s + \pounds_\xi s = 0 \rightarrow \delta s + \xi^i\nabla_i s = 0 \rightarrow$$
$$\delta s = -\xi^i\nabla_i s. \tag{2.18}$$

The velocity of the fluid is given by:

$$\Delta u^i = \delta u^i + \pounds_\xi u^i \rightarrow \partial_t\xi^i = \delta u^i + \xi^j\nabla_j u^i - u^j\nabla_j\xi^i$$
$$\delta u^i = \partial_t\xi^i + u^j\nabla_j\xi^i - \xi^j\nabla_j u^i. \tag{2.19}$$

Pressure perturbations can be written as:

$$\frac{\Delta p}{p} = \gamma\frac{\Delta\rho}{\rho} \rightarrow \delta p + \pounds_\xi p = p\gamma\frac{(-\rho\nabla_i\xi^i)}{\rho} \rightarrow$$
$$\delta p = -\gamma p\nabla_i\xi^i - \xi^i\nabla_i p. \tag{2.20}$$

Finally, for the gravitational potential, using equation (2.5), we have:

$$\nabla^2\delta\Phi = 4\pi G\delta\rho \rightarrow \nabla^2\delta\Phi = -4\pi G\nabla_j(\rho\xi^j). \tag{2.21}$$

Now, we can extract the equation of motion of the perturbed configuration, in terms of the displacement ξ^i.

$$\rho\Delta\left[(\partial_t + u^k\nabla_k)u_i + \frac{1}{\rho}\nabla_i p + \nabla_i\Phi\right] = 0 \rightarrow$$

$$\rho\left[\Delta(\partial_t u_i) + \Delta(u^k\nabla_k u_i) + \Delta\left(\frac{1}{\rho}\nabla_i p\right) + \Delta(\nabla_i\Phi)\right] = 0. \tag{2.22}$$

We will analyze each term individually. For the first term, we have:

$$\begin{aligned}
\Delta(\partial_t u_i) &= \delta(\partial_t u_i) + \pounds_\xi(\partial_t u_i) \\
&= \partial_t(\delta u_i) + \pounds_\xi(\partial_t u_i) \\
&= \partial_t\left(\partial_t\xi_i + u^j\nabla_j\xi_i - \xi^j\nabla_j u_i\right) + \xi^j\nabla_j(\partial_t u_i) + (\partial_t u_j)(\nabla_i\xi^j) \\
&= \partial_t^2\xi_i + (\partial_t u^j)(\nabla_j\xi_i) + u^j\nabla_j(\partial_t\xi_i) - (\partial_t\xi^j)(\nabla_j u_i) - \xi^j\nabla_j(\partial_t u_i) \\
&\qquad +\xi^j\nabla_j(\partial_t u_i) \qquad\qquad \rightarrow
\end{aligned}$$

$$\Delta(\partial_t u_i) = \partial_t^2\xi_i + u^j\nabla_j(\partial_t\xi_i) - (\partial_t\xi^j)(\nabla_j u_i). \tag{2.23}$$

The second term of equation (2.22) gives:

$$\begin{aligned}
\Delta(u^k\nabla_k u_i) &= \delta(u^k\nabla_k u_i) + \pounds_\xi(u^k\nabla_k u_i) \\
&= (\delta u^k)(\nabla_k u_i) + u^k\nabla_k(\delta u_i) + \pounds_\xi(u^k\nabla_k u_i) \\
&= \left(\partial_t\xi^k + u^j\nabla_j\xi^k - \xi^j\nabla_j u^k\right)(\nabla_k u_i) + u^k\nabla_k\left(\partial_t\xi_i + u^j\nabla_j\xi_i - \xi^j\nabla_j u_i\right) \\
&\qquad +\xi^j\nabla_j(u^k\nabla_k u_i) + (u^k\nabla_k u_j)(\nabla_i\xi_j) \\
&= (\partial_t\xi^k)(\nabla_k u_i) + u^j(\nabla_j\xi^k)(\nabla_k u_i) - \xi^j(\nabla_j u^k)(\nabla_k u_i) + u^k\nabla_k(\partial_t\xi_i) \\
&\qquad +u^k\nabla_k(u^j\nabla_j\xi_i) - u^k\nabla_k(\xi^j\nabla_j u_i) + \xi^j(\nabla_j u^k)(\nabla_k u_i) \\
&\qquad +\xi^j u^k\nabla_j\nabla_k u_i + u^k(\nabla_k u_j)(\nabla_i\xi^j) \\
&= (\partial_t\xi^k)(\nabla_k u_i) + u^j(\nabla_j\xi^k)(\nabla_k u_i) - \xi^j(\nabla_j u^k)(\nabla_k u_i) + u^k\nabla_k(\partial_t\xi_i) \\
&\qquad +(u^k\nabla_k)^2\xi_i - u^k(\nabla_k\xi^j)(\nabla_j u_i) - u^k\xi^j\nabla_k\nabla_j u_i \\
&\qquad +\xi^j(\nabla_j u^k)(\nabla_k u_i) + u^k\xi^j\nabla_k\nabla_j u_i + u^k(\nabla_k u_j)(\nabla_i\xi^j) \rightarrow
\end{aligned}$$

$$\Delta(u^k\nabla_k u_i) = (\partial_t\xi^k)(\nabla_k u_i) + u^k\nabla_k(\partial_t\xi_i) + (u^k\nabla_k)^2\xi_i + u^k(\nabla_k u_j)(\nabla_i\xi^j). \tag{2.24}$$

The third term gives:

$$\begin{aligned}
\Delta\left(\frac{1}{\rho}\nabla_i p\right) &= \delta\left(\frac{1}{\rho}\nabla_i p\right) + \pounds_\xi\left(\frac{1}{\rho}\nabla_i p\right) \\
&= \delta\left(\frac{1}{\rho}\right)(\nabla_i p) + \frac{1}{\rho}\nabla_i(\delta p) + \pounds_\xi\left(\frac{1}{\rho}\nabla_i p\right) \rightarrow
\end{aligned}$$

$$\begin{aligned}
\Delta\left(\frac{1}{\rho}\nabla_i p\right) &= -\frac{\delta\rho}{\rho^2}(\nabla_i p) + \frac{1}{\rho}\nabla_i\left(-\gamma p\nabla_j\xi^j - \xi^j(\nabla_j p)\right) + \xi^j\nabla_j\left(\frac{1}{\rho}\nabla_i p\right) + \left(\frac{1}{\rho}\nabla_j p\right)(\nabla_i\xi^j) \\
&= \frac{1}{\rho^2}\nabla_j(\rho\xi^j)(\nabla_i p) - \frac{1}{\rho}\nabla_i(\gamma p\nabla_j\xi^j) - \frac{1}{\rho}(\nabla_i\xi^j)(\nabla_j p) - \frac{1}{\rho}\xi^j\nabla_i\nabla_j p \\
&\qquad +\xi^j\left(\nabla_j\frac{1}{\rho}\right)(\nabla_i p) + \frac{1}{\rho}\xi^j\nabla_j\nabla_i p + \frac{1}{\rho}(\nabla_j p)(\nabla_i\xi^j) \\
&= \frac{1}{\rho}(\nabla_j\xi^j)(\nabla_i p) + \frac{1}{\rho^2}\xi^j(\nabla_j\rho)(\nabla_i p) - \frac{1}{\rho}\nabla_i(\gamma p\nabla_j\xi^j) - \frac{1}{\rho}(\nabla_i\xi^j)(\nabla_j p) \\
&\qquad -\frac{1}{\rho^2}\xi^j(\nabla_j\rho)(\nabla_i p) + \frac{1}{\rho}(\nabla_j p)(\nabla_i\xi^j) \rightarrow
\end{aligned}$$

$$\Delta\left(\frac{1}{\rho}\nabla_i p\right) = -\frac{1}{\rho}\nabla_i(\gamma p \nabla_j \xi^j) + \frac{1}{\rho}(\nabla_j p)(\nabla_i \xi^j). \tag{2.25}$$

Finally, the last term gives:

$$\Delta(\nabla_i \Phi) = \delta(\nabla_i \Phi) + \pounds_\xi(\nabla_i \Phi) = \nabla_i \delta\Phi + \xi^j \nabla_j \nabla_i \Phi + (\nabla_j \Phi)(\nabla_i \xi^j). \tag{2.26}$$

The equation of motion (2.22) combined with equations (2.23), (2.24), (2.25), (2.26), gives:

$$\begin{aligned}
\rho\Big\{ &\partial_t^2 \xi_i + u^j \nabla_j(\partial_t \xi_i) - (\partial_t \xi^j)(\nabla_j u_i) + (\partial_t \xi^k)(\nabla_k u_i) + u^k \nabla_k(\partial_t \xi_i) + (u^k \nabla_k)^2 \xi_i \\
&+ u^k (\nabla_k u_j)(\nabla_i \xi^j) + \frac{1}{\rho}(\nabla_j \xi^j)(\nabla_i p) - \frac{1}{\rho}\nabla_i(\gamma p \nabla_j \xi^j) + \nabla_i \delta\Phi \\
&+ \xi^j \nabla_j \nabla_i \Phi + (\nabla_j \Phi)(\nabla_i \xi^j) = 0 \rightarrow \\
\rho\Big\{ &\partial_t^2 \xi_i + 2u^j \nabla_j(\partial_t \xi_i) + (u^j \nabla_j)^2 \xi_i + u^k (\nabla_k u_j)(\nabla_i \xi^j) + \frac{1}{\rho}(\nabla_j \xi^j)(\nabla_i p) \\
&- \frac{1}{\rho}\nabla_i(\gamma p \nabla_j \xi^j) + \nabla_i \delta\Phi + \xi^j \nabla_j \nabla_i \Phi + (\nabla_j \Phi)(\nabla_i \xi^j)\Big\} = 0 \rightarrow \\
\rho\Big\{ &\partial_t^2 \xi_i + 2u^j \nabla_j(\partial_t \xi_i) + (u^j \nabla_j)^2 \xi_i + u^k (\nabla_k u_j)(\nabla_i \xi^j) + \frac{1}{\rho}(\nabla_j \xi^j)(\nabla_i p) \\
&- \frac{1}{\rho}\nabla_i(\gamma p \nabla_j \xi^j) + \nabla_i \delta\Phi + \xi^j \nabla_j \nabla_i \Phi + (-u^k \nabla_k u_j - \frac{1}{\rho}\nabla_j p)(\nabla_i \xi^j)\Big\} = 0
\end{aligned}$$

where we have substituted the last term from equation (2.4). Finally, the equation of motion takes the form:

$$\begin{aligned}
\rho\Big\{ &\partial_t^2 \xi_i + 2u^j \nabla_j(\partial_t \xi_i) + (u^j \nabla_j)^2 \xi_i + \frac{1}{\rho}(\nabla_i p)(\nabla_j \xi^j) - \frac{1}{\rho}\nabla_i(\gamma p \nabla_j \xi^j) \\
&- \frac{1}{\rho}(\nabla_i \xi^j)(\nabla_j p) + \nabla_i \delta\Phi + \xi^j \nabla_j \nabla_i \Phi\Big\} = 0 \Leftrightarrow \qquad (2.27) \\
&A_{ij}\partial_t^2 \xi^j + B_{ij}\partial_t \xi^j + C_{ij}\xi^j = 0. \qquad (2.28)
\end{aligned}$$

At this point, it should be emphasized the fact that equations (2.17), (2.18), (2.19), (2.20), which connect initial perturbations with the displacement vector ξ^i, hold true only if the total mass and entropy of the configurations are constant.

2.2 Conserved quantities

Any Lagrangian system can be associated with a symplectic structure, that is a dynamically conserved antisymmetric product involving the configuration space variables and their conjugate momenta. In our configuration, where we have the vector ξ^i as the space variable,

the conjugate momentum [2] is:

$$\frac{\partial L}{\partial \dot{\xi}^i} = A^i_j \dot{\xi}^j + \frac{1}{2} B^i_j \xi^j = \rho \dot{\xi}^i + \rho u^j \nabla_j \xi^i. \tag{2.30}$$

The symplectic structure W has the form:

$$W(\eta, \xi) = \langle \eta, A\dot{\xi} + \frac{1}{2} B\xi \rangle - \langle A\dot{\eta} + \frac{1}{2} B\eta, \xi \rangle \tag{2.31}$$

where we have introduced the notation $\langle \eta, \xi \rangle = \int \eta^* \xi dV$ to express the inner product.

If η, ξ are solutions to equation (2.28), then $W(\eta, \xi)$ is a conserved quantity over time:

$$\begin{aligned}
\partial_t W(\eta,\xi) &= \langle \dot{\eta}, A\dot{\xi} + \frac{1}{2}B\xi \rangle + \langle \eta, A\ddot{\xi} + \frac{1}{2}B\dot{\xi} \rangle - \langle A\ddot{\eta} + \frac{1}{2}B\dot{\eta}, \xi \rangle - \langle A\dot{\eta} + \frac{1}{2}B\eta, \dot{\xi} \rangle \\
&= \langle \dot{\eta}, A\dot{\xi} + \frac{1}{2}B\xi \rangle + \langle \eta, -\frac{1}{2}B\dot{\xi} - C\xi \rangle - \langle -\frac{1}{2}B\dot{\eta} - C\eta, \xi \rangle - \langle A\dot{\eta} + \frac{1}{2}B\eta, \dot{\xi} \rangle \\
&= \langle \dot{\eta}, A\dot{\xi} \rangle + \langle \dot{\eta}, \frac{1}{2}B\xi \rangle + \langle \eta, -\frac{1}{2}B\dot{\xi} \rangle + \langle \eta, -C\xi \rangle \\
&\qquad -\langle -\frac{1}{2}B\dot{\eta}, \xi \rangle - \langle -C\eta, \xi \rangle - \langle A\dot{\eta}, \dot{\xi} \rangle - \langle \frac{1}{2}B\eta, \dot{\xi} \rangle \\
&= \langle \dot{\eta}, A\dot{\xi} - \langle \dot{\eta}, A\dot{\xi} \rangle - \frac{1}{2}\left(\langle \dot{\eta}, B\xi \rangle - \langle \dot{\eta}, B\xi \rangle \right) - \frac{1}{2}\Big(\langle \eta, B\dot{\xi} \rangle - \langle \eta, B\dot{\xi} \rangle \Big) \\
&\qquad + \langle \eta, C\xi \rangle - \langle \eta, C\xi \rangle \qquad \rightarrow
\end{aligned}$$

$$\partial_t W(\eta, \xi) = 0, \tag{2.32}$$

where we have used the fact that the operators A_{ij} and C_{ij} are symmetric, while B_{ij} is antisymmetric. In addition, due to the fact that the background is stationary, the operators A_{ij}, B_{ij} and C_{ij} are time independent. It follows that if ξ^i is a solution to equation (2.28), $\partial_t \xi^i$ is also a solution, since the operators A_{ij}, B_{ij} and C_{ij} commute with the time derivative, and $W(\partial_t \xi, \eta)$ is also a conserved quantity. Expressing the perturbation in cylindrical coordinates:

$$\xi^i = \xi^i(\varpi, \theta) e^{i(\omega t + m\phi)}, \tag{2.33}$$

[2] We express conjugate momentum, using the result from Chandrasekhar [14] and later from Lynden-Bell and Ostriker [15], who have derived the equation of motion (2.28) using a variational principle, with action:

$$S = \int L dV = \frac{1}{2} \int (\dot{\xi}_i A_{ij} \dot{\xi}^j + \dot{\xi}_i B_{ij} \xi^j - \xi_i C_{ij} \xi^j) dV. \tag{2.29}$$

we can compute the canonical energy of the displacement:

$$\begin{aligned}
E_c(\xi) &= \frac{1}{2}W(\dot{\xi},\xi) \\
&= \frac{1}{2}\langle\dot{\xi},A\dot{\xi}\rangle + \frac{1}{2}\langle\xi,B\xi\rangle - \frac{1}{2}\langle A\ddot{\xi}\rangle + \frac{1}{2}\langle B\dot{\xi},\xi\rangle \\
&= \frac{1}{2}\langle\dot{\xi},A\dot{\xi}\rangle - \frac{1}{2}\langle A\ddot{\xi},\xi\rangle + \frac{1}{4}\langle\dot{\xi},B\xi\rangle - \frac{1}{4}\langle B\dot{\xi},\xi\rangle \\
&= \frac{1}{2}(-i\omega^*)(i\omega)\langle\xi,A\xi\rangle - \frac{1}{2}(-\omega^*)^2\langle A\xi,\xi\rangle + \frac{1}{4}(-i\omega^*)\langle\xi,B\xi\rangle - \frac{1}{4}(-i\omega^*)\langle B\xi,\xi\rangle \\
&= \frac{1}{2}\left(\omega\omega^*\langle\xi,A\xi\rangle + (\omega^*)^2\langle\xi,A\xi\rangle\right) - \frac{1}{2}i\omega^*\langle\xi,B\xi\rangle \\
&= \frac{1}{2}\omega^*(\omega+\omega^*)\langle\xi,A\xi\rangle - \frac{1}{2}i\omega^*\langle\xi,B\xi\rangle.
\end{aligned}$$

The canonical energy of the system must be a real number, therefore we write it as:

$$E_c(\xi) = \omega^*\left(\mathrm{Re}(\omega)\langle\xi,A\xi\rangle - \frac{1}{2}\langle\xi,iB\xi\rangle\right), \tag{2.34}$$

or, equivalently, substituting the operators A^i_j and B^i_j:

$$E_c(\xi) = \omega^*\left(\mathrm{Re}(\omega)\langle\xi,\rho\xi\rangle - \langle\xi,i\rho u^j\nabla_j\xi\rangle\right), \tag{2.35}$$

where the expression in the parenthesis is real. The fact that the canonical energy of the mode must be a real quantity, implies that ω must be a real number, otherwise $E_c = 0$. This result can be interpreted in other words as follows; if the quantity E_c is conserved and we have an exponentially growing or dampening mode, then the only scenario where this can happen, is if $E_c = 0$.

Similarly, if the equilibrium configuration is axisymmetric with respect to a rotational vector ϕ^i, we can derive the canonical angular momentum of the mode ξ^i mentioned above:

$$\begin{aligned}
J_c(\xi) &= -\frac{1}{2}W(\partial_\phi\xi,\xi) \\
&= -\frac{1}{2}\left\{\langle\partial_\phi\xi,A\dot{\xi}+\frac{1}{2}B\xi\rangle - \langle A(\partial_\phi\dot{\xi}) + \frac{1}{2}B(\partial_\phi\xi),\xi\rangle\right\} \\
&= -\frac{1}{2}\left\{\langle\partial_\phi\xi,A\dot{\xi}\rangle + \frac{1}{2}\langle\partial_\phi\xi,B\xi\rangle - \langle A(\partial_\phi\dot{\xi}),\xi\rangle - \frac{1}{2}\langle B(\partial_\phi\xi),\xi\rangle\right\} \\
&= -\frac{1}{2}\left\{(-im)(i\omega)\langle\xi,A\xi\rangle + \frac{1}{2}(-im)\langle\xi,B\xi\rangle - (-m\omega^*)\langle A\xi,\xi\rangle - \frac{1}{2}(-im)\langle B\xi,\xi\rangle\right\} \\
&= -\frac{1}{2}\left\{m\omega\langle\xi,A\xi\rangle - \frac{1}{2}im\langle\xi,B\xi\rangle + m\omega^*\langle A\xi,\xi\rangle + \frac{1}{2}im\langle B\xi,\xi\rangle\right\} \\
&= -\frac{1}{2}m\left\{(\omega+\omega^*)\langle\xi,A\xi\rangle - \langle\xi,iB\xi\rangle\right\} \rightarrow \\
&\qquad J_c = -m\{\mathrm{Re}(\omega)\langle\xi,A\xi\rangle - \frac{1}{2}\langle\xi,iB\xi\rangle\}
\end{aligned}$$

or

$$J_c = -m\{\mathrm{Re}(\omega)\langle\xi,\rho\xi\rangle - \langle\xi,i\rho u^j\nabla_j\xi\rangle\}. \tag{2.36}$$

Again, $J_c = 0$ if ω is not real.

2.3 The onset of instability

For real frequency modes, we can write the pattern speed of the mode, i.e. the angular velocity of surfaces of constant phase:

$$\frac{E_c}{J_c} = -\frac{\omega}{m} \equiv \sigma_p. \tag{2.37}$$

Using equation (2.35), the above equation an be rewritten as:

$$\begin{aligned} J_c &= \frac{\omega^2\langle\xi,\rho\xi\rangle - \omega\langle\xi, i\rho u^j\nabla_j\xi\rangle}{\sigma_p} \quad \rightarrow \\ J_c &= -m\omega\langle\xi,\rho\xi\rangle + m\langle\xi, i\rho u^j\nabla_j\xi\rangle \quad \rightarrow \\ \frac{J_c}{\langle\xi,\rho\xi\rangle} &= -m\omega + m\frac{\langle\xi, i\rho u^j\nabla_j\xi\rangle}{\langle\xi,\rho\xi\rangle}. \end{aligned} \tag{2.38}$$

At this point, we will express our vectors in cylindrical coordinates,

$$u^i = (u^\varpi, u^\phi, u^z) = (0, \Omega\varpi, 0),$$

assuming uniform rotation and we also assume that the displacement vector can be written as $\xi^i = (\xi^\varpi(\varpi), \xi^\phi(\phi), \xi^z(z))$. Under these assumptions, we can estimate the quantity that appears in the inner product of equation (2.38):

$$\langle\xi, i\rho u^j\nabla_j\xi\rangle \quad = \int_V i\rho\xi_i^* u^j\nabla_j\xi^i dV.$$

First, we have:

$$\begin{aligned} u^j\nabla_j\xi^i &= \left[u_\varpi\frac{\partial\xi^\varpi}{\partial\varpi} + \frac{1}{\varpi}\frac{\partial\xi^\varpi}{\partial\phi} + u_z\frac{\partial\xi^\varpi}{\partial z} - \frac{1}{\varpi}u_\phi\xi^\phi\right]\hat{\varpi} + \\ &\quad + \left[u_\varpi\frac{\partial\xi^\phi}{\partial\varpi} + \frac{1}{\varpi}u_\phi\frac{\partial\xi^\phi}{\partial\phi} + u_z\frac{\partial\xi^\phi}{\partial z} + \frac{1}{\varpi}u_\phi\xi^\varpi\right]\hat{\phi} + \\ &\quad + \left[u_\varpi\frac{\partial\xi^z}{\partial\varpi} + \frac{1}{\varpi}u_\phi\frac{\partial\xi^z}{\partial\phi} + u_z\frac{\partial\xi^z}{\partial z}\right]\hat{z} \\ &= -\frac{1}{\varpi}u_\phi\xi^\phi\hat{\varpi} + \left(\frac{1}{\varpi}u_\phi\frac{\partial\xi^\phi}{\partial\phi} + \frac{1}{\varpi}u_\phi\xi^\varpi\right)\hat{\phi} \rightarrow \\ u^j\nabla_j\xi^i &= -\frac{1}{\varpi}u_\phi\xi^\phi\delta^i_\varpi + \frac{1}{\varpi}u_\phi\frac{\partial\xi^\phi}{\partial\phi}\delta^i_\phi + \frac{1}{\varpi}u_\phi\xi^\varpi\delta^i_\phi, \end{aligned}$$

where δ^i_j is Kronecker delta. Constructing the aforementioned quantity inside the integral, we have:

$$\begin{aligned}\xi_i^* u^j \nabla_j \xi^i &= -\frac{1}{\varpi} u_\phi \xi^\phi (\xi^\varpi)^* + \frac{1}{\varpi} u_\phi \frac{\partial \xi^\phi}{\partial \phi} (\xi^\phi)^* + \frac{1}{\varpi} u_\phi \xi^\varpi (\xi^\phi)^* \\ &= \frac{1}{\varpi} u_\phi [\xi^\varpi (\xi^\phi)^* - \xi^\phi (\xi^\varpi)^*] + \frac{1}{\varpi} u_\phi i m \|\xi\|^2 \\ &= \frac{1}{\varpi} u_\phi [i m \|\xi\|^2 + (\xi^* \times \xi)_z] \rightarrow \end{aligned}$$

$$-i\rho \xi_i^* u^j \nabla_j \xi^i = \rho \Omega [m\|\xi\|^2 + i(\xi^* \times \xi)_z]. \tag{2.39}$$

However, from Schwartz inequality we know that:

$$\|(\xi^* \times \xi)_z\| \leq \|\xi\|^2, \tag{2.40}$$

so,

$$\begin{aligned}\rho\Omega(m\|\xi\|^2 - \|\xi\|^2) \leq -i\rho\xi_i^* u^j \nabla_j \xi^i \leq \rho\Omega(m\|\xi\|^2 + \|\xi\|^2) \\ \Omega(m-1) \leq \frac{-\langle \xi, i\rho u^j \nabla_j \xi\rangle}{\langle \xi, \rho\xi\rangle} \leq \Omega(m+1) \\ -m\Omega(m+1) \leq \frac{m\langle \xi, i\rho u^j \nabla_j \xi\rangle}{\langle \xi, \rho\xi\rangle} \leq -m\Omega(m-1) \\ -m\omega - m\Omega(m+1) \leq -m\omega + \frac{m\langle \xi, i\rho u^j \nabla_j \xi\rangle}{\langle \xi, \rho\xi\rangle} \leq -m\omega - m\Omega(m-1) \\ -m\omega - m\Omega(m+1) \leq \frac{J_c}{\langle \xi, \rho\xi\rangle} \leq -m\omega - m\Omega(m-1) \\ \sigma_p - \Omega\left(1 + \frac{1}{m}\right) \leq \frac{J_c/m^2}{\langle \xi, \rho\xi\rangle} \leq \sigma_p - \Omega\left(1 - \frac{1}{m}\right).\end{aligned} \tag{2.41}$$

Relation (2.41) is very helpful to demonstrate that rotating perfect fluid stars are generically unstable in the presence of radiation. To begin with, let us consider a very slowly rotating star, i.e. in the limit $\Omega \to 0$, as seen by an inertial distant observer, and a normal mode with finite frequency, so that $\omega \neq 0$. For any $m > 0$ the normal modes divide naturally in two classes, co-rotating ($\sigma_p > 0$) and counter-rotating ($\sigma_p < 0$). In this regime, we can assume that the quantity $1/m \equiv \epsilon$ is a small number and relation (2.41) is rewritten:

$$\begin{aligned}\sigma_p - \Omega(1+\epsilon) \leq \frac{J_c/m^2}{\langle \xi, \rho\xi\rangle} \leq \sigma_p - \Omega(1-\epsilon) \\ \sigma_p - \Omega\epsilon \leq \frac{J_c/m^2}{\langle \xi, \rho\xi\rangle} \leq \sigma_p + \Omega\epsilon,\end{aligned} \tag{2.42}$$

where $0 < \Omega\epsilon \ll 1$. Relation (2.42) implies that for co-rotating modes, i.e. $\sigma_p > 0$, we also have $J_c > 0$ and by virtue of equation (2.37), $E_c > 0$. For counter-rotating modes, $\sigma_p < 0$ and once more, from the relations (2.42) and (2.37) we find that $J_c < 0$ and $E_c > 0$, respectively. Both of these modes have positive canonical energy, thus they are stable.

Further on, at the onset of instability in a mode, its frequency and equivalently its pattern speed vanishes. So, let us consider a small region near a point, where $\sigma_p = 0$ at a finite rotation rate ($\Omega \neq 0$). Typically, this corresponds to a point where the initially counter-rotating mode becomes co-rotating. Relation (2.41) is now written as:

$$-\Omega(1+\epsilon) \leq \frac{J_c/m^2}{\langle \xi, \rho\xi \rangle} \leq -\Omega(1-\epsilon). \tag{2.43}$$

In this regime, the canonical angular momentum is negative $J_c < 0$, as a result of relation (2.43), while $E_c = 0$ in virtue of equation (2.37). Prior to this point of instability, $E_c > 0$ and beyond this point $E_c < 0$. So, the canonical energy will change sign at the point where σ_p vanishes and since the mode was stable in the non-rotating limit, this change of sign indicates the onset of instability at a critical rotation rate Ω. As a result, the instability sets in when a counter-rotating mode (stable) becomes co-rotating (unstable) and this is happening when the angular velocity ω_p exceeds the mode's pattern speed in the rotating frame ω_r,

$$\Omega > \frac{\omega_r}{m}. \tag{2.44}$$

2.4 Gravitational radiation-driven secular instability

Secular instabilities, require a dissipation mechanism coupled to the fluid. This dissipation mechanism is associated with electromagnetic or gravitational wave emission and viscosity. We will assume that the secular instability is only caused by gravitational radiation, but similar results hold true when there is another operational mechanism. The reason why we will only consider the case of gravitational wave-driven instabilities, is because gravitational radiation is almost always the dominant mechanism leading to the CFS secular instability.

In linearized perturbation theory, unstable non-axisymmetric perturbations of an axisymmetric background will grow without bound, radiating infinite energy. On the other hand, stable perturbations radiate finite amount of energy before they eventually settle down to the previously axisymmetric configuration.

The canonical energy we derived in a previous section, given by (2.34), depends only on the initial data $(\xi, \dot{\xi})$ of the perturbation at a given time. The condition for stability in terms of canonical energy can be phrased as following:

- If $E_c < 0$ for some initial conditions $(\xi, \dot{\xi})$, then the configuration is unstable or marginally unstable. One can find non-axisymmetric perturbations that will not die away with time.
- If $E_c \geq 0$ for all initial conditions $(\xi, \dot{\xi})$, the configuration is stable in the sense that no perturbation radiates infinite energy, so the value of E_c is bounded.

When dissipation is present, the equation of motion (2.28) is written

$$A_{ij}\partial_t^2 \xi^j + B_{ij}\partial_t \xi^j + C_{ij}\xi^j = F_i, \tag{2.45}$$

where the extra term F_i represents the radiation force. In this case the canonical energy and angular momentum will no longer be conserved quantities, but their time dependence will be given by

$$\frac{dE_c}{dt} = \mathrm{Re}\langle \partial_t \xi, F \rangle, \tag{2.46}$$

$$\frac{dJ_c}{dt} = \mathrm{Re}\langle \partial_\phi \xi, F \rangle. \tag{2.47}$$

Similar to the dissipationless case we examined at the beginning, when we introduce solutions to equation (2.45), having harmonic time dependence, to equations (2.46) and (2.47), we obtain the pattern speed

$$\frac{\dot{E}_c}{\dot{J}_c} = \sigma_p, \tag{2.48}$$

and in this case, σ_p may also be complex.

Since $\dot{E}_c < 0$ for any radiative solution to the perturbation equations, no radiative oscillation which has harmonic time dependence can have purely real frequency. The complex part is responsible for the excitation of unstable modes, leading to the instability.

Chapter 3

Gravitational waves

In this chapter, we will examine some fundamental aspects of Einstein's theory of General Relativity, in order to study the generation of gravitational waves from isolated neutron stars. We will use the linear approximation, in order to derive the Einstein's equation in the weak field approximation. To do so, we will use the Einstein notation to describe the physical parameters and express the equations involved. Greek small letters in indices are used to represent only the space coordinates, for example the Cartesian coordinates x, y, z and take the values $1, 2, 3$, while English small letters represent the spacetime coordinates t, x, y, z or in general $0, 1, 2, 3$.

3.1 Introduction

Gravitational waves are small deformations of spacetime, traveling at the speed of light. They are a fundamental consequence of Einstein's General theory of Relativity, and are similar to the electromagnetic radiation, in the context that gravitational waves transport energy and propagate at the speed of light. The most powerful gravitational waves are emitted in the latest stages of the merging process of massive compact objects, i.e. black holes, neutron stars and white dwarfs.

The existence of gravitational waves was theoretically predicted in the early 1900s, but the technology was then far from being able to detect them. The first indirect evidence of their existence came in 1974 when Hulse and Taylor discovered the first binary neutron star system, which was named after them. Using pulsar timing observations, it is evident that the system's orbit is decaying with time, and this decay matches the energy and angular momentum losses due to gravitational wave emission, as predicted by General Relativity. However, the first direct detection of gravitational waves happened in 2015, when the LIGO interferometers detected the gravitational wave from the merging of two black holes, with masses around $36M_{\odot}$ and $29M_{\odot}$ respectively. Since the first signal, according to the last catalogue published by LIGO and VIRGO collaboration [16], the total amount of gravitational wave signals detected has risen to twenty. Apart from one binary neutron star system, the rest of the signals originate from binary black hole systems.

Besides binary systems, which produce the most powerful gravitational waves that current detectors are capable of detecting, there are many other gravitational wave sources that could be detected in the future with the next generation of detectors. Among these sources are spinning neutron stars with time-dependent quadrupole moment, supernovae explosions and the inflation epoch of the early Universe.

3.2 Linearization of Einstein's equations

We will begin with the Einsten's equation in geometrized units, where $c = G = 1$,

$$G^{\mu\nu} = 8\pi T^{\mu\nu}, \tag{3.1}$$

where $G^{\mu\nu}$ is the Einstein's tensor and describes the geometry of spacetime, and $T^{\mu\nu}$ describes the distribution and motion of masses. In order to derive the equations of describing a weak gravitational field, we will linearize our theory. This assumption is valid, since in the absence of gravity, the spacetime is flat. As a result, a weak gravitational field will distort so slightly the spacetime, that we can assume it is nearly flat. This allows us to split our metric $g_{\alpha\beta}$ to two components; $\eta_{\alpha\beta}$ corresponding to the flat spacetime; i.e. a Minkowski background spacetime, and $h_{\alpha\beta}$, which describes the small perturbations of the flat spacetime,

$$g_{\alpha\beta} = \eta_{\alpha\beta} + h_{\alpha\beta}. \tag{3.2}$$

At this point, it should be emphasized that we have taken $\|h_{\alpha\beta}\| \ll 1$, so that we can construct the linearized equations using the methods of perturbation theory.

We will calculate the terms involved in equation (3.1), and see the form they take when we impose a weak gravitational field, starting from $G^{\mu\nu}$. In order to linearize $G^{\mu\nu}$, first we have to calculate the Riemann curvature tensor, as it describes the intrinsic curvature of spacetime. The Riemann curvature tensor is given from the expression,

$$R^{\alpha}_{\beta\mu\nu} = \Gamma^{\alpha}_{\beta\nu,\mu} - \Gamma^{\alpha}_{\beta\mu,\nu} + \Gamma^{\alpha}_{\sigma\mu}\Gamma^{\sigma}_{\beta\nu} - \Gamma^{\alpha}_{\sigma\nu}\Gamma^{\sigma}_{\beta\mu}, \tag{3.3}$$

where $\Gamma^{\alpha}_{\mu\nu}$ are the Christoffel symbols,

$$\Gamma^{\alpha}_{\mu\nu} = \frac{1}{2}g^{\alpha\beta}(g_{\beta\mu,\nu} + g_{\beta\nu,\mu} - g_{\mu\nu,\beta}). \tag{3.4}$$

Calculating the partial derivatives of the Christoffel symbols, we have that

$$\Gamma^{\alpha}_{\mu\nu,\sigma} = \frac{1}{2}g^{\alpha\beta}(g_{\beta\mu,\nu\sigma} + g_{\beta\nu,\mu\sigma} - g_{\mu\nu,\beta\sigma}). \tag{3.5}$$

So, inserting equations (3.4) and (3.5) to equation (3.3), we have

$$\begin{aligned} R^{\alpha}_{\beta\mu\nu} = {} & \frac{1}{2}g^{\alpha\sigma}(g_{\sigma\beta,\nu\mu} + g_{\sigma\nu,\beta\mu} - g_{\beta\nu,\sigma\mu}) + \frac{1}{2}g^{\alpha\sigma}(g_{\sigma\beta,\mu\nu} + g_{\sigma\mu,\beta\nu} - g_{\beta\mu,\sigma\nu}) \\ & + \frac{1}{4}g^{\alpha\beta}(g_{\beta\sigma,\mu} + g_{\beta\mu,\sigma} - g_{\sigma\mu,\beta})g^{\sigma\alpha}(g_{\alpha\beta,\nu} + g_{\alpha\nu,\beta} - g_{\beta\nu,\alpha}) \\ & - \frac{1}{4}g^{\alpha\beta}(g_{\beta\sigma,\nu} + g_{\beta\nu,\sigma} - g_{\sigma\nu,\beta})g^{\sigma\alpha}(g_{\alpha\beta,\mu} + g_{\alpha\mu,\beta} - g_{\beta\mu,\alpha}). \end{aligned} \tag{3.6}$$

If we can interchange the index ν with μ, in the last line of equation (3.6), it is easy to see that we end up with the same expression as the line above it, so the terms cancel with each other, leading to the expression

$$R^{\alpha}_{\beta\mu\nu} = \frac{1}{2}g^{\alpha\sigma}(g_{\sigma\beta,\nu\mu} + g_{\sigma\nu,\beta\mu} - g_{\beta\nu,\sigma\mu} - g_{\sigma\beta,\mu\nu} - g_{\sigma\mu,\beta\nu} + g_{\beta\mu,\sigma\nu}). \tag{3.7}$$

Now, using the symmetry of $g_{\alpha\beta}$ and the fact that partial derivatives always commute,

$$g_{\alpha\beta,\mu\nu} = g_{\alpha\beta,\nu\mu}, \tag{3.8}$$

the Riemann curvature tensor can be written as

$$R^{\alpha}_{\beta\mu\nu} = \frac{1}{2}g^{\alpha\sigma}(g_{\sigma\nu,\beta\mu} - g_{\beta\nu,\sigma\mu} - g_{\sigma\mu,\beta\nu} + g_{\beta\mu,\sigma\nu}) \qquad \text{and} \tag{3.9}$$

$$R_{\alpha\beta\mu\nu} = g_{\alpha\lambda}R^{\lambda}_{\beta\mu\nu}. \tag{3.10}$$

Ultimately, we want to find the linearized expression of the Riemann curvature tensor, in the weak gravitational field approximation. As a result, our next step is to insert the metric (3.2) to equation (3.9), which yields

$$\begin{aligned}
R_{\alpha\beta\mu\nu} &= g_{\alpha\lambda}R^{\lambda}_{\beta\mu\nu} \\
&= \frac{1}{2}g_{\alpha\lambda}g^{\lambda\sigma}(\cancelto{0}{\eta_{\sigma\nu,\beta\mu}} + h_{\sigma\nu,\beta\mu} - \cancelto{0}{\eta_{\beta\nu,\sigma\mu}} - h_{\beta\nu,\sigma\mu} - \cancelto{0}{\eta_{\sigma\mu,\beta\nu}} - h_{\sigma\mu,\beta\nu} + \cancelto{0}{\eta_{\beta\mu,\sigma\nu}} + h_{\beta\mu,\sigma\nu}) \\
&= \frac{1}{2}g^{\sigma}_{\alpha}(h_{\sigma\nu,\beta\mu} - h_{\beta\nu,\sigma\mu} - h_{\sigma\mu,\beta\nu} + h_{\beta\mu,\sigma\nu}) \\
&= \frac{1}{2}(\eta^{\sigma}_{\alpha} + h^{\sigma}_{\alpha})(h_{\sigma\nu,\beta\mu} - h_{\beta\nu,\sigma\mu} - h_{\sigma\mu,\beta\nu} + h_{\beta\mu,\sigma\nu}),
\end{aligned}$$

and keeping only the first-order terms with respect to $h_{\mu\nu}$ we have,

$$R_{\alpha\beta\mu\nu} = \frac{1}{2}(h_{\alpha\nu,\beta\mu} - h_{\beta\nu,\alpha\mu} - h_{\alpha\mu,\beta\nu} + h_{\beta\mu,\alpha\nu}). \tag{3.11}$$

Now, the Einstein tensor is by definition dependent on the Riemann curvature tensor, through the equation

$$G^{\alpha\beta} = R^{\alpha\beta} - \frac{1}{2}g^{\alpha\beta}R, \tag{3.12}$$

where R is the Ricci scalar, given by

$$R = g^{\alpha\beta}R_{\alpha\beta} = g^{\alpha\beta}g^{\mu\nu}R_{\mu\alpha\nu\beta}, \tag{3.13}$$

and

$$R_{\alpha\beta} = R^{\mu}_{\alpha\mu\beta}, \tag{3.14}$$

which is the Ricci tensor. We will now derive the linearized expression for the Ricci tensor. From equation (3.9) we have,

$$\begin{aligned}
R^{\alpha}{}_{\beta\mu\nu} &= \frac{1}{2}\eta^{\alpha\sigma}(h_{\sigma\nu,\beta\mu} - h_{\beta\nu,\sigma\mu} - h_{\sigma\mu,\beta\nu} + h_{\beta\mu,\sigma\nu}) \\
&= \frac{1}{2}(h^{\alpha}{}_{\nu,\beta\mu} - h_{\beta\nu}{}^{,\alpha}{}_{,\mu} - h^{\alpha}{}_{\mu,\beta\nu} + h_{\beta\mu}{}^{,\alpha}{}_{,\nu}),
\end{aligned} \tag{3.15}$$

so

$$R_{\alpha\beta} = R^{\mu}{}_{\alpha\mu\beta} = \frac{1}{2}(h^{\mu}{}_{\beta,\alpha\mu} - h_{\alpha\beta}{}^{,\mu}{}_{,\mu} - h^{\mu}{}_{\mu,\alpha\beta} + h_{\alpha\mu}{}^{,\mu}{}_{,\beta}). \tag{3.16}$$

The expression above can be somewhat simplified, by inserting the trace $h = h^{\alpha}{}_{\alpha}$ and the D' Alembertian, or wave operator, $\Box = \partial^{\alpha}\partial_{\alpha}$. As a result, the Ricci tensor can be rewritten as,

$$R_{\alpha\beta} = \frac{1}{2}(h^{\mu}{}_{\beta,\alpha\mu} - \Box h_{\alpha\beta} - h_{,\alpha\beta} + h_{\alpha\mu}{}^{,\mu}{}_{,\beta}). \tag{3.17}$$

As for the Ricci scalar, we have

$$\begin{aligned} R &= g^{\alpha\beta}R_{\alpha\beta} = \eta^{\alpha\beta}R_{\alpha\beta} \\ &= \frac{1}{2}\eta^{\alpha\beta}(h^{\mu}{}_{\beta,\alpha\mu} - \Box h_{\alpha\beta} - h_{,\alpha\beta} + h_{\alpha\mu}{}^{,\mu}{}_{,\beta}) \\ &= \frac{1}{2}(h^{\alpha\mu}{}_{,\alpha\mu} - \Box h^{\alpha}{}_{\alpha} - h^{\alpha}{}_{,\alpha} + h_{\alpha\mu}{}^{,\alpha\mu}) \\ &= \frac{1}{2}(h^{\alpha\mu}{}_{,\alpha\mu} - \Box h - \Box h + h^{\alpha\mu}{}_{\alpha\mu}) \\ R &= h^{\alpha\mu}{}_{,\alpha\mu} - \Box h. \end{aligned} \tag{3.18}$$

Combining equations (3.17) and (3.18) and introducing them to (3.12), the linearized Einstein's tensor, is calculated to be

$$\begin{aligned} G_{\alpha\beta} &= R_{\alpha\beta} - \frac{1}{2}g_{\alpha\beta}R = R_{\alpha\beta} - \frac{1}{2}\eta_{\alpha\beta}R \\ &= \frac{1}{2}(h^{\mu}{}_{\beta,\alpha\mu} - \Box h_{\alpha\beta} - h_{,\alpha\beta} + h_{\alpha\mu}{}^{,\mu}{}_{,\beta} - \eta_{\alpha\beta}h^{\nu\mu}{}_{,\nu\mu} - \eta_{\alpha\beta}\Box h). \end{aligned} \tag{3.19}$$

Finally, the linearized Einstein's equation is given by

$$h^{\mu}{}_{\beta,\alpha\mu} - \Box h_{\alpha\beta} - h_{,\alpha\beta} + h_{\alpha\mu}{}^{,\mu}{}_{,\beta} - \eta_{\alpha\beta}h^{\nu\mu}{}_{,\nu\mu} - \eta_{\alpha\beta}\Box h = 16\pi T_{\alpha\beta}. \tag{3.20}$$

However, equation (3.20) seems to be cumbersome, so we will endeavor to simplify its form, by introducing some transformations. To begin with, we define the trace-reversed metric perturbation tensor,

$$\bar{h}_{\alpha\beta} = h_{\alpha\beta} - \frac{1}{2}\eta_{\alpha\beta}h \quad \rightarrow \quad h_{\alpha\beta} = \bar{h}_{\alpha\beta} - \frac{1}{2}\eta_{\alpha\beta}\bar{h}, \tag{3.21}$$

where $\bar{h} = \bar{h}^{\alpha}{}_{\alpha} = -h$, hence the name of the variable. This new quantity, $\bar{h}_{\alpha\beta}$ is actually describing the weak gravitational field.

Under this transformation, equation (3.19) is now rewritten,

$$\begin{aligned} G_{\alpha\beta} &= \bar{h}^{\mu}{}_{\beta,\mu\alpha} - \Box\bar{h}_{\alpha\beta} + \frac{1}{2}\eta_{\alpha\beta}\Box\bar{h} - \bar{h}_{,\alpha\beta} + \bar{h}_{\alpha\mu}{}^{,\mu}{}_{,\beta} - \eta_{\alpha\beta}\bar{h}^{\mu\nu}{}_{,\mu\nu} - \eta_{\alpha\beta}\Box\bar{h} + \frac{1}{2}\eta_{\alpha\beta}\Box\bar{h} \\ &= -\Box\bar{h}_{\alpha\beta} + \bar{h}_{\beta\mu}{}^{,\mu}{}_{,\alpha} + \bar{h}_{\alpha\mu}{}^{,\mu}{}_{,\beta} - \eta_{\alpha\beta}\bar{h}^{\mu\nu}{}_{,\mu\nu}. \end{aligned} \tag{3.22}$$

The next step in order to simplify as much as possible the expression for $G_{\alpha\beta}$ in the weak gravitational field approximation, is to choose a suitable gauge transformation. It can

be shown that equation (3.22) obtains its simplest form, if we assume that $h_{\alpha\beta}$ satisfies the condition

$$\bar{h}^{\alpha\beta}{}_{,\beta} = 0. \tag{3.23}$$

This is often called the Lorentz gauge condition, by analogy with electromagnetism. As a consequence, inserting the aforementioned gauge condition to equation (3.22), it is trivial to find that $G_{\alpha\beta}$ is

$$G^{\mu\nu} = \Box\bar{h}^{\mu\nu}, \tag{3.24}$$

and the Einstein's equation (3.1) that we started with, can now be rewritten as

$$\Box\bar{h}^{\mu\nu} = 16\pi T^{\mu\nu}, \tag{3.25}$$

or equivalently, if we substitute the form of the D' Alembertian operator,

$$\left(-\frac{\partial^2}{\partial t^2} + \nabla^2\right)\bar{h}^{\mu\nu} = -16\pi T^{\mu\nu}, \tag{3.26}$$

which is the wave equation. We will see in the following paragraph that the solutions to equation (3.26) are gravitational perturbations that propagate in empty space, traveling at the speed of light, similar to the ones of electromagnetism. Once again, it should be noted that $h_{\mu\nu}$ is the metric perturbation and $\bar{h}_{\mu\nu}$ is a tensor quantity related to $h_{\mu\nu}$.

3.3 The generation of gravitational waves

In this section, we aim to solve equation (3.26) and use the results to calculate a few characteristics of gravitational waves. In this attempt, we will make a few assumptions that will not greatly affect the results, however they will simplify our calculations. Our first assumption is about the time-dependent part of $T^{\mu\nu}$, which we will assume to be described by a sinusoidal oscillation with frequency ω. That is interpreted as taking the real part of the equation

$$T_{\mu\nu} = S_{\mu\nu}(x^j)e^{-i\omega t}. \tag{3.27}$$

This assumption is logical, since it is possible to convert any time-dependent function, to a sum of sines and cosines through Fourier analysis. The second assumption that we make, is that the typical velocity inside the area that the gravitational waves are generated, is less that the speed of light, i.e. in our geometrized units $\omega l \ll 1$, where l denotes the size of the source region.

Having stated our assumptions above, we are now ready to look for solutions to the wave equation (3.26). Similar to electromagnetism, we look for a solution for $\bar{h}_{\mu\nu}$ of the form

$$\bar{h}_{\mu\nu} = B_{\mu\nu}(x^j)e^{-i\omega t}. \tag{3.28}$$

At the end, we will keep only the real part of relation (3.28), in order to be consistent with equations (3.26) and the initial assumption we stated at the beginning of this section.

Substituting equations (3.27) and (3.28) to equation (3.26), we have

$$\left(-\frac{\partial^2}{\partial t^2}+\nabla^2\right)B_{\mu\nu}(x^j)e^{-i\omega t}=-16\pi S_{\mu\nu}(x^j)e^{-i\omega t} \qquad \rightarrow$$
$$(\omega^2+\nabla^2)B_{\mu\nu}(x^j)=-16\pi S_{\mu\nu}(x^j) \tag{3.29}$$

The source is extended in the region where $S_{\mu\nu}\neq 0$. We choose the origin of our coordinate system to lie inside the source, and define r as the radial polar coordinate. On the region outside the source, the solution we derive for $B_{\mu\nu}$ from equation (3.29) is

$$B_{\mu\nu}=\frac{A_{\mu\nu}}{r}e^{i\omega r}+\frac{Z_{\mu\nu}}{r}e^{-i\omega r}, \tag{3.30}$$

where $A_{\mu\nu}$ and $Z_{\mu\nu}$ are constants. The first term represents an outgoing traveling wave, while the second term corresponds to an ingoing wave. Since we are concerned with waves generated from the source, we ignore the ingoing term and set $Z_{\mu\nu}=0$. As a result, the relation giving $B_{\mu\nu}$ outside the source is,

$$B_{\mu\nu}=\frac{A_{\mu\nu}}{r}e^{i\omega r}. \tag{3.31}$$

If the source is nonzero only inside a sphere of radius $\epsilon \ll \frac{2\pi}{\omega}$, and integrate equation (3.29), we get

$$\int(\omega^2+\nabla^2)B_{\mu\nu}d^3x=-16\pi\int S_{\mu\nu}d^3x$$
$$\int\omega^2 B_{\mu\nu}d^3x+\int\nabla^2 B_{\mu\nu}d^3x=-16\pi\int S_{\mu\nu}d^3x. \tag{3.32}$$

We will integrate each term individually. For the first term we calculate that

$$\int\omega^2 B_{\mu\nu}d^3x\leq\omega^2\|B_{\mu\nu\,\max}\|\frac{4\pi}{3}\epsilon^3, \tag{3.33}$$

where $B_{\mu\nu\,\max}$ is the maximum value that $B_{\mu\nu}$ takes inside the source. The second term, using Gauss's theorem to reduce the volume integral to a surface integral, along with the relation (3.31), yields

$$\int\nabla^2 B_{\mu\nu}d^3x=\oint_S\mathbf{n}\cdot\nabla B_{\mu\nu}dS=\oint_S\frac{dB_{\mu\nu}}{dr}\Big|_{r=\epsilon}dS=\left(-\frac{A_{\mu\nu}e^{i\omega\epsilon}}{\epsilon^2}+\frac{A_{\mu\nu}}{\epsilon}i\omega e^{i\omega\epsilon}\right)4\pi\epsilon^2$$
$$\int\nabla^2 B_{\mu\nu}d^3x=-4\pi A_{\mu\nu}e^{i\omega\epsilon}(1-i\omega\epsilon). \tag{3.34}$$

For the last term, we define

$$J_{\mu\nu}=\int S_{\mu\nu}d^3x, \tag{3.35}$$

and we can easily see that it is related to $T_{\mu\nu}$ tensor, by

$$J_{\mu\nu}e^{-i\omega t} = \int S_{\mu\nu}e^{-i\omega t}d^3x = \int T_{\mu\nu}d^3x. \tag{3.36}$$

Combining the equations (3.29), (3.34) and (3.35), we have

$$\int \omega^2 B_{\mu\nu}d^3x - 4\pi A_{\mu\nu}e^{i\omega\epsilon}(1 - i\omega\epsilon) = -16\pi J_{\mu\nu}. \tag{3.37}$$

In the limit $\epsilon \to 0$, the first term, by virtue of equation (3.33), disappears, so the above relation yields

$$A_{\mu\nu} = 4J_{\mu\nu}. \tag{3.38}$$

This leads to

$$B_{\mu\nu} = \frac{4J_{\mu\nu}}{r}e^{i\omega r} \tag{3.39}$$

and consequently, from equation (3.28),

$$\bar{h}_{\mu\nu} = \frac{4J_{\mu\nu}}{r}e^{i\omega(r-t)}. \tag{3.40}$$

In the last few calculations, we have been treating $\bar{h}_{\mu\nu}$ as an arbitrary function. However, the truth is that $\{\bar{h}_{\mu\nu}\}$ are components of a single tensor, thus we should start taking this under consideration. Calculating the time derivative of equation (3.36), we have that

$$-i\omega J^{\mu 0}e^{-i\omega t} = \int T^{\mu 0}{}_{,0}\, d^3x \tag{3.41}$$

The conservation of mass and energy in General theory of Relativity, is expressed through the conservation of $T^{\mu\nu}$, thus we have

$$T^{\mu\nu}{}_{,\nu} = 0 \quad \to \quad T^{\mu 0}{}_{,0} = -T^{\mu\kappa}{}_{,\kappa}\,. \tag{3.42}$$

Substituting equation (3.42) to (3.41), we have

$$i\omega J^{\mu 0}e^{-i\omega t} = \int T^{\mu\kappa}{}_{,\kappa}\, d^3x, \tag{3.43}$$

and once again, using Gauss's theorem for the right-hand side we obtain

$$i\omega J^{\mu 0}e^{-i\omega t} = \oint_S n_\kappa T^{\mu\kappa} dS. \tag{3.44}$$

The surface integral of equation (3.44) is to be calculated at the surface of an arbitrary volume that fully contains the source. This implies that on the boundary surface of this volume, where we have to calculate the integral, $T^{\mu\nu} = 0$ and as a result, equation (3.44) is rewritten as

$$i\omega J^{\mu 0}e^{-i\omega t} = 0. \tag{3.45}$$

For $\omega \neq 0$ this relation translates to $J^{\mu 0} = 0$, or equivalently by virtue of equation (3.28), $\bar{h}^{\mu 0} = 0$. This implies that our linearized approximation on the weak gravitational-field regime is not self-consistent. The inconsistency in our approximation entered when we assumed that the conservation of the energy-tensor $T^{\mu\nu}$ is linked to the partial derivative, when in reality it should be linked to the covariant derivative. As a result, equation (3.42) should be replaced with

$$T^{\mu\nu}{}_{;\nu}\,, \tag{3.46}$$

to study the problem in the full non-linear Einstein gravity regime. However, this treatment is quite complicated and we will not focus more on this subject. Instead, we will adopt a different approach, to express $J^{\mu\nu}$, remaining in the weak-gravitational field linearized theory.

From equation (3.42) and for a bounded region of space, i.e. $T^{\mu\nu} = 0$ outside that boundary, we calculate that

$$\begin{aligned}\frac{\partial^2}{\partial t^2}\int T^{00}x^i x^j d^3x &= \frac{\partial}{\partial t}\int (T^{00}{}_{,0}\,x^i x^j + T^{00}x^i{}_{,0}x^j + T^{00}x^i x^j{}_{,0})d^3x \\ &= \frac{\partial}{\partial t}\int \left(T^{00}{}_{,0}\,x^i x^j + T^{00}u^i x^j + T^{00}x^i u^j\right) d^3x \rightarrow\end{aligned}$$

$$\begin{aligned}\frac{\partial^2}{\partial t^2}\int T^{00}x^i x^j d^3x = \int (&T^{00}{}_{,00}\,x^i x^j + T^{00}{}_{,0}\,u^i x^j + T^{00}{}_{,0}\,x^i u^j + T^{00}{}_{,0}\,u^i x^j + T^{00}u^i{}_{,0}x^j + \\ &+T^{00}u^i u^j + T^{00}{}_{,0}\,x^i u^j + T^{00}u^i u^j + T^{00}x^i u^j{}_{,0})d^3x \\ &= 2\int T^{00}x^i{}_{,0}x^j{}_{,0}d^3x = 2\int T^{00}u^i u^j d^3x \quad \rightarrow\end{aligned}$$

$$\frac{\partial^2}{\partial t^2}\int T^{00}x^i x^j d^3x = 2\int T^{ij}d^3x. \tag{3.47}$$

For a source in slow motion, the T^{00} component of the energy tensor corresponds to the density of that mass, $T^{00} = \rho$. So, the second order time-derivative of the quadrupole moment tensor, is equal to twice the energy moment. This is called the tensor virial theorem and we will use it to link the quadrupole moment tensor of the mass with the characteristics of the emitted gravitational waves.

The quadrupole moment tensor is defined as

$$Q^{ij} = \int T^{00}x^i x^j d^3x = D^{ij}e^{-i\omega t}. \tag{3.48}$$

Our aim is to calculate the expression of $\bar{h}^{ij}$, so first we need to specify the form of J^{ij} in terms of the quadrupole moment tensor. From equation (3.36), substituting (3.48), we obtain

$$\begin{aligned}J^{ij}e^{-i\omega t} = \frac{1}{2}\frac{d^2Q^{ij}}{dt^2} = \frac{1}{2}\frac{\partial^2}{\partial t^2}(D^{ij}e^{-i\omega t}) \rightarrow \\ J^{ij} = -\frac{1}{2}\omega^2 D^{ij}.\end{aligned} \tag{3.49}$$

Now, introducing equation (3.49) to (3.40) yields

$$\bar{h}^{ij} = 2\left(\frac{d^2Q^{ij}}{dt^2}\right)\frac{e^{i\omega r}}{r}e^{-i\omega t} \tag{3.50}$$

or equivalently,

$$\bar{h}^{ij} = -2\omega^2 D^{ij}\frac{e^{i\omega(r-t)}}{r}. \tag{3.51}$$

Due to the fact that equation (3.50) is linked to the quadrupole moment tensor of the mass distribution, it is often called the quadrupole approximation for gravitational radiation. It should be noted at this point, that our conclusion for $\bar{h}^{ij}$ is a simplified approximation. We have neglected $1/r^2$ terms or higher-order, since they are not dominant in the slow-motion approximation.

In most cases, one is not likely to encounter the expression of $\bar{h}^{ij}$ we derived earlier. Instead of equation (3.51), a transverse-traceless gauge (from now on we will use the abbreviation TT when we refer to this gauge) is widely used to acquire the simplest form of the waves. Basically what this gauge includes, is that we ask for a wave solution that is purely spatial,

$$\bar{h}^{0\nu} = 0, \tag{3.52}$$

satisfies the traceless condition

$$\bar{h}^{i}{}_{i} = 0. \tag{3.53}$$

In this regime, the spatial perturbation is transverse to the direction of motion of the wave. The Lorentz gauge can now be rewritten as

$$\bar{h}^{ij}{}_{,i} = 0. \tag{3.54}$$

For instance, let us assume that the gravitational waves propagate along the $z-$ axis. By imposing the TT gauge, the components of $\bar{h}^{ij}$ given by equation (3.51), reduce to

$$\bar{h}^{TT}_{zi} = 0, \tag{3.55}$$

$$\bar{h}^{TT}_{xx} = -\bar{h}^{TT}_{yy} = -\omega^2(q_{xx} - q_{yy})\frac{e^{i\omega r}}{r}, \tag{3.56}$$

$$\bar{h}^{TT}_{xy} = -2\omega^2 q_{xy}\frac{e^{i\omega r}}{r}, \tag{3.57}$$

where $q_{ij} = Q_{ij} - \frac{1}{3}\delta_{ij}Q^{k}{}_{k}$, is the traceless quadrupole moment tensor. Another way to write the equations (3.55), (3.56) and (3.57) in a general form is

$$\bar{h}_{ij}(t, x^i) = \frac{2}{r}q_{ij,00}(t-r) \quad \Leftrightarrow \quad \bar{h}_{ij}(t, x^i) = \frac{2}{r}\ddot{q}_{ij}(t-r) \tag{3.58}$$

It can be clearly seen from equation (3.58) that the gravitational waves are perturbations on the flat spacetime continuum and their amplitude is proportional to the second order time-derivative of the trace-free quadrupole moment tensor, i.e. the quantity that describes how much the object deviates from spherical symmetry. Furthermore, equations (3.56) and (3.57)

show that any body in the path of a gravitational wave will feel an oscillating gravitational force that acts in a plane perpendicular to the direction of the wave's propagation.

The gravitational wave analysis of this section includes a lot more physical substance than what we have presented here, but as it is not considered relevant to the point of this thesis, we refer anyone interested in the theory of gravitational waves to [17], [18] for an in depth study on the topic.

3.4 The energy carried away due to gravitational radiation

Our next step, will be to calculate the energy that is emitted from a system, in the form of gravitational waves. This is of fundamental importance, since there are circumstances, in which even though we may not be able to directly observe the gravitational waves themselves, we can observe the consequences of such radiation, through the system's energy loss[1].

The total gravitational energy flux of a wave of frequency ω can be written as [17],

$$F = \frac{1}{32\pi}\omega^2\langle \bar{h}^{TT}_{\mu\nu}\bar{h}^{TT\mu\nu}\rangle, \tag{3.59}$$

where the angle brackets denote an average over several periods. Assuming the simple case, where we have a radiative system, radiating according to equations (3.48) - (3.57), we substitute equations (3.56) and (3.57) to equation (3.59), in order to calculate at a distance r along the z- axis, the energy flux,

$$\begin{aligned} F &= \frac{1}{32\pi}\omega^2\langle 2\bar{h}_{xx}\bar{h}^{xx} + 2\bar{h}_{xy}\bar{h}^{xy}\rangle \\ &= \frac{1}{32\pi}\omega^2\langle \frac{2\omega^4}{r^2}(q_{xx}-q_{yy})^2 + \frac{8\omega^4}{r^2}q_{xy}^2\rangle \\ &= \frac{\omega^6}{16\pi r^2}\langle (q_{xx}-q_{yy})^2 + 4q_{xy}^2\rangle \\ &= \frac{\omega^6}{16\pi r^2}\langle q_{xx}^2 + q_{yy}^2 - 2q_{xx}q_{yy} + 4q_{xy}^2\rangle \\ &= \frac{\omega^6}{16\pi r^2}\langle 2q_{xx}^2 + 2q_{yy}^2 - q_{zz}^2 + 4q_{xy}^2\rangle, \end{aligned} \tag{3.60}$$

where we have used the identity

$$q_i{}^i = q_{xx} + q_{yy} + q_{zz} = 0. \tag{3.61}$$

Furthermore, we can rewrite the previous equation in the general form,

$$F = \frac{\omega^6}{16\pi r^2}\langle 2q_{ij}q^{ij} - 4q_{zj}q_z{}^j + q_{zz}^2\rangle. \tag{3.62}$$

[1] An example to this, is the famous Hulse-Taylor binary neutron star system. Long before the detection of gravitational waves in 2015 from a binary black hole system, it was known that the system is constantly losing energy while the neutron stars are emitting gravitational waves and are coming closer together. Although the gravitational waves emitted from the Hulse-Taylor system have not been detected to this day, the "lost" energy of the system, matches the energy that is carried away from gravitational waves.

The z- index has been distinguished from the other ones, since it is the direction where the radiation comes from.

Ultimately, we want to calculate the energy losses of a system, due to the emission of gravitational radiation. To do so, we have to integrate equation (3.62) over a sphere surrounding the system. We define the unit vector, normal to the surface of the sphere that includes our source, as

$$n^j = \frac{x^j}{r}, \tag{3.63}$$

where r, is the radius of the sphere, and substitute to equation (3.62), which gives

$$F = \frac{\omega^6}{16\pi r^2}\langle 2q_{ij}q^{ij} - 4n^j n^k q_{ji}q_k{}^i + n^i n^j n^k n^l q_{ij}q_{kl}\rangle. \tag{3.64}$$

Integration of (3.64) over the surface of the sphere of radius r gives

$$\begin{aligned}
L = -\langle \dot{E}\rangle &= \int F r^2 d\Omega \\
&= \langle \int_0^{2\pi}\int_0^{\pi} \frac{\omega^6}{16\pi r^2}(2q_{ij}q^{ij} - 4n^j n^k q_{ji}q_k{}^i + n^i n^j n^k n^l q_{ij}q_{kl}) r^2 \sin\theta d\theta d\phi\rangle \\
&= \frac{\omega^6}{16\pi}\langle \int_0^{2\pi}\int_0^{\pi} 2q_{ij}q^{ij}\sin\theta d\theta d\phi - 4\int_0^{2\pi}\int_0^{\pi} n^j n^k q_{ij}q_k{}^i \sin\theta d\theta d\phi + \int_0^{2\pi}\int_0^{\pi} n^i n^j n^k n^l q_{ij}q_{kl}\sin\theta d\theta d\phi\rangle \\
&= \frac{\omega^6}{16\pi}\langle 2\cdot 4\pi q_{ij}q^{ij} - 4\cdot\frac{4\pi}{3}\delta^{jk}q_{ij}q_k{}^i + \frac{4\pi}{15}(\delta^{ij}\delta^{kl} + \delta^{ik}\delta^{jl} + \delta^{il}\delta^{jk})q_{ij}q_{kl}\rangle \\
&= \frac{\omega^6}{4}\langle 2q_{ij}q^{ij} - \frac{4}{3}q_{ij}q^{ij} + \frac{1}{15}(\cancelto{0}{q_i{}^i q_k{}^k} + q_{jk}q^{jk} + q_{lj}q^{lj})\rangle \rightarrow
\end{aligned}$$

$$L = \frac{\omega^6}{5}\langle q_{ij}q^{ij}\rangle. \tag{3.65}$$

We will now generalize (3.65) to cases where q_{ij} has a more general time-dependence[19]. In a nearly inertial frame of linearized theory, the effective stress-energy tensor of gravitational waves is given by

$$T_{\mu\nu} = \frac{1}{32\pi}\langle \bar{h}^{TT}_{ij,\mu}\bar{h}^{TT}_{ij,\nu}\rangle, \tag{3.66}$$

and the flux of the radiation is given by the components

$$\begin{aligned}
F = T_{00} = T_{0r} = T_{r0} = T_{rr} &= \frac{1}{32\pi}\langle \bar{h}^{TT}_{ij,0}\bar{h}^{TT}_{ij,0}\rangle \\
&= \frac{1}{8\pi r^2}\langle \dddot{q}_{ij}\dddot{q}_{ij}\rangle \\
&= \frac{1}{8\pi r^2}\langle \ddot{q}_{jk}\ddot{q}_{jk} - 2n^i n^k \dddot{q}_{ij}\ddot{q}_{jk} + \frac{1}{2}(n^j \dddot{q}_{jk} n^k)^2\rangle
\end{aligned} \tag{3.67}$$

where we have substitited equation (3.58). Integrating the flux again, over the surface of a sphere containing the source, we calculate that

$$L^{GW} = \frac{1}{8\pi r^2}\langle \int_0^{2\pi}\int_0^{\pi}\left[\ddot{q}_{jk}\ddot{q}_{jk} - 2n^i n^k \dddot{q}_{ij}\ddot{q}_{jk} + \frac{1}{2}(n^j \ddot{q}_{jk} n^k)^2\right] r^2 \sin\theta d\theta d\phi\rangle \rightarrow$$

$$L = \frac{1}{5}\langle \dddot{q}_{ij} \ \dddot{q}^{ij} \rangle. \tag{3.68}$$

As a result, in the general case where the quadrupole moment tensor has an arbitrary time-dependence, the luminosity of the gravitational wave radiation is found to be analogous to the 3^{rd}- order time derivative of the traceless quadrupole moment of the source.

Chapter 4

Figures of equilibrium

4.1 Brief historical overview

The study of the equilibrium configuration of a self gravitating, homogeneous uniformly rotating liquid body dates back to Newton's days. His work on the topic can be found in *Principia Mathematica, Book 3 [20]* in which, while he was studying the shape of the earth, he argued that even a small rotation will alter the spherical configuration of the body, into a slightly elliptic shape, oblate at the plane passing through the axis of rotation, a meridian.

The next important theoretical step was in 1742, due to Maclaurin [21], who generalized Newton's results to cases where the ellipticity caused by rotation cannot be considered small. Maclaurin calculated the attraction of an oblate spheroid[1] at an internal point, and by considering the difference between the acceleration due to gravity at the equator and at the poles of the spheroid, he associated the eccentricity of the spheroid with its angular velocity. A noteworthy implication of Maclaurin's formula is that for any angular velocity

[1]By the term *spheroid* we imply the shape one obtains from a rotating ellipse, about one of its principal axes. Depending on the axis of rotation, one has two possible spheroids; an *oblate* spheroid if the ellipse is rotating about its minor axis, or a *prolate* spheroid if the rotation is about the major axis.

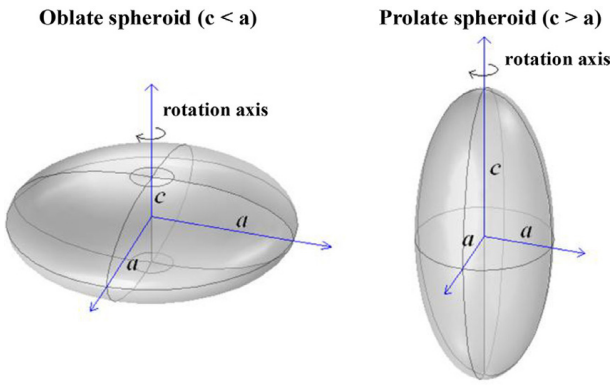

Figure 4.1: The oblate and prolate spheroids. Image taken from: https://www.researchgate.net/figure/The-oblate-and-prolate-spheroids-18_fig2_317259645

less than a critical maximum value, there are two possible configurations regarding the shape of the rotating body. For instance, in the slowly rotating regime $\Omega \to 0$, we can either have a spheroid of small eccentricity or a highly flattened spheroid. As a result we cannot deduce the exact shape of the spheroid just from measuring the angular velocity of the rotating body. This is a very important implication and we will discuss it further in the following chapters.

Until 1834, it was considered that the only admissible solution to the problem of the equilibrium of uniformly rotating homogeneous masses is that of a Maclaurin spheroid. At the time, Jacobi [22] pointed out that ellipsoids with three unequal axes, i.e. triaxial ellipsoids can also be figures of equilibrium. A few years later, in 1842, Meyer examined the relationship between the Maclaurin spheroids and the Jacobi ellipsoids. He showed that there is an angular velocity where the Maclaurin sequence bifurcates to the Jacobian sequence and with the work of Liouville, it was proven that the Jacobian ellipsoids are stable after this bifurcation point, due to the fact that they have lower angular momentum than the corresponding Maclaurin spheroids. Furthermore, it was later proven that there exist no figures of equilibrium for uniformly rotating masses when the angular velocity exceeds a certain limit.

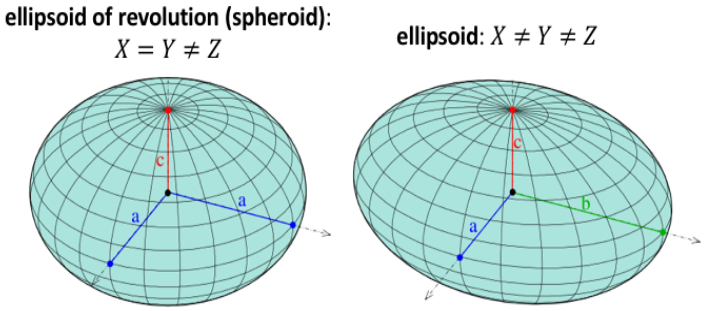

Figure 4.2: The shape of a triaxial ellipsoid in contrast to a spheroid. Source: https://learngis.org/textbook/section-three-mathematically-measuring-earth

The only way to produce a figure of equilibrium with larger angular velocity than the aforementioned limit, is by allowing the fluid to have internal flow and circulate within the ellipsoid. These are called Dedekind ellipsoids and, while they are congruent to the Jacobi ellipsoids, they are stationary with respect to a distant inertial observer and maintain the ellipsoidal figure by internal motions of the fluid.

Riemann [23], in 1861 gave a complete solution to the figures of equilibrium restricting to motions, which are linear in the coordinates. He showed that there are three cases, in

which ellipsoidal figures of equilibrium are possible. The first case, on which we will focus our study in the next sections, is that of uniform rotation with no internal motions. This scenario leads to the sequences of the Maclaurin spheroids and Jacobi ellipsoids.

Poincaré further investigated the problem of the ellipsoidal figures of equilibrium and in 1885, he discovered that along the Jacobian sequence, there is a bifurcation point similar to the one along the Maclaurin sequence. This bifurcation leads to a new sequence of pear-shaped configurations, or in more technical terminology, at the bifurcation point the Jacobian sequence allows a neutral mode of oscillation belonging to the third harmonic. Furthermore, he also showed that there must be more bifurcation points along the Jacobian sequence, where the ellipsoid allows neutral modes of oscillation that belong to higher harmonics. Concluding our historical overview, the last significant contribution was made by Cartan in 1924, who established that the Jacobi ellipsoid becomes unstable at its first bifurcation point. This comes in contrast with the case of the Maclaurin spheroid, which in the absence of any dissipative mechanism, is stable on either side of the bifurcation point where the Jacobian sequence appears.

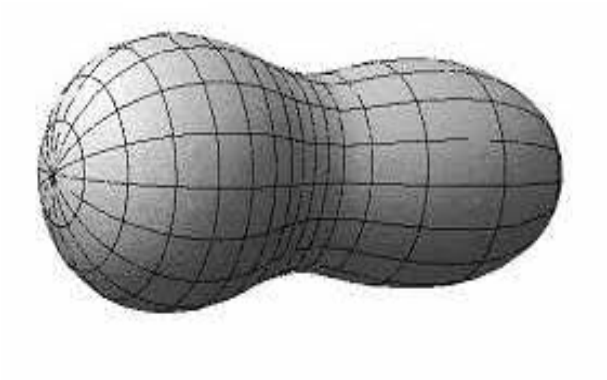

Figure 4.3: Poincaré pear-shaped figure of equilibrium. Source: https://indico.in2p3.fr/event/12970/contributions/12298/attachments/10464/12976/Mazurek.pdf

4.2 The potential of a Maclaurin spheroid

In this paragraph, we will calculate the potential of an oblate spheroid, assuming homogeneous mass distribution with density ρ. These objects are also referred to as Maclaurin spheroids, named after the mathematician Colin Maclaurin, who formulated these spheroids for the shape of the Earth.

To begin with, we will place the origin of the coordinates at the center of the spheroid, and the z-axis along the axis of rotation. Considering an arbitrary point $P(x, y, z)$, as shown in figure (4.4), far from the spheroid's surface, at a distance R from the origin O of the axes, we will calculate the potential from a mass element dm at that point $P(x, y, z)$.

Assuming that the mass element dm is located at a point $A(u, v, w)$, and define the

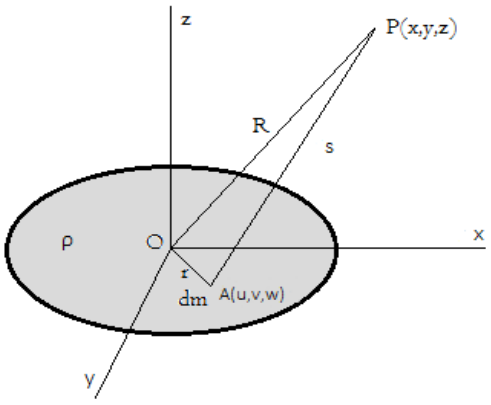

Figure 4.4: The point $P(x, y, z)$ is remote compared to the dimensions of the spheroid.

distance $AP = s$, then the potential at the point P is given by

$$V = -G \int_S \frac{dm}{s}, \tag{4.1}$$

where

$$s = \sqrt{(x-u)^2 + (y-v)^2 + (z-w)^2}. \tag{4.2}$$

Furthermore, we express the distance R, from the origin of the coordinates O to the point P and the distance r, from O to the mass element dm

$$R = \sqrt{x^2 + y^2 + z^2} \tag{4.3}$$

and

$$r = \sqrt{u^2 + v^2 + w^2} \tag{4.4}$$

Equation (4.1) implies that we need to calculate the term $1/s$ in order to describe the potential from a homogeneous oblate spheroid at an exterior point P. So, substituting equation (4.2) to equation (4.1) we have

$$\begin{aligned}
\frac{1}{s} &= \frac{1}{\sqrt{(x-u)^2 + (y-v)^2 + (z-w)^2}} \\
\frac{1}{s} &= \frac{1}{\sqrt{x^2 + u^2 + y^2 + v^2 + z^2 + w^2 - 2(xu + yv + zw)}} \\
\frac{1}{s} &= \frac{1}{\sqrt{R^2 + r^2 - 2(xu + yv + zw)}} \\
\frac{1}{s} &= \frac{1}{R} \frac{1}{\sqrt{1 + \frac{r^2 - 2(xu+yv+zw)}{R^2}}}.
\end{aligned} \tag{4.5}$$

Assuming that the quantities $\frac{u}{R}, \frac{v}{R}$ and $\frac{w}{R}$ are sufficiently small, we can expand the expression above as

$$(1+\epsilon)^{-1/2} \approx 1 - \frac{1}{2}\epsilon + \frac{3}{8}\epsilon^2 + \mathcal{O}(\epsilon^3) \tag{4.6}$$

so

$$\begin{aligned}\frac{1}{s} &\approx \frac{1}{R}\left\{1 - \frac{1}{2R^2}\Big[r^2 - 2(xu+yv+zw)\Big] + \frac{3}{8R^4}\Big[r^2 - 2(xu+yv+zw)\Big]^2\right\} \\ \frac{1}{s} &= \frac{1}{R}\left\{1 + \frac{xu+yv+zw}{R^2} - \frac{r^2}{2R^2} + \frac{3}{2}\frac{x^2u^2+y^2v^2+z^2w^2+2xyuv+2yzvw+2xzuw}{R^4}\right\}.\end{aligned} \tag{4.7}$$

As a result, substituting equation (4.7) to equation (4.1), we calculate the potential

$$\begin{aligned}-\frac{V}{G} \approx \int_S \frac{1}{R}dm + \int_S \frac{xu+yv+zw}{R^3}dm - \int_S \frac{r^2}{2R^3}dm \quad + \\ + \frac{3}{2}\int \frac{x^2u^2+y^2v^2+z^2w^2+2xyuv+2yzvw+2xzuw}{R^5}dm \rightarrow\end{aligned}$$

$$\begin{aligned}-\frac{V}{G} \approx \frac{M}{R} + \frac{1}{R^3}\left\{x\int_S udm + y\int_S vdm + z\int_S wdm\right\} \\ - \frac{1}{2R^3}\int_S r^2dm + \frac{3}{2R^5}\left\{x^2\int_S u^2dm + y^2\int_S v^2dm + z^2\int_S w^2dm\right\} \\ + \frac{3}{R^5}\left\{xy\int_S uvdm + yz\int_S vwdm + xz\int_S uwdm\right\},\end{aligned} \tag{4.8}$$

where, by M we represent the total mass of the spheroid.

We will switch to spherical coordinates to calculate the integrals of equation (4.8). Let

$$u = r\cos\theta\cos\phi \tag{4.9}$$
$$v = r\cos\theta\sin\phi \tag{4.10}$$
$$w = r\sin\theta \tag{4.11}$$

where θ ranges from $[-\frac{\pi}{2}, \frac{\pi}{2}]$ and ϕ from $[0, 2\pi]$. Furthermore, letting ρ represent the density of the spheroid, we can express the mass element as

$$dm = \rho r^2\cos\theta dr d\theta d\phi. \tag{4.12}$$

Equation (4.8) is rewritten using the relations (4.22), (4.23), (4.24) and (4.12) as

$$
\begin{aligned}
-\frac{V}{G} \approx \frac{M}{R} &+ \frac{\rho}{R^3}\left\{x\int_S r^3\cos^2\theta\cos\phi dr d\theta d\phi + y\int_S r^3\cos^2\theta\sin\phi dr d\theta d\phi + z\int_S r^3\sin\theta\cos\theta dr d\theta d\phi\right\} \\
&- \frac{\rho}{2R^3}\int_S r^4\cos\theta dr d\theta d\phi + \frac{3\rho}{2R^5}x^2\int_S r^4\cos^3\theta\cos^2\phi dr d\theta d\phi + \frac{3\rho}{2R^5}y^2\int_S r^4\cos^3\theta\sin^2\phi dr d\theta d\phi \\
&+ \frac{3\rho}{2R^5}z^2\int_S r^4\sin^2\theta\cos\theta dr d\theta d\phi + \frac{3\rho}{R^5}xy\int_S r^4\cos^3\theta\sin\phi\cos\phi dr d\theta d\phi \\
&+ \frac{3\rho}{R^5}yz\int_S r^4\sin\theta\cos^2\theta\sin\phi dr d\theta d\phi + \frac{3\rho}{R^5}xz\int_S r^4\sin\theta\cos^2\theta\cos\phi dr d\theta d\phi \rightarrow \\
-\frac{V}{G} \approx \frac{M}{R} &- \frac{\pi\rho}{R^3}\int_{-\pi/2}^{\pi/2}\int_0^r r^4\cos\theta dr d\theta + \frac{3\pi\rho x^2}{2R^5}\int_{-\pi/2}^{\pi/2}\int_0^r r^4\cos^3\theta dr d\theta \\
&+ \frac{3\pi\rho y^2}{2R^5}\int_{-\pi/2}^{\pi/2}\int_0^r r^4\cos^3\theta dr d\theta + \frac{3\pi\rho z^2}{R^5}\int_{-\pi/2}^{\pi/2}\int_0^r r^4\sin^2\theta\cos\theta dr d\theta. \qquad (4.13)
\end{aligned}
$$

Since r depends on the angle θ, we have to further manipulate equation (4.13) in order to calculate the potential of the spheroid. To do so, let a and c represent the major and the minor semi-axes of the spheroid, respectively and e represent the eccentricity. Then,

$$r^2 = \frac{c^2}{1 - e^2\cos^2\theta}, \qquad (4.14)$$

so substituting to equation (4.13) and integrating with respect to r, we have

$$
\begin{aligned}
-\frac{V}{G} &\approx \frac{M}{R} - \frac{\pi\rho}{R^3}\int_{-\pi/2}^{\pi/2}\frac{r^5}{5}\cos\theta d\theta + \frac{3\pi\rho(x^2+y^2)}{2R^5}\int_{-\pi/2}^{\pi/2}\frac{r^5}{5}\cos^3\theta d\theta + \frac{3\pi\rho z^2}{R^5}\int_{-\pi/2}^{\pi/2}\frac{r^5}{5}\sin^2\theta\cos\theta d\theta \\
&= \frac{M}{R} - \frac{\pi\rho c^5}{5R^3}\int_{-\pi/2}^{\pi/2}\frac{1}{(1-e^2\cos^2\theta)^{5/2}}\cos\theta d\theta + \frac{3\pi\rho c^5(x^2+y^2)}{10R^5}\int_{-\pi/2}^{\pi/2}\frac{1}{(1-e^2\cos^2\theta)^{5/2}}\cos^3\theta d\theta \\
&+ \frac{3\pi\rho c^5 z^2}{5R^5}\int_{-\pi/2}^{\pi/2}\frac{1}{(1-e^2\cos^2\theta)^{5/2}}\sin^2\theta\cos\theta d\theta. \qquad (4.15)
\end{aligned}
$$

Expanding in Taylor series, we have

$$\frac{1}{(1-e^2\cos^2\theta)^{5/2}} \approx 1 + \frac{5}{2}e^2\cos^2\theta + \mathcal{O}(e^4\cos^4\theta), \qquad (4.16)$$

and if we substitute the expansion to the integral, keeping only up to second-order terms

with respect to $e\cos\theta$, we find

$$
\begin{aligned}
-\frac{V}{G} \approx \frac{M}{R} &- \frac{\pi\rho c^5}{5R^3}\int_{-\pi/2}^{\pi/2}\left(1+\frac{5}{2}e^2\cos^2\theta\right)\cos\theta d\theta \\
&+ \frac{3\pi\rho c^5(x^2+y^2)}{10R^5}\int_{-\pi/2}^{\pi/2}\left(1+\frac{5}{2}e^2\cos^2\theta\right)\cos^3\theta d\theta \\
&+ \frac{3\pi\rho c^5 z^2}{5R^5}\int_{-\pi/2}^{\pi/2}\left(1+\frac{5}{2}e^2\cos^2\theta\right)\sin^2\theta\cos\theta d\theta \rightarrow \\
-\frac{V}{G} \approx \frac{M}{R} &- \frac{\pi\rho c^5}{5R^3}\left(\int_{-\pi/2}^{\pi/2}\cos\theta d\theta + \frac{5}{2}e^2\int_{-\pi/2}^{\pi/2}\cos^3\theta d\theta\right) \\
&+ \frac{3\pi\rho c^5(x^2+y^2)}{10R^5}\left(\int_{-\pi/2}^{\pi/2}\cos^3\theta d\theta + \frac{5}{2}e^2\int_{-\pi/2}^{\pi/2}\cos^5\theta d\theta\right) \\
&+ \frac{3\pi\rho c^5 z^2}{5R^5}\left(\int_{-\pi/2}^{\pi/2}\sin^2\theta\cos\theta d\theta + \frac{5}{2}e^2\int_{-\pi/2}^{\pi/2}\sin^2\theta\cos^3\theta d\theta\right) \rightarrow \\
-\frac{V}{G} \approx \frac{M}{R} &- \frac{2}{5}\frac{\pi\rho c^5}{R^3} - \frac{2}{3}\frac{\pi\rho c^5}{R^3}e^2 + \frac{2}{5}\frac{\pi\rho c^5}{R^5}(x^2+y^2) \\
&+ \frac{4}{5}\frac{\pi\rho c^5}{R^5}(x^2+y^2)e^2 + \frac{2}{5}\frac{\pi\rho c^5}{R^5}z^2 + \frac{2}{5}\frac{\pi\rho c^5}{R^5}z^2e^2 \rightarrow \\
-\frac{V}{G} \approx \frac{M}{R} &+ \frac{2}{5}\frac{\pi\rho c^5}{R^5}(x^2+y^2+z^2-R^2) + \frac{2}{15}\frac{\pi\rho c^5}{R^5}e^2(6x^2+6y^2+3z^2-5R^2),
\end{aligned}
$$

and by virtue of equation (4.3), the expression for the potential of an oblate spheroid of uniform density becomes

$$V = -\frac{GM}{R} - \frac{2}{5}\frac{\pi G\rho c^5}{R^5}(x^2+y^2-2z^2). \tag{4.17}$$

Our final step to simplify the expression of the potential (4.17), is to substitute the total mass of the spheroid

$$M = \frac{4}{3}\pi\rho a^2 c, \tag{4.18}$$

and by introducing the eccentricity once more

$$e^2 = 1 - \frac{c^2}{a^2}, \tag{4.19}$$

we end up with the relation

$$V = -\frac{GM}{R}\left[1 + \frac{c^2}{10}\frac{(x^2+y^2-2z^2)}{R^4}e^2\right]. \tag{4.20}$$

If the spheroid becomes a sphere ($e = 0$) then the potential (4.20) reduces to the classic Newtonian expression of the point mass potential.

4.3 The potential of a Jacobi ellipsoid

In this paragraph, we will calculate the potential of a Jacobi ellipsoid, i.e. a triaxial ellipsoid, assuming homogeneous mass distribution with density ρ.

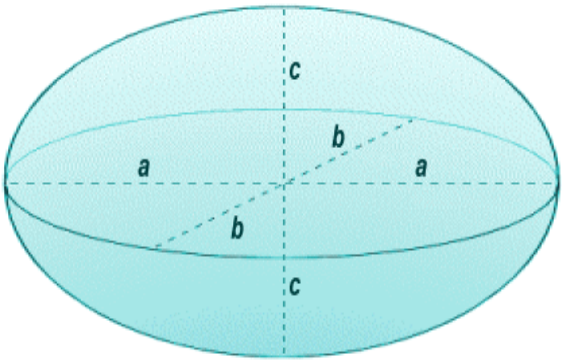

Figure 4.5: The general case of a triaxial ellipsoid, with semi-axes $a > b > c$. . Image taken from: http://www.technologyuk.net/mathematics/geometry/ellipsoids.shtml

We will assume that the surface of the ellipsoid is given in Cartesian coordinates, by the equation

$$\frac{u^2}{a^2} + \frac{v^2}{b^2} + \frac{w^2}{c^2} = 1 \tag{4.21}$$

and we will consider a particle at a point $P(x, y, z)$ in the interior of the ellipsoid. Furthermore, we will assume the point P to be the origin of the spherical m coordinate system that we will adopt, r, θ, ϕ. If we cut the ellipsoid into discrete planes, parallel to the first Cartesian coordinates, then we can relate them with the new coordinate system, by the equations

$$u = x + r\cos\theta\cos\phi \tag{4.22}$$

$$v = y + r\cos\theta\sin\phi \tag{4.23}$$

$$w = z + r\sin\theta, \tag{4.24}$$

where r ranges from 0 to r', θ takes values in the range $[-\pi/2, \pi/2]$ and ϕ in the range $[0, 2\pi]$. The potential of the ellipsoid upon the particle P, is

$$V = -G\int \frac{dm}{r}, \tag{4.25}$$

however, for a homogeneous ellipsoid of density ρ, we have that

$$dm = \rho r^2\cos\theta dr d\theta d\phi.$$

Substituting to equation (4.25), we calculate that

$$V = -G\rho\int_V r\cos\theta dr d\theta d\phi = -\frac{G\rho}{2}\int_0^{2\pi}\int_{-\pi/2}^{\pi/2} r'^2\cos\theta d\theta d\phi. \tag{4.26}$$

Since r' depends on the coordinates θ, ϕ we have to manipulate equation (4.26) in order to perform the integrations. If we substitute equations (4.22), (4.23) and (4.24) to (4.21) we have

$$\frac{x^2}{a^2} + \frac{r'^2\cos^2\theta\cos^2\phi}{a^2} + 2\frac{xr'\cos\theta\cos\phi}{a^2} + \frac{y^2}{b^2} + \frac{r'^2\cos^2\theta\sin^2\phi}{b^2} + 2\frac{yr'\cos\theta\sin\phi}{b^2} + \frac{z^2}{c^2} + \frac{r'^2\sin^2\theta}{c^2} + 2\frac{zr'\sin\theta}{c^2} = 1 \rightarrow$$

$$\left\{\frac{\cos^2\theta\cos^2\phi}{a^2} + \frac{\cos^2\theta\sin^2\phi}{b^2} + \frac{\sin^2\theta}{c^2}\right\} r'^2 \quad + \\ +2\left\{\frac{x\cos\theta\cos\phi}{a^2} + \frac{y\cos\theta\sin\phi}{b^2} + \frac{z\sin\theta}{c^2}\right\} r' \quad + \\ + \left\{\frac{x^2}{a^2} + \frac{y^2}{b^2} + \frac{z^2}{c^2} - 1\right\} = 0. \tag{4.27}$$

Equation (4.27) can be rewritten in the simpler form

$$Ar'^2 + 2Br' + C = 0, \tag{4.28}$$

where

$$A = \frac{\cos^2\theta\cos^2\phi}{a^2} + \frac{\cos^2\theta\sin^2\phi}{b^2} + \frac{\sin^2\theta}{c^2}, \tag{4.29}$$

$$B = \frac{x\cos\theta\cos\phi}{a^2} + \frac{y\cos\theta\sin\phi}{b^2} + \frac{z\sin\theta}{c^2}, \quad \text{and} \tag{4.30}$$

$$C = \frac{x^2}{a^2} + \frac{y^2}{b^2} + \frac{z^2}{c^2} - 1. \tag{4.31}$$

The only acceptable solutions to equation (4.28) are of the form

$$r' = \frac{-B \pm \sqrt{B^2 - AC}}{A} \tag{4.32}$$

for which, we obtain a positive value of r'. From equation (4.27), we notice that A is always positive and C is negative, since we have assumed a point mass $P(x, y, z)$ that lies within the surface of the ellipsoid. As a result the aforementioned meaningful solution holds true for the positive sign of the radical, since

$$\sqrt{B^2 - AC} > \|B\|. \tag{4.33}$$

Substituting the result of equation (4.32) to equation (4.26) we find for the integral that

$$V = -\frac{G\rho}{2}\int_{-\pi/2}^{\pi/2}\int_0^{2\pi} \frac{2B^2 - 2B\sqrt{B^2 - AC} - AC}{A^2}\cos\theta d\theta d\phi \rightarrow$$

$$V = -\frac{G\rho}{2}\int_{-\pi/2}^{\pi/2}\int_0^{2\pi} \frac{2B^2 - AC}{A^2}\cos\theta d\theta d\phi, \tag{4.34}$$

since the elements in the term

$$\int_{-\pi/2}^{\pi/2}\int_{0}^{2\pi}\frac{B\sqrt{B^2-AC}}{A^2}\cos\theta d\theta d\phi \tag{4.35}$$

cancel each other out. This can be seen if we interchange θ with $-\theta$ and ϕ with $\phi+\pi$ in the expression for B,

$$\begin{aligned}B(-\theta,\phi+\pi) &= \frac{x\cos(-\theta)\cos(\phi+\pi)}{a^2}+\frac{y\cos(-\theta)\sin(\phi+\pi)}{b^2}+\frac{z\sin(-\theta)}{c^2}\\ &= -\frac{x\cos\theta\cos\phi}{a^2}-\frac{y\cos\theta\sin\phi}{b^2}-\frac{z\sin\theta}{c^2}\\ &= -B(\theta,\phi)\end{aligned} \tag{4.36}$$

The term $\dfrac{\sqrt{B^2-AC}}{A^2}$ is even, with respect to the aforementioned angle exchanges, so the vanishing terms result from the fact that B is odd.

Before we move on to evaluate the integral in equation (4.34), we will calculate and simplify the nominator as much as possible.

$$\begin{aligned}B^2 &= \left[\frac{x\cos\theta\cos\phi}{a^2}+\frac{y\cos\theta\sin\phi}{b^2}+\frac{z\sin\theta}{c^2}\right]^2\\ &= \left(\frac{x\cos\theta\cos\phi}{a^2}\right)^2+\left(\frac{y\cos\theta\sin\phi}{b^2}\right)^2+\left(\frac{z\sin\theta}{c^2}\right)^2+\\ &+2\left[\frac{x\cos\theta\cos\phi}{a^2}\cdot\frac{y\cos\theta\sin\phi}{b^2}+\frac{y\cos\theta\sin\phi}{b^2}\cdot\frac{z\sin\theta}{c^2}+\frac{x\cos\theta\cos\phi}{a^2}\cdot\frac{z\sin\theta}{c^2}\right].\end{aligned} \tag{4.37}$$

$$\begin{aligned}AC &= \left[\frac{\cos^2\theta\cos^2\phi}{a^2}+\frac{\cos^2\theta\sin^2\phi}{b^2}+\frac{\sin^2\theta}{c^2}\right]\cdot\left[\frac{x^2}{a^2}+\frac{y^2}{b^2}+\frac{z^2}{c^2}-1\right]\\ &= \left(\frac{x\cos\theta\cos\phi}{a^2}\right)^2+\left(\frac{y\cos\theta\sin\phi}{b^2}\right)^2+\left(\frac{z\sin\theta}{c^2}\right)^2+\\ &+\left(\frac{y^2}{b^2}+\frac{z^2}{c^2}-1\right)\frac{\cos^2\theta\cos^2\phi}{a^2}+\left(\frac{x^2}{a^2}+\frac{z^2}{c^2}-1\right)\frac{\cos^2\theta\sin^2\phi}{b^2}+\left(\frac{x^2}{a^2}+\frac{y^2}{b^2}-1\right)\frac{\sin^2\theta}{c^2}.\end{aligned} \tag{4.38}$$

So,

$$
\begin{aligned}
2B^2 - AC = &\left(\frac{x\cos\theta\cos\phi}{a^2}\right)^2 + \left(\frac{y\cos\theta\sin\phi}{b^2}\right)^2 + \left(\frac{z\sin\theta}{c^2}\right)^2 + \\
&+ 4\left[\frac{x\cos\theta\cos\phi}{a^2}\cdot\frac{y\cos\theta\sin\phi}{b^2} + \frac{y\cos\theta\sin\phi}{b^2}\cdot\frac{z\sin\theta}{c^2} + \frac{x\cos\theta\cos\phi}{a^2}\cdot\frac{z\sin\theta}{c^2}\right] + \\
&+ \left(\frac{x^2}{a^2} - C\right)\frac{\cos^2\theta\cos^2\phi}{a^2} + \left(\frac{y^2}{b^2} - C\right)\frac{\cos^2\theta\sin^2\phi}{b^2} + \left(\frac{z^2}{c^2} - C\right)\frac{\sin^2\theta}{c^2} \rightarrow \\
2B^2 - AC = &\, 4\left[\frac{x\cos\theta\cos\phi}{a^2}\cdot\frac{y\cos\theta\sin\phi}{b^2} + \frac{y\cos\theta\sin\phi}{b^2}\cdot\frac{z\sin\theta}{c^2} + \frac{x\cos\theta\cos\phi}{a^2}\cdot\frac{z\sin\theta}{c^2}\right] + \\
&+ \left(\frac{2x^2}{a^2} - C\right)\frac{\cos^2\theta\cos^2\phi}{a^2} + \left(\frac{2y^2}{b^2} - C\right)\frac{\cos^2\theta\sin^2\phi}{b^2} + \left(\frac{2z^2}{c^2} - C\right)\frac{\sin^2\theta}{c^2}.
\end{aligned}
\tag{4.39}
$$

Inserting equation (4.39) to equation (4.34), we have

$$
\begin{aligned}
V = &-\frac{G\rho}{2}\int_{-\pi/2}^{\pi/2}\int_0^{2\pi}\frac{2B^2 - AC}{A^2}\cos\theta d\theta d\phi \\
= &-2G\rho\int_{-\pi/2}^{\pi/2}\int_0^{2\pi}\frac{x\cos\theta\cos\phi}{a^2}\cdot\frac{y\cos\theta\sin\phi}{b^2}\frac{\cos\theta d\theta d\phi}{A^2} + \\
&- 2G\rho\int_{-\pi/2}^{\pi/2}\int_0^{2\pi}\frac{y\cos\theta\sin\phi}{b^2}\cdot\frac{z\sin\theta}{c^2}\frac{\cos\theta d\theta d\phi}{A^2} + \\
&- 2G\rho\int_{-\pi/2}^{\pi/2}\int_0^{2\pi}\frac{x\cos\theta\cos\phi}{a^2}\cdot\frac{z\sin\theta}{c^2}\frac{\cos\theta d\theta d\phi}{A^2} + \\
&- \frac{G\rho}{2}\int_{-\pi/2}^{\pi/2}\int_0^{2\pi}\left(\frac{2x^2}{a^2} - C\right)\frac{\cos^2\theta\cos^2\phi}{a^2}\frac{\cos\theta d\theta d\phi}{A^2} + \\
&- \frac{G\rho}{2}\int_{-\pi/2}^{\pi/2}\int_0^{2\pi}\left(\frac{2y^2}{b^2} - C\right)\frac{\cos^2\theta\sin^2\phi}{b^2}\frac{\cos\theta d\theta d\phi}{A^2} + \\
&- \frac{G\rho}{2}\int_{-\pi/2}^{\pi/2}\int_0^{2\pi}\left(\frac{2z^2}{c^2} - C\right)\frac{\sin^2\theta}{c^2}\frac{\cos\theta d\theta d\phi}{A^2} \rightarrow \\
V = &-2G\rho\int_{-\pi/2}^{\pi/2}\int_0^{2\pi}\frac{xy\cos^3\theta\cos\phi\sin\phi d\theta d\phi}{a^2b^2A^2} - 2G\rho\int_{-\pi/2}^{\pi/2}\int_0^{2\pi}\frac{yz\cos^2\theta\sin\theta\sin\phi d\theta d\phi}{b^2c^2A^2} - \\
&- 2G\rho\int_{-\pi/2}^{\pi/2}\int_0^{2\pi}\frac{xz\cos^2\theta\sin\theta\cos\phi d\theta d\phi}{a^2c^2A^2} - \frac{G\rho}{2}\int_{-\pi/2}^{\pi/2}\int_0^{2\pi}\left(\frac{2x^2}{a^2} - C\right)\frac{\cos^3\theta\cos^2\phi d\theta d\phi}{a^2A^2} + \\
&- \frac{G\rho}{2}\int_{-\pi/2}^{\pi/2}\int_0^{2\pi}\left(\frac{2y^2}{b^2} - C\right)\frac{\cos^3\theta\sin^2\phi d\theta d\phi}{b^2A^2} - \frac{G\rho}{2}\int_{-\pi/2}^{\pi/2}\int_0^{2\pi}\left(\frac{2z^2}{c^2} - C\right)\frac{\cos\theta\sin^2\theta d\theta d\phi}{c^2A^2}.
\end{aligned}
\tag{4.40}
$$

The first three terms of equation (4.40) vanish, using the symmetry properties of the

integrated functions, with respect to ϕ. Now, let

$$W = \frac{G\rho}{2}\int_{-\pi/2}^{\pi/2}\int_{0}^{2\pi}\frac{\cos\theta d\theta d\phi}{\frac{\cos^2\theta\cos^2\phi}{a^2}+\frac{\cos^2\theta\sin^2\phi}{b^2}+\frac{\sin^2\theta}{c^2}}, \tag{4.41}$$

where the partial derivatives are

$$\begin{aligned}\frac{\partial W}{\partial a} &= \frac{G\rho}{2}\int_{-\pi/2}^{\pi/2}\int_{0}^{2\pi}\frac{2\cos^2\phi\cos^3\theta d\theta d\phi}{a^3\left(\frac{\cos^2\phi\cos^2\theta}{a^2}+\frac{\cos^2\theta\sin^2\phi}{b^2}+\frac{\sin^2\theta}{c^2}\right)^2}\\ &= \frac{2}{a}\cdot\frac{G\rho}{2}\int_{-\pi/2}^{\pi/2}\int_{0}^{2\pi}\frac{\cos^3\theta\cos^2\phi d\theta d\phi}{a^2A^2},\end{aligned} \tag{4.42}$$

$$\begin{aligned}\frac{\partial W}{\partial b} &= \frac{G\rho}{2}\int_{-\pi/2}^{\pi/2}\int_{0}^{2\pi}\frac{2\sin^2\phi\cos^3\theta d\theta d\phi}{b^3\left(\frac{\cos^2\phi\cos^2\theta}{a^2}+\frac{\sin^2\phi\cos^2\theta}{b^2}+\frac{\sin^2\theta}{c^2}\right)^2}\\ &= \frac{2}{b}\cdot\frac{G\rho}{2}\int_{-\pi/2}^{\pi/2}\int_{0}^{2\pi}\frac{\sin^2\phi\cos^3\theta d\theta d\phi}{b^2A^2},\end{aligned} \tag{4.43}$$

$$\begin{aligned}\frac{\partial W}{\partial c} &= \frac{G\rho}{2}\int_{-\pi/2}^{\pi/2}\int_{0}^{2\pi}\frac{2\cos\theta\sin^2\theta d\theta d\phi}{c^3\left(\frac{\cos^2\phi\cos^2\theta}{a^2}+\frac{\sin^2\phi\cos^2\theta}{b^2}+\frac{\sin^2\theta}{c^2}\right)^2}\\ &= \frac{2}{c}\cdot\frac{G\rho}{2}\int_{-\pi/2}^{\pi/2}\int_{0}^{2\pi}\frac{\cos\theta\sin^2\theta d\theta d\phi}{c^2A^2}.\end{aligned} \tag{4.44}$$

Inserting equations (4.42), (4.43), (4.44) to equation (4.40), the potential of a solid homogeneous ellipsoid can be rewritten as

$$\begin{aligned}-V &= \left(\frac{2x^2}{a^2}-C\right)\frac{a}{2}\frac{\partial W}{\partial a}+\left(\frac{2y^2}{b^2}-C\right)\frac{b}{2}\frac{\partial W}{\partial b}+\left(\frac{2z^2}{c^2}-C\right)\frac{c}{2}\frac{\partial W}{\partial c}\\ &= \frac{x^2}{a}\frac{\partial W}{\partial a}+\frac{y^2}{b}\frac{\partial W}{\partial b}+\frac{z^2}{c}\frac{\partial W}{\partial c}-C\left[\frac{a}{2}\frac{\partial W}{\partial a}+\frac{b}{2}\frac{\partial W}{\partial b}+\frac{c}{2}\frac{\partial W}{\partial c}\right]\\ &= \frac{x^2}{a}\frac{\partial W}{\partial a}+\frac{y^2}{b}\frac{\partial W}{\partial b}+\frac{z^2}{c}\frac{\partial W}{\partial c}-C\frac{\rho}{2}\int_{-\pi/2}^{\pi/2}\int_{0}^{2\pi}\left(\frac{\cos^3\theta\cos^2\phi}{a^2A^2}+\frac{\cos^3\theta\sin^2\phi}{b^2A^2}+\frac{\cos\theta\sin^2\theta}{c^2A^2}\right)d\theta d\phi\\ &= \frac{x^2}{a}\frac{\partial W}{\partial a}+\frac{y^2}{b}\frac{\partial W}{\partial b}+\frac{z^2}{c}\frac{\partial W}{\partial c}-C\frac{\rho}{2}\int_{-\pi/2}^{\pi/2}\int_{0}^{2\pi}\left[\frac{\cos\theta}{A^2}\left(\frac{\cos^2\theta\cos^2\phi}{a^2}+\frac{\cos^2\theta\sin^2\phi}{b^2}+\frac{\sin^2\theta}{c^2}\right)\right]d\theta d\phi\\ &\overset{(4.29)}{=} \frac{x^2}{a}\frac{\partial W}{\partial a}+\frac{y^2}{b}\frac{\partial W}{\partial b}+\frac{z^2}{c}\frac{\partial W}{\partial c}-C\frac{\rho}{2}\int_{-\pi/2}^{\pi/2}\int_{0}^{2\pi}\left(\frac{\cos\theta}{A^2}Ad\theta d\phi\right)\rightarrow\end{aligned}$$

$$-V = \frac{x^2}{a}\frac{\partial W}{\partial a}+\frac{y^2}{b}\frac{\partial W}{\partial b}+\frac{z^2}{c}\frac{\partial W}{\partial c}-CW. \tag{4.45}$$

For a given ellipsoid, W is constant. As a result, equation (4.45) implies that the equation of the level surfaces has the form

$$\frac{x^2}{C_1}+\frac{y^2}{C_2}+\frac{z^2}{C_3} = \text{constant}, \tag{4.46}$$

where

$$\frac{1}{C_1} = \frac{1}{a}\frac{\partial W}{\partial a} = \frac{\rho}{a^4}\int_{-\pi/2}^{\pi/2}\int_0^{2\pi} \frac{\cos^3\theta\cos^2\phi d\theta d\phi}{A^2}, \tag{4.47}$$

$$\frac{1}{C_2} = \frac{1}{b}\frac{\partial W}{\partial b} = \frac{\rho}{b^4}\int_{-\pi/2}^{\pi/2}\int_0^{2\pi} \frac{\cos^3\theta\sin^2\phi d\theta d\phi}{A^2}, \tag{4.48}$$

$$\frac{1}{C_3} = \frac{1}{c}\frac{\partial W}{\partial c} = \frac{\rho}{c^4}\int_{-\pi/2}^{\pi/2}\int_0^{2\pi} \frac{\cos\theta\sin^2\theta d\theta d\phi}{A^2}. \tag{4.49}$$

This is the equation of concentric similar ellipsoids, whose axes a, b, and c are proportional to $\sqrt{C_1}, \sqrt{C_2}$ and $\sqrt{C_3}$, respectively.

For a rotating Jacobi ellipsoid, revolving about the $z-$axis with constant angular velocity Ω, we need to take into account the centrifugal potential,

$$V_{\text{centr}} = \frac{1}{2}\Omega^2(x^2+y^2). \tag{4.50}$$

The effective potential of the Jacobi ellipsoid will be given by the sum of the gravitational potential and the centrifugal potential, thus

$$V_{\text{eff}} = \frac{1}{2}\Omega^2(x^2+y^2) - \left(\frac{x^2}{C_1}+\frac{y^2}{C_2}+\frac{z^2}{C_3}\right) + CW$$

$$V_{\text{eff}} = \frac{x^2}{C'_1}+\frac{y^2}{C'_2}+\frac{z^2}{C_3}+CW, \tag{4.51}$$

where,

$$C'_1 = \frac{\Omega^2}{2} - \frac{1}{C_1}, \qquad \text{and} \tag{4.52}$$

$$C'_2 = \frac{\Omega^2}{2} - \frac{1}{C_2}, \tag{4.53}$$

and the semi-axes along the x and y axes are proportional to $\sqrt{C'_1}$ and $\sqrt{C'_2}$, respectively. Once more, the level surfaces according to the effective potential we derived, are concentric ellipsoids.

We will proceed with some further manipulation, in order to reduce the equations (4.45) and (4.41), to an integrable form. First, we introduce

$$M = \frac{\cos^2\theta}{a^2} + \frac{\sin^2\theta}{c^2} \tag{4.54}$$

$$N = \frac{\cos^2\theta}{b^2} + \frac{\sin^2\theta}{c^2} \tag{4.55}$$

to equation (4.41). Thus, we obtain,

$$W = \frac{\rho}{2}\int_{-\pi/2}^{\pi/2}\int_0^{2\pi} \frac{\cos\theta d\theta d\phi}{M\cos^2\phi + N\sin^2\phi}$$

$$= 4\rho\int_0^{\pi/2}\int_0^{\pi/2} \frac{\cos\theta d\theta d\phi}{M\cos^2\phi + N\sin^2\phi}.$$

Since M and N are functions only of θ, we can integrate separately with respect to ϕ, which results in

$$W = 2\pi\rho \int_0^{\pi/2} \frac{\cos\theta d\theta}{\sqrt{MN}}$$
$$= 2\pi\rho abc^2 \int_0^{\pi/2} \frac{\cos\theta d\theta}{\sqrt{(a^2\sin^2\theta + c^2\cos^2\theta)(b^2\sin^2\theta + c^2\cos^2\theta)}}. \tag{4.56}$$

In order to regain a symmetric expression of W in a, b and c, as in equation (4.41), we introduce the transformation

$$\sin\theta = \frac{c}{\sqrt{c^2+u}}, \tag{4.57}$$

where

$$\cos\theta d\theta = -\frac{cdu}{2\sqrt{c^2+u}^3}, \tag{4.58}$$

and finally, we have the expression for W,

$$W = \pi\rho abc \int_0^{\infty} \frac{du}{\sqrt{(a^2+u)(b^2+u)(c^2+u)}}. \tag{4.59}$$

Calculating the derivatives of (4.59) with respect to a, b and c, we reconstruct equation (4.45), to find the final expression for the potential of a Jacobi ellipsoid,

$$V = -\pi\rho abc \int_0^{\infty} \left(1 - \frac{x^2}{a^2+u} - \frac{y^2}{b^2+u} - \frac{z^2}{c^2+u}\right) \frac{du}{\sqrt{(a^2+u)(b^2+u)(c^2+u)}}. \tag{4.60}$$

4.4 Equilibrium of the Maclaurin spheroid

In this section we will study the equilibrium of the Maclaurin spheroid, which arises when a homogeneous body starts to rotate with a uniform angular velocity. Our analysis will be based upon the Chandrasekhar's second - order virial equations [2], which are expressed as

$$W_{ij} + \Omega^2(I_{ij} - \delta_{i3}I_{3j}) = -\delta_{ij}\Pi, \tag{4.67}$$

[2]The Chandrasekhar virial equations, are ultimately the Euler equations for fluid dynamics, expressed in terms of moment equations. The general form of the second-order virial equation in tensor notation is

$$\frac{1}{2}\frac{d^2I_{ij}}{dt^2} = 2T_{ij} + W_{ij} + \delta_{ij}\Pi, \tag{4.61}$$

where

$$I_{ij} = \int_V \rho x_i x_j d^3x, \tag{4.62}$$

is the density moment

$$T_{ij} = \frac{1}{2}\int_V \rho u_i u_j d^3x, \tag{4.63}$$

is the kinetic energy tensor,

$$W_{ij} = -\frac{1}{2}\int_V \rho\Phi_{ij} d^3x, \tag{4.64}$$

assuming the axis of rotation is along the $z-$axis , which is also considered to be the axis of symmetry of the Maclaurin spheroid described by the equation of its surface,

$$\frac{x^2+y^2}{a^2}+\frac{z^2}{c^2}=1. \tag{4.68}$$

Under these circumstances, we calculate each component of equation (4.81), so

$$\begin{aligned} W_{11}+\Omega^2 I_{11} &= -\Pi \\ W_{12}+\Omega^2 I_{12} &= 0 \\ W_{13}+\Omega^2 I_{13} &= 0 \end{aligned} \tag{4.69}$$

$$\begin{aligned} W_{21}+\Omega^2 I_{21} &= 0 \\ W_{22}+\Omega^2 I_{22} &= -\Pi \\ W_{23}+\Omega^2 I_{23} &= 0 \end{aligned} \tag{4.70}$$

$$\begin{aligned} W_{31} &= 0 \\ W_{32} &= 0 \\ W_{33} &= -\Pi, \end{aligned} \tag{4.71}$$

which lead to the following relations

$$I_{11}=I_{22}, \tag{4.72}$$

$$W_{11}=W_{22} \tag{4.73}$$

and

$$W_{11}+\Omega^2 I_{11}=W_{33}=-\Pi, \tag{4.74}$$

as a consequence of the fact that we assumed symmetry with respect to the $z-$axis. Substituting the expressions that correspond to the potential energy and moment of inertia tensors,

---

is the gravitational potential energy tensor, with $\Phi_{ij}=G\int_V \rho(\mathbf{x}')\frac{(x_i-x_i')(x_j-x_j')}{\|\mathbf{x}-\mathbf{x}'\|^3}d^3x'$, and the final term,

$$\Pi_{ij}=\int_V p x_i x_j d^3x, \tag{4.65}$$

is the pressure moment. Mainly, we are concerned with configurations that are rotating uniformly, with angular velocity Ω. As a result, it is convenient to refer the equations above, to a frame of reference that is rotating with the same angular velocity. Without any loss of generality, we will assume that our configuration is rotating about the z-axis. In this rotating frame, the steady state second - order virial equation (4.61) can be replaced by

$$W_{ij}+\Omega^2(I_{ij}-\delta_{i3}I_{3j})=-\delta_{ij}\Pi. \tag{4.66}$$

following Chandrasekhar [14] and expressing Ω in units $\sqrt{\pi G\rho}$, we have

$$\begin{aligned}
\Omega^2 &= 2\left(\frac{\sqrt{1-e^2}}{e^3}\arcsin e - \frac{1-e^2}{e^2} - \frac{c^2}{a^2}\left(\frac{2}{e^2} - 2\frac{\sqrt{1-e^2}}{e^3}\arcsin e\right)\right) \\
&= 2\left(\frac{\sqrt{1-e^2}}{e^3}\arcsin e - \frac{1-e^2}{e^2} - (1-e^2)\left(\frac{2}{e^2} - 2\frac{\sqrt{1-e^2}}{e^3}\arcsin e\right)\right) \\
&= \frac{2\sqrt{1-e^2}}{e^3}\arcsin e - \frac{2(1-e^2)}{e^2} - \frac{4(1-e^2)}{e^2} + \frac{4(1-e^2)\sqrt{1-e^2}}{e^3}\arcsin e \rightarrow \\
\Omega^2 &= \frac{2\sqrt{1-e^2}}{e^3}(3-2e^2)\arcsin e - \frac{6(1-e^2)}{e^2}. \qquad (4.75)
\end{aligned}$$

By retrieving the units of Ω, we have the Maclaurin formula for spheroids,

$$\frac{\Omega^2}{\pi G\rho} = \frac{2\sqrt{1-e^2}}{e^3}(3-2e^2)\arcsin e - \frac{6(1-e^2)}{e^2}, \qquad (4.76)$$

where $e = \sqrt{1-\frac{c^2}{a^2}}$ is the eccentricity in the $x-z$ plane.

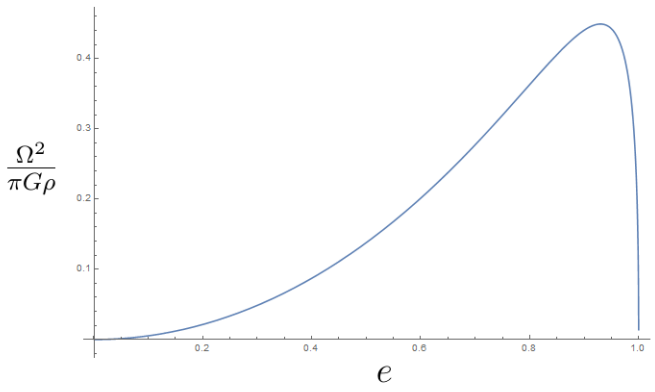

Figure 4.6: The square of angular velocity as a function of the eccentricity in the $x-z$ plane, for the Maclaurin spheroid. This plot is created using *Wolfram Mathematica.*

We have also constructed the plots of the evolution of the semi-axes of the Maclaurin spheroid, to better visualize the effects of rotation on the axes. As we can see in figures 4.7 and 4.8 the length of the major semi-axis a is constantly growing as we increase the rotation rate of the mass, while the minor semi- axis c becomes shorter.

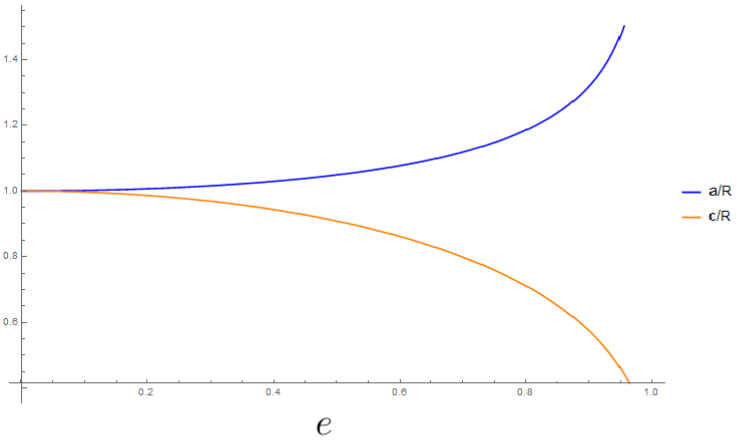

Figure 4.7: The evolution of the normalized semi-axes, to the radius of a sphere that has the same volume as our spheroid, as a function of the eccentricity in the $x-z$ plane, for the Maclaurin spheroid. This plot has been created using *Wolfram Mathematica.*

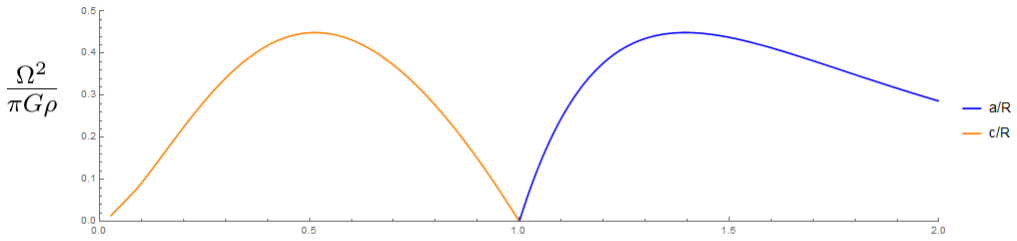

Figure 4.8: The evolution of the normalized semi-axes, as a function of the square of angular velocity, for the Maclaurin spheroid. This plot has been created using *Wolfram Mathematica.*

Furthermore, we can use the expression (4.76) for the angular velocity to further calculate the angular momentum of the Maclaurin spheroid,

$$L = I\Omega \rightarrow \frac{L}{\sqrt{GM^3R}} = \frac{\sqrt{3}}{5}(1-e^2)^{1/3}\sqrt{\frac{\Omega^2}{\pi G\rho}}, \tag{4.77}$$

where $I = 2Ma^2/5$ is the moment of inertia of the spheroid with respect to $z-$ axis, which we assume to be the axis of rotation and $R = (a^2c)^{1/3}$ the radius of a sphere of the same volume as our spheroid.

As we can see in figure 4.6, it is possible to have the same value for $\Omega^2/\pi G\rho$ for two different values of the eccentricity, i.e. two completely different shapes - one will tend more to

a sphere while the other will tend to a disk, while $\Omega \to 0$. This will in turn lead to two values of eccentricity that correspond to the same angular momentum. From this brief analysis, one has to answer the question, what is the most convenient parameter that describes uniquely the shape of equilibrium along the sequence. As we have already mentioned, the angular momentum J is not a good choice, as it depends on Ω which does not increase monotonically with respect to the eccentricity. The best parameter to use when we want to describe the evolution of the figure along the sequence, is the ratio β which is the fraction of the rotational kinetic energy K over the gravitational potential energy W,

$$\beta = \frac{K}{W}. \tag{4.78}$$

This $\beta-$ parameter takes values in the space [0,0.5][3] and is the parameter used vastly when one studies the dynamical instabilities occurred in neutron stars. However, we will keep studying the evolution of the Maclaurin spheroid and later the Jacobi ellipsoid with respect to Ω for pedagogical reasons.

Another important aspect that should be noted, is that the Maclaurin sequence is not stable for all eccentricities. It has been proven that at eccentricity $e \approx 0.81$ the Maclaurin sequence branches off to the Jacobi sequence, forming a triaxial ellipsoid. The underlying cause of this bifurcation, is that a Jacobi ellipsoid having the same angular momentum as a Maclaurin spheroid, will have a lower total energy. As a result, a small perturbation on the fluid composing the spheroid will break the symmetry and gradually elongate the spheroid into a triaxial ellipsoid.

4.5 Equilibrium of the Jacobi ellipsoid

As we have already mentioned, the Jacobi ellipsoid is a figure of equilibrium for a self-gravitating body of uniform density, rotating with a constant angular velocity. A Jacobi ellipsoid is described by the general form

$$\frac{x^2}{a^2} + \frac{y^2}{b^2} + \frac{z^2}{c^2} \leq 1, \tag{4.80}$$

where a, b, c are the semi-major axes, assuming that $a > b > c$ and that it rotates about the z axis with constant angular velocity Ω. Using Chandrasekhar's second - order virial equation, accounting for the rotation of the ellipsoid, we have that

$$W_{ij} + \Omega^2(I_{ij} - \delta_{i3}I_{3j}) = -\delta_{ij}\Pi, \tag{4.81}$$

[3]Using the virial theorem, we have

$$2K - \|W\| + 3\int_V p d^3x = 0,$$

where p is the pressure. The volume integral over the pressure is always a non-negative quantity, so the parameter β is limited according to:

$$0 \leq \beta \leq \frac{1}{2}. \tag{4.79}$$

while it should be noted at this point, that Ω is measured in units $\sqrt{\pi G\rho}$. Explicitly written out, equation (4.81) gives

$$\begin{aligned} W_{11} + \Omega^2 I_{11} &= -\Pi \\ W_{12} + \Omega^2 I_{12} &= 0 \\ W_{13} + \Omega^2 I_{13} &= 0 \end{aligned} \tag{4.82}$$

$$\begin{aligned} W_{21} + \Omega^2 I_{21} &= 0 \\ W_{22} + \Omega^2 I_{22} &= -\Pi \\ W_{23} + \Omega^2 I_{23} &= 0 \end{aligned} \tag{4.83}$$

$$\begin{aligned} W_{31} &= 0 \\ W_{32} &= 0 \\ W_{33} &= -\Pi. \end{aligned} \tag{4.84}$$

As a result, we have the following three equalities

$$W_{11} + \Omega^2 I_{11} = W_{22} + \Omega^2 I_{22} = W_{33}, \tag{4.85}$$

which, after inserting the expressions for the potential energy of an ellipsoid with semi-axes a, b and c, and the moment of inertia tensors, will give

$$\Omega^2 a^2 - 2a^3 bc \int_0^\infty \frac{du}{(a^2+u)\Delta} = \Omega^2 b^2 - 2ab^3 c \int_0^\infty \frac{du}{(b^2+u)\Delta} = -2abc^3 \int_0^\infty \frac{du}{(c^2+u)\Delta}, \tag{4.86}$$

where

$$\Delta = \sqrt{(a^2+u)(b^2+u)(c^2+u)}.$$

Following Chandrasekhar[14], we add the quantity

$$2a^3 b^3 c \int_0^\infty \frac{du}{(a^2+u)(b^2+u)\Delta}$$

to each side of the equalities above, so we obtain the relations

$$\begin{aligned} \Omega^2 a^2 - 2a^3 bc \int_0^\infty \frac{du}{(a^2+u)\Delta} + 2a^3 b^3 c \int_0^\infty \frac{du}{(a^2+u)(b^2+u)\Delta} &= \\ \Omega^2 b^2 - 2ab^3 c \int_0^\infty \frac{du}{(b^2+u)\Delta} + 2a^3 b^3 c \int_0^\infty \frac{du}{(a^2+u)(b^2+u)\Delta} &= \\ - 2abc^3 \int_0^\infty \frac{du}{(c^2+u)\Delta} + 2a^3 b^3 c \int_0^\infty \frac{du}{(a^2+u)(b^2+u)\Delta} \qquad &\rightarrow \end{aligned}$$

$$\begin{aligned} a^2 \left[\Omega^2 - 2abc \left(\int_0^\infty \frac{du}{(a^2+u)\Delta} - b^2 \int_0^\infty \frac{du}{(a^2+u)(b^2+u)\Delta} \right) \right] &= \\ b^2 \left[\Omega^2 - 2abc \left(\int_0^\infty \frac{du}{(b^2+u)\Delta} - a^2 \int_0^\infty \frac{du}{(a^2+u)(b^2+u)\Delta} \right) \right] &= \\ 2abc \left[a^2 b^2 \int_0^\infty \frac{du}{(a^2+u)(b^2+u)\Delta} - c^2 \int_0^\infty \frac{du}{(c^2+u)\Delta} \right] \qquad &\rightarrow \end{aligned}$$

$$a^2\left[\Omega^2 - 2abc\int_0^\infty \frac{udu}{(a^2+u)(b^2+u)\Delta}\right] = b^2\left[\Omega^2 - 2abc\int_0^\infty \frac{udu}{(a^2+u)(b^2+u)\Delta}\right]$$
$$= 2abc\left[a^2b^2\int_0^\infty \frac{du}{(a^2+u)(b^2+u)\Delta} - c^2\int_0^\infty \frac{du}{(c^2+u)\Delta}\right]. \tag{4.87}$$

From equations (4.87) it is obvious, that if one allows only for solutions with $a \neq b$, the following two conditions emerge; a geometric restriction on the ellipsoid

$$a^2b^2\int_0^\infty \frac{du}{(a^2+u)(b^2+u)\Delta} = c^2\int_0^\infty \frac{du}{(c^2+u)\Delta}, \tag{4.88}$$

which determines a unique relation between the ellipsoid's semi-axes, and

$$\Omega^2 = 2abc\int_0^\infty \frac{udu}{(a^2+u)(b^2+u)\Delta}. \tag{4.89}$$

Retrieving the units of Ω in equation (4.89) for our configuration, the Jacobi formula [22] can be written

$$\frac{\Omega^2}{\pi G\rho} = 2abc\int_0^\infty \frac{udu}{(a^2+u)(b^2+u)\Delta}. \tag{4.90}$$

Instead of equation (4.90), we will use a more convenient expression relating the square of the angular velocity Ω with the eccentricities of the $x-y$ and $x-z$ planes. To begin with, we define the eccentricities of the $x-y$ and $x-z$ planes

$$e_{xy}^2 = 1 - \frac{b^2}{a^2} \quad \rightarrow \quad \frac{b^2}{a^2} = 1 - e_{xy}^2 \qquad \text{and} \tag{4.91}$$

$$e_{xz}^2 = 1 - \frac{c^2}{a^2} \quad \rightarrow \quad \frac{c^2}{a^2} = 1 - e_{xz}^2 \tag{4.92}$$

respectively. One can easily infer that in the cases where $e_{xy} = 0$ or $e_{xz} = 0$, the corresponding planar cross section is reduced to a circle, while on the other limiting case of $e_{xy} \to 1$ or $e_{xz} \to 1$ the ellipse stretches to an infinite line. Manipulating equation (4.90) and substituting equations (4.91) and (4.92) we have

$$\frac{\Omega^2}{\pi G\rho} = 2abc\int_0^\infty \frac{udu}{a^4(1+\frac{u}{a^2})(\frac{b^2}{a^2}+\frac{u}{a^2})\sqrt{a^6(1+\frac{u}{a^2})(\frac{b^2}{a^2}+\frac{u}{a^2})(\frac{c^2}{a^2}+\frac{u}{a^2})}}$$
$$\frac{\Omega^2}{\pi G\rho} = 2bc\frac{1}{a^6}\int_0^\infty \frac{udu}{(1+\frac{u}{a^2})(1-e_{xy}^2+\frac{u}{a^2})\sqrt{(1+\frac{u}{a^2})(1-e_{xy}^2+\frac{u}{a^2})(1-e_{xz}^2+\frac{u}{a^2})}}. \tag{4.93}$$

Substituting $\frac{u}{a^2} = w$, we have

$$\frac{\Omega^2}{\pi G\rho} = 2\frac{bc}{a^6}\int_0^\infty \frac{wa^4 dw}{(1+w)(1-e_{xy}^2+w)\sqrt{(1+w)(1-e_{xy}^2+w)(1-e_{xz}^2+w)}}$$

$$\frac{\Omega^2}{\pi G\rho} = 2\frac{b}{a}\frac{c}{a}\int_0^\infty \frac{wdw}{(1+w)(1+w-e_{xy}^2)\sqrt{(1+w)(1+w-e_{xy}^2)(1+w-e_{xz}^2)}}$$

$$\frac{\Omega^2}{\pi G\rho} = 2\sqrt{(1-e_{xy}^2)(1-e_{xz}^2)}\int_0^\infty \frac{wdw}{(1+w)(1+w-e_{xy}^2)\sqrt{(1+w)(1+w-e_{xy}^2)(1+w-e_{xz}^2)}}$$

$$\frac{\Omega^2}{\pi G\rho} = 2\sqrt{(1-e_{xy}^2)(1-e_{xz}^2)}\int_0^\infty \frac{wdw}{\sqrt{(1+w)^3(1+w-e_{xy}^2)^3(1+w-e_{xz}^2)}}. \tag{4.94}$$

Equation (4.94) will be very helpful for our numerical evaluations, as it enables us to use the eccentricities, which take values in the finite range $[0,1]$, as opposed to the semi-axes a, b, c.

We will repeat the same process for equation (4.88). We have,

$$a^2b^2\int_0^\infty \frac{du}{\sqrt{(a^2+u)^3(b^2+u)^3(c^2+u)}} = c^2\int_0^\infty \frac{du}{\sqrt{(a^2+u)(b^2+u)(c^2+u)^3}}$$

$$a^2b^2\int_0^\infty \frac{du}{\sqrt{a^{14}(1+\frac{u}{a^2})^3(\frac{b^2}{a^2}+\frac{u}{a^2})^3(\frac{c^2}{a^2}+\frac{u}{a^2})}} = c^2\int_0^\infty \frac{du}{\sqrt{a^{10}(1+\frac{u}{a^2})(\frac{b^2}{a^2}+\frac{u}{a^2})(\frac{c^2}{a^2}+\frac{u}{a^2})^3}}. \tag{4.95}$$

Again, we make the substitution $\frac{u}{a^2} = w$ and make use of the relations for the eccentricities (4.91) and (4.92), so the equation above can be rewritten as

$$b^2\int_0^\infty \frac{dw}{\sqrt{(1+w)^3(1+w+e_{xy}^2)^3(1+w+e_{xz}^2)}} = c^2\int_0^\infty \frac{dw}{\sqrt{(1+w)(1+w+e_{xy}^2)(1+w+e_{xz}^2)^3}}$$

$$\int_0^\infty \frac{\sqrt{1-e_{xy}^2}dw}{\sqrt{(1+w)^3(1+w+e_{xy}^2)^3(1+w+e_{xz}^2)}} = \int_0^\infty \frac{\sqrt{1-e_{xz}^2}dw}{\sqrt{(1+w)(1+w+e_{xy}^2)(1+w+e_{xz}^2)^3}}. \tag{4.96}$$

Imposing the geometric condition (4.96), we recreate the three-dimensional plot 4.9 of the function (4.94), along with the Maclaurin sequence.

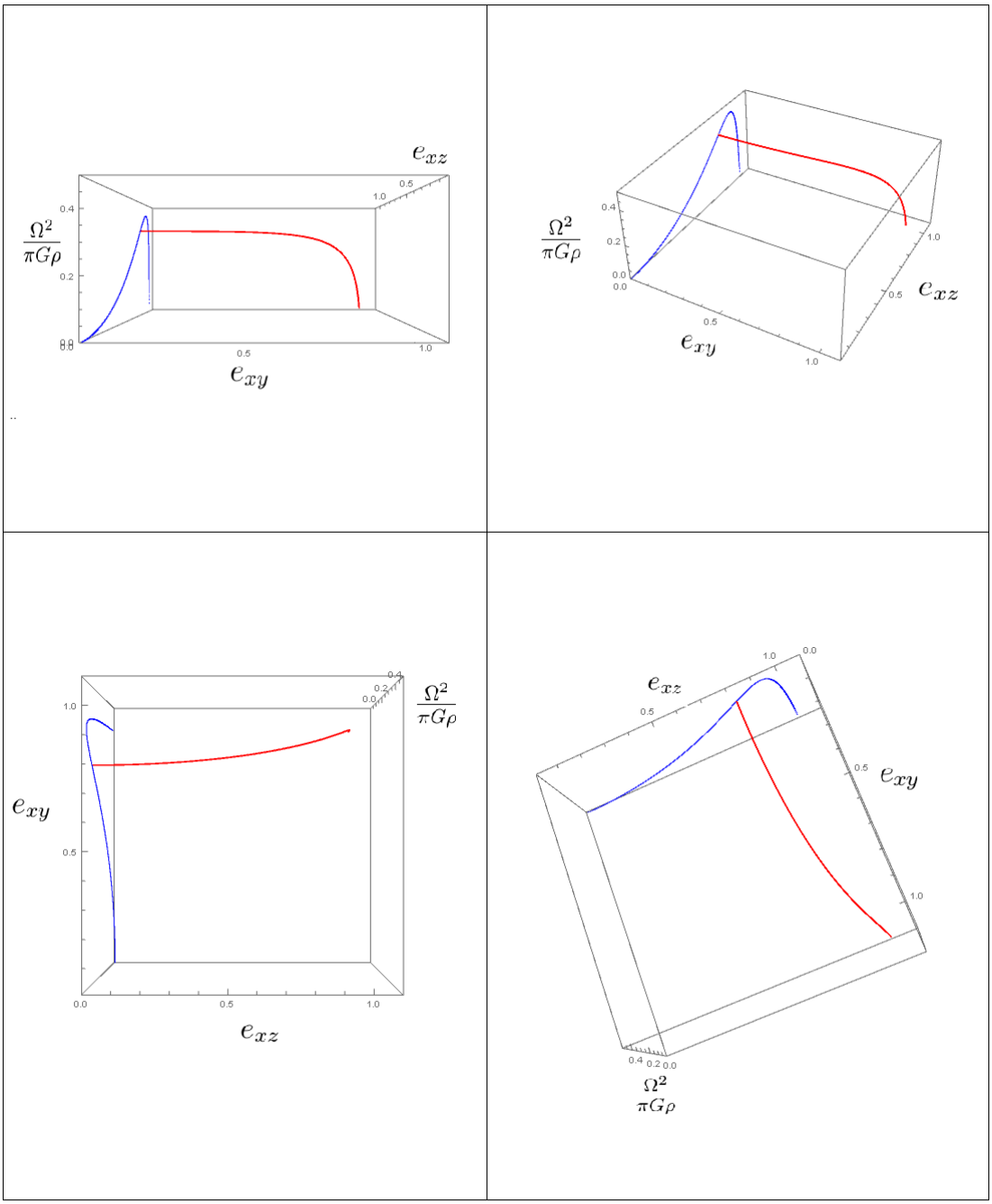

Figure 4.9: The square of angular velocity of a Jacobi ellipsoid with respect to the eccentricity in the $x-y$ plane, e_{xy} and the eccentricity in the $x-z$ plane, e_{xz}. The blue line corresponds to the Maclaurin spheroid sequence, while the red line corresponds to the Jacobi ellipsoid sequence. This plot has been created using *Wolfram Mathematica*.

The angular momentum of the Jacobi ellipsoid is given by the equation,

$$L = I\sqrt{\frac{\Omega^2}{\pi G\rho}} \rightarrow \frac{L}{\sqrt{GM^3R}} = \frac{\sqrt{3}}{10}\frac{a^2+b^2}{R^2}\sqrt{\frac{\Omega^2}{\pi G\rho}}, \tag{4.97}$$

where we have substituted the moment of inertia $I = M(a^2 + b^2)/5$ of the ellipsoid, with respect to $z-$axis of rotation, and $R = (abc)^{1/3}$ is the radius of a sphere with volume equal to the volume of the ellipsoid.

4.6 Multipole moment expansion

The shape of an isolated, non-rotating, self-gravitating fluid mass is a sphere, but as soon as it starts to rotate, it will diverge from the spherically symmetric configuration. As a result, the gravitational potential of such a configuration at some point r, outside the boundary of our mass, will be different than the typical gravitational potential of a point mass distribution,

$$V(r) = -\frac{GM}{r}. \tag{4.98}$$

In this section we will calculate the quadrupole moment of inertia of an irregularly shaped mass M at some distance r. We will start with the the usual expression for the potential at a point r due to a mass distribution, characterized by mass density $\rho(r')$,

$$\begin{aligned} V(\mathbf{r}) &= -\int_V \frac{G}{\|\mathbf{r}-\mathbf{r}'\|} dm' = -\int_V \frac{G\rho(\mathbf{r})}{\|\mathbf{r}-\mathbf{r}'\|} dV' \\ &= -\int_V \frac{G\rho(\mathbf{r})}{(r^2 - 2\mathbf{r}\mathbf{r}' + r'^2)^{1/2}} dV' \\ &= -\int_V \frac{G\rho(\mathbf{r})}{r\left(1 - 2\left(\frac{r'}{r}\right)\cos\theta' + \left(\frac{r'}{r}\right)^2\right)^{1/2}} dV'. \end{aligned} \tag{4.99}$$

Assuming that $r'/r \ll 1$, we can Taylor expand the denominator of equation (4.99),

$$\left(1 + \left(\frac{r'}{r}\right)^2 - 2\left(\frac{r'}{r}\right)\cos\theta'\right)^{1/2} = (1+x)^{1/2}, \tag{4.100}$$

where $x \equiv \left(\frac{r'}{r}\right)^2 - 2\left(\frac{r'}{r}\right)\cos\theta'$. The expansion of our series will give

$$\begin{aligned} (1+x)^{-1/2} &\approx 1 - \frac{1}{2}x + \frac{3}{8}x^2 + \mathcal{O}(x^3) \\ &= 1 - \frac{1}{2}\left(\frac{r'}{r}\right)^2 + \left(\frac{r'}{r}\right)\cos\theta' + \frac{3}{8}\left[\left(\frac{r'}{r}\right)^2 - 2\left(\frac{r'}{r}\right)\cos\theta'\right]^2 \\ &= 1 - \frac{1}{2}\left(\frac{r'}{r}\right)^2 + \left(\frac{r'}{r}\right)\cos\theta' + \frac{3}{2}\left(\frac{r'}{r}\right)^2\cos^2\theta' + \mathcal{O}\{(r'/r)^3\} \\ &= 1 + \left(\frac{r'}{r}\right)\cos\theta' + \frac{1}{2}\left(\frac{r'}{r}\right)^2(3\cos^3\theta' - 1) + \mathcal{O}\{(r'/r)^3\}. \end{aligned} \tag{4.101}$$

Using the Taylor expansion from relation (4.101), we can now express the gravitational potential for our irregular mass distribution:

$$V(\mathbf{r}) = -G \int_V \left[\frac{1}{r} + \frac{r' \cos\theta'}{r^2} + \frac{r'^2(3\cos^2\theta' - 1)}{2r^3} + \mathcal{O}\{(r'/r)^3\} \right] dm', \tag{4.102}$$

or equivalently

$$V(\mathbf{r}) = -\frac{GM}{r} + \frac{G}{r^2} \int_V r' \cos\theta' dm' + \frac{G}{2r^3} \int_V r'^2(3\cos^2\theta' - 1) dm' + \dots \ . \tag{4.103}$$

The first term is the classical result expected from a point mass distribution, having the same total mass M as our configuration, i.e. the monopole. The monopole moment is independent from the origin of our coordinate system, as it contains the total mass and not its distribution in space. The second term, also referred to as the dipole moment, will vanish if we suitably choose the origin of the frame of reference to coincide with the center of mass of our distribution [4]. This is the reason why a mass dipole cannot generate gravitational waves. The third term is the quadrupole moment of the mass, which we will denote by $Q(\hat{\mathbf{r}})$. In fact, the quadrupole moment is a rank-two tensor Q_{ij}. For a continuous mass system the components of the tensor are written:

$$Q_{ij} = 3 \int_V x'_i x'_j dm' \tag{4.104}$$

and the traceless part of Q_{ij}, if the mass density is given by $\rho(\mathbf{r}')$, can be written as

$$Q_{ij} = \int_V \rho(\mathbf{r}')(3x'_i x'_j - r'^2 \delta_{ij}) d^3 r' \tag{4.105}$$

where the indices i, j run over the Cartesian coordinates x, y, z. The quadrupole moment plays a key role in general relativity, because if it is time-dependent, it will produce gravitational radiation in a similar way to the electromagnetic radiation produced by accelerating electromagnetic charges. In contrast to the electromagnetic radiation, in gravitational radiation the lowest-order contribution comes from the quadrupole moment and this is the reason why we will focus on this term, neglecting any higher order contributions.

As we mentioned previously, the quadrupole moment shows up in the third term of the equation (4.103), i.e.

$$Q(\hat{\mathbf{r}'}) = \int_V \left[\frac{3(r'\cos\theta')^2 - 1}{2} \right] dm' = \frac{1}{2} Q_{ij} (\hat{\mathbf{r}})_i (\hat{\mathbf{r}})_j - \frac{1}{6} Q_{ii}, \tag{4.106}$$

[4] That is because for an arbitrary origin, we have

$$\hat{r} \cdot \mathbf{R}_{CM} = \hat{r} \cdot \frac{1}{M} \int_V \mathbf{r}' dm' = \frac{1}{M} \int_V r' \cos\theta' dm',$$

where by $\mathbf{R}_{CM} = \dfrac{1}{M} \displaystyle\int_V \mathbf{r}' dm'$ we denote the vector, pointing from the origin to the center of mass of the mass distribution. As a result, when the origin and the center of mass coincide, $\mathbf{R}_{CM} = 0$, the integral in the second term vanishes as well.

where the notation $(\hat{\mathbf{r}})_i$ refers to the $i-$th coordinate of the unit vector $\hat{\mathbf{r}}$. The most common form in which the quadrupole moment is expressed, is by introducing the traceless part of the tensor Q_{ij},

$$q_{ij} \equiv Q_{ij} - \frac{1}{3}\delta_{ij}Q_{kk}, \tag{4.107}$$

and as a result the gravitational potential of a mass distribution at some distant point r can be written as

$$V(\mathbf{r}) = -\frac{GM}{r} - \frac{Gq_{ij}(\hat{\mathbf{r}})_i(\hat{\mathbf{r}})_j}{2r^3} + \mathcal{O}\left(\frac{1}{r^4}\right). \tag{4.108}$$

For a spherical mass distribution, the quadrupole term and any other higher-order term of the Taylor expansion (4.101) vanish, so the gravitational potential at a distance r, far away from the mass, is described by equation (4.98). However, any divergence from spherical symmetry will result in non vanishing terms of the expansion (4.101).

4.7 The quadrupole moment tensor

In this section, we will calculate the quadrupole moment in the general case of a triaxial ellipsoid of the form

$$\frac{x^2}{a^2} + \frac{y^2}{b^2} + \frac{z^2}{c^2} \leq 1, \tag{4.109}$$

where a, b and c are the principal axes, which we have chosen to coincide with the coordinate axes for convenience. Furthermore, we will assume that the ellipsoid has a uniform density $\rho(r) = \rho_0$, constant.

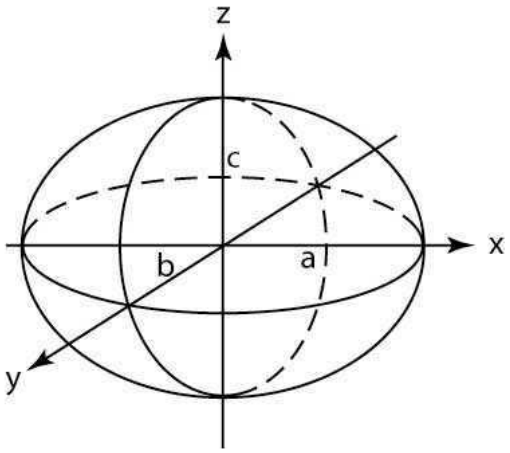

Figure 4.10: Triaxial ellipsoid centered on the origin of the Cartesian coordinate system.

In order to simplify the calculations, we will adopt a suitable ellipsoidal coordinate system (s, θ, ϕ), similar to the spherical coordinate system (r, θ, ϕ). The s-coordinate that we will use instead of the spherical r, is the dimensionless radius variable. We use s as a more

convenient parameter for our calculations, since the three principal axes are assumed to be of different lengths. As a result, we express the Cartesian coordinates in terms of the elliptical (s, θ, ϕ)

$$x = as\sin\theta\cos\phi \tag{4.110}$$
$$y = bs\sin\theta\sin\phi \tag{4.111}$$
$$z = cs\cos\theta. \tag{4.112}$$
$$\tag{4.113}$$

In order to use equation (4.105), we will first need to calculate the transformation of the infinitesimal volume element from the Cartesian to the elliptical coordinates,

$$dxdydz = \|\det(\mathbf{J}_{ij})\|dsd\theta d\phi, \tag{4.114}$$

where $\mathbf{J}_{ij}$ is the Jacobian matrix. We have,

$$\mathbf{J}_{ij} = \begin{bmatrix} \frac{\partial x}{\partial s} & \frac{\partial x}{\partial \theta} & \frac{\partial x}{\partial \phi} \\ \frac{\partial y}{\partial s} & \frac{\partial y}{\partial \theta} & \frac{\partial y}{\partial \phi} \\ \frac{\partial z}{\partial s} & \frac{\partial z}{\partial \theta} & \frac{\partial z}{\partial \phi} \end{bmatrix} = \begin{bmatrix} a\sin\theta\cos\phi & as\cos\theta\cos\phi & -as\sin\theta\sin\phi \\ b\sin\theta\sin\phi & bs\cos\theta\sin\phi & bs\sin\theta\cos\phi \\ c\cos\theta & -cs\sin\theta & 0 \end{bmatrix}$$

and after some simple algebraic calculations for the determinant, we find that

$$dxdydz = abcs^2\sin\theta dsd\theta d\phi. \tag{4.115}$$

At this point, we are ready to calculate the quadrupole moment tensor components using the equation (4.105) and we will begin with the diagonal terms. The first component yields,

$$\begin{aligned} Q_{11} = Q_{xx} &= \rho\int_V [3x^2 - (x^2+y^2+z^2)]dxdydz \\ &= \rho\int_V (2x^2 - y^2 - z^2)dxdydz \\ &= \rho\int_V (2a^2s^2\sin^2\theta\cos^2\phi - b^2s^2\sin^2\theta\sin^2\phi - c^2s^2\cos^2\theta)abcs^2\sin\theta dsd\theta d\phi \\ &= abc\rho\int_V s^4(2a^2\sin^3\theta\cos^2\phi - b^2\sin^3\theta\sin^2\phi - c^2\sin\theta\cos^2\theta)dsd\theta d\phi \\ &= abc\rho\int_0^1 s^4 ds\Big(2a^2\int_0^\pi\int_0^{2\pi}\sin^3\theta\cos^2\phi d\theta d\phi - b^2\int_0^\pi\int_0^{2\pi}\sin^3\theta\sin^2\phi d\theta d\phi \\ &\qquad - c^2\int_0^\pi\int_0^{2\pi}\sin\theta\cos^2\theta d\theta d\phi\Big) \\ &= abc\rho\frac{1}{5}\left(\frac{8\pi a^2}{3} - \frac{4\pi b^2}{3} - \frac{4\pi c^2}{3}\right) \rightarrow \end{aligned}$$

$$Q_{11} = \frac{4\pi}{15}\rho abc(2a^2 - b^2 - c^2). \tag{4.116}$$

For Q_{22} we have,

$$\begin{aligned}
Q_{22} = Q_{yy} &= \rho \int_V [3y^2 - (x^2 + y^2 + z^2)] dxdydz \\
&= \rho \int_V (2y^2 - x^2 - z^2) dxdydz \\
&= \rho \int_V (2b^2 \sin^3\theta \sin^2\phi - a^2 \sin^3\theta \cos^2\phi - c^2 \cos^2\theta \sin\theta) abcs^4 \sin\theta ds d\theta d\phi \\
&= abc\rho \frac{1}{5} \Big(2b^2 \int_0^{\pi} \int_0^{2\pi} \sin^3\theta \sin^2\phi d\theta d\phi - a^2 \int_0^{\pi} \int_0^{2\pi} \sin^3\theta \cos^2\phi d\theta d\phi \\
&\qquad\qquad - c^2 \int_0^{\pi} \int_0^{2\pi} \cos^2\theta \sin\theta d\theta d\phi \Big) \\
&= \frac{1}{5} abc\rho \left(\frac{8\pi b^2}{3} - \frac{4\pi a^2}{3} - \frac{4\pi c^2}{3} \right) \rightarrow
\end{aligned}$$

$$Q_{22} = \frac{4\pi}{15} \rho abc(2b^2 - a^2 - c^2). \tag{4.117}$$

For Q_{33} we have,

$$\begin{aligned}
Q_{33} = Q_{zz} &= \rho \int_V [3z^2 - (x^2 + y^2 + z^2)] dxdydz \\
&= \rho \int_V (2z^2 - x^2 - y^2) dxdydz \\
&= \rho \int_V (2c^2 \cos^2\theta - a^2 \sin^2\theta \cos^2\phi - b^2 \sin^2\theta \sin^2\phi) abcs^4 \sin\theta ds d\theta d\phi \\
&= \frac{1}{5} abc\rho \left(\frac{8\pi c^2}{3} - \frac{4\pi a^2}{3} - \frac{4\pi b^2}{3} \right) \rightarrow
\end{aligned}$$

$$Q_{33} = \frac{4\pi}{15} \rho abc(2c^2 - a^2 - b^2). \tag{4.118}$$

Now, for the non-diagonal terms, we have

$$\begin{aligned}
Q_{12} = Q_{xy} &= \rho \int_V \rho xy dxdydz \\
&= 3\rho \int_V as \sin\theta \cos\phi bs \sin\theta \sin\phi abcs^2 \sin\theta ds d\theta d\phi \\
&= 3\rho (ab)^2 c \int_V s^4 \sin^3\theta \cos\phi \sin\phi ds d\theta d\phi \\
&= 0,
\end{aligned} \tag{4.119}$$

since $\int_0^{2\pi} \cos\phi \sin\phi d\phi = 0$. For similar reasons, every other component of the quadrupole moment tensor, except for the diagonal components, vanishes. Using the results from equations (4.116),(4.117), (4.118) and (4.119) we end up with the traceless quadrupole moment

tensor

$$q_{ij} = \frac{4\pi}{15}\rho abc \begin{pmatrix} (2a^2 - b^2 - c^2) & 0 & 0 \\ 0 & (2b^2 - a^2 - c^2) & 0 \\ 0 & 0 & (2c^2 - a^2 - b^2) \end{pmatrix}. \tag{4.120}$$

Additionally, if we introduce the radius R of an equivalent sphere occupying the same volume as our ellipsoid, we have

$$V_{sph} = V_{ell} \rightarrow \frac{4\pi R^3}{3} = \frac{4\pi abc}{3} \rightarrow R^3 = abc. \tag{4.121}$$

and we can rewrite the density ρ as

$$\rho = \frac{3M}{4\pi R^3}. \tag{4.122}$$

Inserting equation (4.121) to the quadrupole moment tensor, we have that

$$\frac{q_{ij}}{\rho R^5} = \frac{4\pi}{15}\frac{abc}{R^5} \begin{pmatrix} 2a^2 - b^2 - c^2 & 0 & 0 \\ 0 & 2b^2 - a^2 - c^2 & 0 \\ 0 & 0 & 2c^2 - a^2 - b^2 \end{pmatrix}. \tag{4.123}$$

This way of expressing the quadrupole moment tensor will be very convenient for the calculations that we will make in a following section.

4.8 Gravitational waves from a Maclaurin spheroid

We will use the results we obtained in chapter 3 and section 4.7, in order to calculate the gravitational wave emission of the Maclaurin spheroid. For start, we will assume a Maclaurin spheroid given by

$$\frac{x^2}{a^2} + \frac{y^2}{a^2} + \frac{z^2}{c^2} \leq 1. \tag{4.124}$$

From equation (4.123) and by making use of the fact that $a = b$ in our case, we find the quadrupole moment tensor to be

$$\frac{q_{ij}^{Mc}}{\rho R^5} = \frac{4\pi}{15}\frac{a^2 c}{R^3} \begin{pmatrix} \frac{a^2}{R^2} - \frac{c^2}{R^2} & 0 & 0 \\ 0 & \frac{a^2}{R^2} - \frac{c^2}{R^2} & 0 \\ 0 & 0 & 2\frac{c^2}{R^2} - 2\frac{a^2}{R^2} \end{pmatrix} \rightarrow$$

$$\frac{q_{ij}^{Mc}}{\rho R^5} = \frac{4\pi}{15}\frac{a^2 c}{R^5}(a^2 - c^2) \begin{pmatrix} 1 & 0 & 0 \\ 0 & 1 & 0 \\ 0 & 0 & -2 \end{pmatrix}. \tag{4.125}$$

However, since our mass is rotating about the $z-$axis, we need to apply the rotation matrix $\mathbf{R}_{ij}$ on the quadrupole moment tensor. So, we calculate

$$\mathbf{R}_{ik}\mathbf{R}_{lj}\frac{q_{ij}^{Mc}}{\rho R^5} = \frac{4\pi}{15}\frac{a^2 c}{R^5}(a^2-c^2)\begin{pmatrix}\cos\omega t & -\sin\omega t & 0\\ \sin\omega t & \cos\omega t & 0\\ 0 & 0 & 1\end{pmatrix}\begin{pmatrix}1 & 0 & 0\\ 0 & 1 & 0\\ 0 & 0 & -2\end{pmatrix}\begin{pmatrix}\cos\omega t & \sin\omega t & 0\\ -\sin\omega t & \cos\omega t & 0\\ 0 & 0 & 1\end{pmatrix} \rightarrow$$

$$\mathbf{R}_{ik}\mathbf{R}_{lj}\frac{q_{ij}^{Mc}}{\rho R^5} = \frac{4\pi}{15}\frac{a^2 c}{R^5}(a^2-c^2)\begin{pmatrix}\cos^2\omega t+\sin^2\omega t & 0 & 0\\ 0 & \sin^2\omega t+\cos^2\omega t & 0\\ 0 & 0 & -2\end{pmatrix} \rightarrow \tag{4.126}$$

$$\mathbf{R}_{ik}\mathbf{R}_{lj}\frac{q_{ij}^{Mc}}{\rho R^5} = \frac{4\pi}{15}\frac{a^2 c}{R^5}(a^2-c^2)\begin{pmatrix}1 & 0 & 0\\ 0 & 1 & 0\\ 0 & 0 & -2\end{pmatrix}. \tag{4.127}$$

As we can see from equation (4.127), the Maclaurin spheroid quadrupole moment does not have any time-dependent component. If we recall the equations we derived in chapter 3 for the characteristics of the gravitational wave, they are given by equation (3.57),

$$\bar{h}_{ij} = \frac{2}{r}\ddot{q_{ij}}(t-\frac{r}{c}),$$

and (3.68)

$$L = \frac{1}{5}\langle \dddot{q_{ij}}\ \ddot{q}^{ij}\rangle,$$

where the geometrized units have been used.

It is trivial that the Maclaurin spheroid cannot be a gravitational wave source, as it has a constant quadrupole moment tensor, resulting to the trivial zero- solution of the gravitational wave equation.

4.9 Gravitational waves from a Jacobi ellipsoid

We will now calculate the gravitational waves emitted by a Jacobi ellipsoid which is described by the equation

$$\frac{x^2}{a^2}+\frac{y^2}{b^2}+\frac{z^2}{c^2}\leq 1. \tag{4.127}$$

As in the case of the Maclaurin spheroid, we will start with equation (4.123) and act on q_{ij}^J with the rotation matrix $\mathbf{R}_{ij}$ assuming that the ellipsoid is rotating about the $z-$axis. Thus,

we have

$$\mathcal{I}_{ij} = \mathbf{R}_{ik}\mathbf{R}_{lj}q^J_{ij} =$$
$$= \frac{4\pi}{15}\frac{abc}{R^5}\rho R^5 \begin{pmatrix} \cos\omega t & -\sin\omega t & 0 \\ \sin\omega t & \cos\omega t & 0 \\ 0 & 0 & 1 \end{pmatrix} \begin{pmatrix} 2a^2-b^2-c^2 & 0 & 0 \\ 0 & 2b^2-a^2-c^2 & 0 \\ 0 & 0 & 2c^2-a^2-b^2 \end{pmatrix} \begin{pmatrix} \cos\omega t & \sin\omega t & 0 \\ -\sin\omega t & \cos\omega t & 0 \\ 0 & 0 & 1 \end{pmatrix}$$
$$= \frac{4\pi}{15}\frac{abc}{R^5}\rho R^5 \begin{pmatrix} \frac{1}{2}(a^2+b^2-2c^2)+\frac{3}{2}(a^2-b^2)\cos(2\omega t) & \frac{3}{2}(a^2-b^2)\sin(2\omega t) & 0 \\ \frac{3}{2}(a^2-b^2)\sin(2\omega t) & \frac{1}{2}(a^2+b^2-2c^2)-\frac{3}{2}(a^2-b^2)\cos(2\omega t) & 0 \\ 0 & 0 & 2c^2-a^2-b^2 \end{pmatrix} \tag{4.128}$$

We will calculate the luminosity of the generated gravitational waves, using equation (3.68). First, we calculate the time-derivatives of $\mathcal{I}_{ij}$:

$$\dot{\mathcal{I}}_{ij} = \frac{4\pi}{15}\frac{abc}{R^5}\rho R^5 \begin{pmatrix} -3\omega(a^2-b^2)\sin(2\omega t) & 3\omega(a^2-b^2)\cos(2\omega t) & 0 \\ 3\omega(a^2-b^2)\cos(2\omega t) & 3\omega(a^2-b^2)\sin(2\omega t) & 0 \\ 0 & 0 & 0 \end{pmatrix}$$
$$= \frac{4\pi}{5}\frac{abc}{R^5}\rho R^5\omega(a^2-b^2) \begin{pmatrix} -\sin(2\omega t) & \cos(2\omega t) & 0 \\ \cos(2\omega t) &)\sin(2\omega t) & 0 \\ 0 & 0 & 0 \end{pmatrix} \tag{4.129}$$

$$\ddot{\mathcal{I}}_{ij} = \frac{8\pi}{5}\frac{abc}{R^5}\rho R^5\omega^2(a^2-b^2) \begin{pmatrix} -\cos(2\omega t) & -\sin(2\omega t) & 0 \\ -\sin(2\omega t) & \cos(2\omega t) & 0 \\ 0 & 0 & 0 \end{pmatrix} \tag{4.130}$$

$$\dddot{\mathcal{I}}_{ij} = -\frac{16\pi}{5}\frac{abc}{R^5}\rho R^5\omega^3(a^2-b^2) \begin{pmatrix} -\sin(2\omega t) & \cos(2\omega t) & 0 \\ \cos(2\omega t) & \sin(2\omega t) & 0 \\ 0 & 0 & 0 \end{pmatrix} \tag{4.131}$$

The luminosity of the gravitational waves produced by a rotating Jacobi ellipsoid, in standard units, is

$$L = \frac{G}{5c_l^5}\langle \dddot{\mathcal{I}}_{ij}\dddot{\mathcal{I}}^{ij}\rangle \rightarrow$$
$$L = \frac{G}{5c_l^5}\left(-\frac{16\pi}{5}\frac{abc}{R^5}\rho R^5\omega^3(a^2-b^2)\right)^2 \langle 2\sin^2(2\omega t) + 2\cos^2(2\omega t)\rangle \rightarrow$$
$$L = \frac{512\pi^2 G\omega^6}{125c_l^5}\rho^2 R^{10}\left(\frac{abc}{R^5}\right)^2 (a^2-b^2)^2, \tag{4.132}$$

where by c_l we denote the speed of light. From this expression, we notice that if we impose $a = b$, i.e. the Maclaurin sequence, we retrieve $L = 0$, which holds true for the Maclaurin spheroid as we showed in the previous section.

In order to better comprehend the result of equation (4.132), we will assume a sphere with volume equivalent to the volume of the Jacobi ellipsoid,

$$abc = R^3, \tag{4.133}$$

and we will replace the semi-axes a, b, c with the eccentricities of the ellipsoid

$$e_{xy}^2 = 1 - \frac{b^2}{a^2}, \tag{4.134}$$

$$e_{xz}^2 = 1 - \frac{c^2}{a^2}. \tag{4.135}$$

Introducing the relations (4.133), (4.134), (4.135) to equation (4.132), we have

$$\begin{aligned}
L &= \frac{512\pi^2 G\rho^2 R^{10}\omega^6}{125c_l^5}\frac{1}{R^4}a^4(1-\frac{b^2}{a^2})^2 \rightarrow \\
L &= \frac{512\pi^2}{125}\frac{G}{c_l^5}\omega^6\frac{M^2}{R^6}R^6a^4e_{xy}^4 \rightarrow \\
L &= \frac{16\pi^2}{125}\left(\frac{c_l^5}{G}\right)\left(\frac{2GM}{c_l^2}\right)^5\left(\frac{\omega^2}{GM}\right)^3 R^4\frac{e_{xy}^4}{[(1-e-xy^2)(1-e-xz^2)]^6} \rightarrow \\
L &= \frac{16\pi^2}{125}\left(\frac{c_l^5}{G}\right)\left(\frac{R_S}{R}\right)^5\left(\frac{\omega^2}{GM/R^3}\right)^3\frac{e_{xy}^4}{[(1-e_{xy}^2)(1-e_{xz}^2)]^6} \rightarrow \\
L &= \frac{16\pi^5}{125}\left(\frac{c_l^5}{G}\right)\left(\frac{R_S}{R}\right)^5\left(\frac{\omega^2}{\pi G\rho}\right)^3\frac{e_{xy}^4}{[(1-e_{xy}^2)(1-e_{xz}^2)]^6},
\end{aligned} \tag{4.136}$$

where we introduced the Schwarzschild radius $R_S = 2GM/c_l^2$. The most important aspect that is implied from equation (4.136) is that only compact objects can be essentially sources of gravitational waves. Although $\frac{c_l^5}{G} \approx 10^{59}\text{erg}\cdot\text{s}^{-1}$ is a huge number, the quantity $\frac{R_S}{R}$ is very small for ordinary stars, so overall the luminosity of the gravitational waves is significant only in the cases of compact objects, where the size of the object is comparable to its Schwarzschild radius.

Furthermore, equation (4.136) is a complicated function of ω and the eccentricities e_{xy}, e_{xz}. As a result, we can substitute the relation (4.94) for $\omega^2/\pi G\rho$ for the Jacobi ellipsoid, and see how the luminosity of the gravitational waves changes along the Jacobi sequence. So, inserting the relation (4.94) to (4.136), we have

$$L = \frac{128\pi^5}{125}\left(\frac{c_l^5}{G}\right)\left(\frac{R_S}{R}\right)^5\frac{e_{xy}^4}{[(1-e_{xy}^2)(1-e_{xz}^2)]^{9/2}}\left(\int_0^\infty \frac{udu}{\sqrt{(1+u)^3(1+u-e_{xy}^2)^3(1+u-e_{xz}^2)}}\right)^3. \tag{4.137}$$

Figure 4.11 shows clearly that the luminosity of the gravitational waves, that result from a rotating Jacobi ellipsoid, is constantly growing, as the eccentricities of the ellipsoid approach one, i.e. the ellipsoid tends to a bar-shaped figure. Additionally, from figure 4.9, we know that as the eccentricities of the ellipsoid grow larger, the square of the angular velocity - the quantity $\Omega^2/\pi G\rho$ - becomes smaller. Combining these results, one can clearly see that even though the rotation of the ellipsoid tends to zero, the most important contribution to the luminosity of the gravitational waves, comes from the distribution of mass.

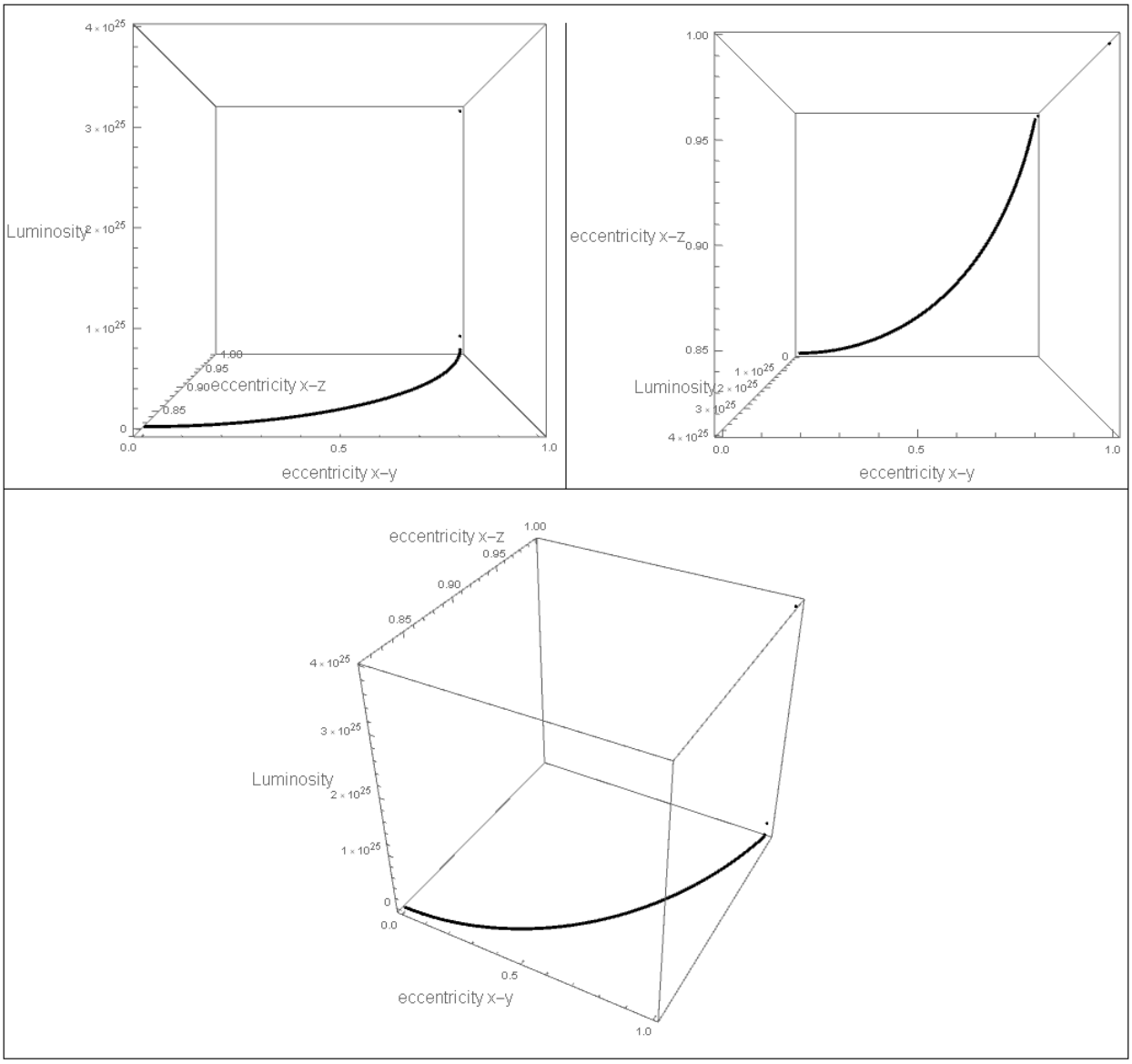

Figure 4.11: The gravitational wave luminosity for a Jacobi ellipsoid as a function of the eccentricities e_{xy}, e_{xz} in the $x-y$ and $x-z$ planes, respectively. The luminosity in this diagram is normalized to 10^58 erg/s, and we assumed an ellipsoid of total mass $M = 1M_\odot$ and equivalent radius $R = 10$km. This plot has been created using *Wolfram Mathematica.*

Bibliography

[1] W. Baade and F. Zwicky. Remarks on super-novae and cosmic rays. *Phys. Rev.*, 46:76–77, Jul 1934. https://link.aps.org/doi/10.1103/PhysRev.46.76.2.

[2] Richard C. Tolman. Static Solutions of Einstein's Field Equations for Spheres of Fluid. *Physical Review*, 55(4):364–373, Feb 1939. https://ui.adsabs.harvard.edu/abs/1939PhRv...55..364T.

[3] J. R. Oppenheimer and G. M. Volkoff. On Massive Neutron Cores. *Physical Review*, 55(4):374–381, Feb 1939. https://ui.adsabs.harvard.edu/abs/1939PhRv...55..374O.

[4] A. G. Cameron. Neutron Star Models. *apj*, 130:884, Nov 1959. https://ui.adsabs.harvard.edu/abs/1959ApJ...130..884C.

[5] A.B. Migdal. Superfluidity and the moments of inertia of nuclei. *Nuclear Physics*, 13(5):655 – 674, 1959. http://www.sciencedirect.com/science/article/pii/0029558259902640.

[6] S. Bowyer, E. T. Byram, T. A. Chubb, and H. Friedman. Lunar Occultation of X-ray Emission from the Crab Nebula. *Science*, 146(3646):912–917, Nov 1964. https://ui.adsabs.harvard.edu/abs/1964Sci...146..912B.

[7] N. S. Kardashev. Magnetic Collapse and the Nature of Intense Sources of Cosmic Radio-Frequency Emission. *azh*, 41:807, Jan 1964. https://ui.adsabs.harvard.edu/abs/1964AZh....41..807K.

[8] A. Hewish, S. J. Bell, J. D. H. Pilkington, P. F. Scott, and R. A. Collins. Observation of a Rapidly Pulsating Radio Source (Reprinted from Nature, February 24, 1968). *nat*, 224(5218):472, Nov 1969. https://ui.adsabs.harvard.edu/abs/1969Natur.224..472H.

[9] F. Pacini. Energy Emission from a Neutron Star. *nat*, 216(5115):567–568, Nov 1967. https://ui.adsabs.harvard.edu/abs/1967Natur.216..567P.

[10] T. Gold. Rotating Neutron Stars as the Origin of the Pulsating Radio Sources. *nat*, 218(5143):731–732, May 1968. https://ui.adsabs.harvard.edu/abs/1968Natur.218..731G.

[11] S. E. Thorsett and D. Chakrabarty. Neutron Star Mass Measurements. I. Radio Pulsars. *apj*, 512:288–299, February 1999. https://ui.adsabs.harvard.edu/abs/1999ApJ...512..288T.

[12] J. L. Friedman and B. F. Schutz. Lagrangian perturbation theory of nonrelativistic fluids. *apj*, 221:937–957, May 1978. http://adsabs.harvard.edu/abs/1978ApJ...221..937F.

[13] J. L. Friedman and B. F. Schutz. Secular instability of rotating Newtonian stars. *apj*, 222:281–296, May 1978. https://ui.adsabs.harvard.edu/abs/1978ApJ...222..281F.

[14] S. Chandrasekhar. *Ellipsoidal figures of equilibrium*. 1987. http://adsabs.harvard.edu/abs/1987efe..book.....C.

[15] D. Lynden-Bell and J. P. Ostriker. On the stability of differentially rotating bodies. *mnras*, 136:293, 1967. http://adsabs.harvard.edu/abs/1967MNRAS.136..293L.

[16] The LIGO Scientific Collaboration, the Virgo Collaboration, B. P. Abbott, R. Abbott, T. D. Abbott, S. Abraham, F. Acernese, K. Ackley, C. Adams, and R. X. Adhikari. GWTC-1: A Gravitational-Wave Transient Catalog of Compact Binary Mergers Observed by LIGO and Virgo during the First and Second Observing Runs. Nov 2018. https://ui.adsabs.harvard.edu/abs/2018arXiv181112907T.

[17] B. Schutz. *A First Course in General Relativity*. 2009. http://adsabs.harvard.edu/abs/2009fcgr.book.....S.

[18] C. W. Misner, K. S. Thorne, and J. A. Wheeler. *Gravitation*. 1973. http://adsabs.harvard.edu/abs/1973grav.book.....M.

[19] Chirata C. M., nov 2011. http://www.tapir.caltech.edu/~chirata/ph236/2011-12/lec14.pdf.

[20] I. Newton. *Philosophiae naturalis principia mathematica*. 1760. http://adsabs.harvard.edu/abs/1760pnpm.book.....N.

[21] C. MacLaurin. *A Treatise on Fluxions*. A Treatise of Fluxions. W. Baynes, 1801. https://books.google.gr/books?id=NUw7AQAAIAAJ.

[22] C. G. J. Jacobi. Ueber die Figur des Gleichgewichts. *Annalen der Physik*, 109(8):229–233, Jan 1834. https://ui.adsabs.harvard.edu/abs/1834AnP...109..229J.

[23] B. Riemann. *Ein Beitrag zu den Untersuchungen über die Bewegung eines flüssigen gleichartigen Ellipsoides*. Abhandlungen der Gesellschaft der Wissenschaften in Göttingen, Mathematisch-Physikalische Klasse. Verlag der Dieterichischen Buchhandlung, 1861. https://books.google.gr/books?id=BzgPAAAAQAAJ.

[24] J. R. Ipser and L. Lindblom. The oscillations of rapidly rotating Newtonian stellar models. *apj*, 1990. http://adsabs.harvard.edu/abs/1990ApJ...355..226I.

[25] N. Stergioulas. Rotating Stars in Relativity. *Living Reviews in Relativity*, 2003. http://adsabs.harvard.edu/abs/2003LRR.....6....3S.

[26] P. H. Roberts and K. Stewartson. On the Stability of a Maclaurin Spheroid of Small Viscosity. *apj*, 137:777, April 1963. http://adsabs.harvard.edu/abs/1963ApJ...137..777R.

[27] Éanna É. Flanagan and Scott A. Hughes. The basics of gravitational wave theory. *New Journal of Physics*, 7(1):204, Sep 2005. https://ui.adsabs.harvard.edu/abs/2005NJPh....7..204F.

[28] Zeldovich Ya.B. The equation of state at ultrahigh densities and its relativistic limitations. *Zh. Eksp. Teor. Fiz.*, ([Engl. transl.: , Sov. Phys.–JETP 14, 1143–1147].), 1962.

[29] Kostas Glampedakis and Leonardo Gualtieri. Gravitational Waves from Single Neutron Stars: An Advanced Detector Era Survey. In *Astrophysics and Space Science Library*, volume 457 of *Astrophysics and Space Science Library*, page 673, Jan 2018. https://ui.adsabs.harvard.edu/abs/2018ASSL..457..673G.

[30] Benjamin J. Owen, Lee Lindblom, Curt Cutler, Bernard F. Schutz, Alberto Vecchio, and Nils Andersson. Gravitational waves from hot young rapidly rotating neutron stars. *prd*, 58(8), Oct 1998. https://ui.adsabs.harvard.edu/abs/1998PhRvD..58h4020O.

[31] R. N. Manchester, G. B. Hobbs, A. Teoh, and M. Hobbs. The Australia Telescope National Facility Pulsar Catalogue. *aj*, 129:1993–2006, April 2005. https://ui.adsabs.harvard.edu/abs/2005AJ....129.1993M.

[32] *Neutron Stars and Pulsars*, volume 357, Jan 2009. https://ui.adsabs.harvard.edu/abs/2009ASSL..357.....B.

[33] P. Haensel, A. Y. Potekhin, and D. G. Yakovlev. Neutron stars 1: Equation of state and structure. *Astrophys. Space Sci. Libr.*, 326:pp.1–619, 2007.